

***THE RIDE COMFORT VERSUS HANDLING
DECISION FOR OFF-ROAD VEHICLES***

**by
Rudolf Bester**

Submitted in partial fulfilment of the requirements for the degree:

Master of Engineering (Mechanical Engineering)

in the

Faculty of Engineering, Built environment and Information Technology (EBIT),
University of Pretoria, Pretoria.

2006

Supervisors: Dr. P.E. Uys and Dr. P.S. Els

Summary

Today, Sport Utility Vehicles are marketed as both on-road and off-road vehicles. This results in a compromise when designing the suspension of the vehicle. If the suspension characteristics are fixed, the vehicle cannot have good handling capabilities on highways and good ride comfort over rough terrain. The rollover propensity of this type of vehicle compared to normal cars is high because it has a combination of a high centre of gravity and a softer suspension.

The 4 State Semi-active Suspension System ($4S_4$) that can switch between two discrete spring characteristics as well as two discrete damper characteristics, has been proven to overcome this compromise. The soft suspension setting (soft spring and low damping) is used for ride comfort, while the hard suspension setting (stiff spring and high damping) is used for handling. The following question arises: when is which setting most appropriate? The two main contributing factors are the terrain profile and the driver's actions.

Ride comfort is primarily dependant on the terrain that the vehicle is travelling over. If the terrain can be identified, certain driving styles can be expected for that specific environment. The terrains range from rough and uncomfortable to smooth with high speed manoeuvring. Terrain classification methods are proposed and tested with measured data from the test vehicle on known terrain types. Good results were obtained from the terrain classification methods. Five terrain types were accurately identified from over an hour's worth of vehicle testing.

Handling manoeuvres happen unexpectedly, often to avoid an accident. To improve the handling and therefore safety of the vehicle, the $4S_4$ can be switched to the hard suspension setting, which results in a reduced body roll angle. This decision should be made quickly with the occupants' safety as the priority. Methods were investigated that will determine when to switch the suspension to the handling mode based on the kinematics of the vehicle. The switching strategies proposed in this study have the potential, with a little refinement, to make the ride versus handling decision correctly.

Samevatting

Vandag word sportnutsvoertuie bemark as beide padvoertuie en veldvoertuie. Gevolglik het die suspensiestelsel wat vir hierdie voertuie ontwerp word 'n kompromie tussen ritgemak en hantering. Wanneer 'n vaste suspensie eienskap gekies word, kan die voertuig nie goeie hanteringsvermoë op snelweë sowel as goeie ritgemak oor rowwe terrein hê nie. Die omrolwaarskynlikheid van hierdie tipe voertuie is ook hoër as dié van normale karre, as gevolg van die kombinasie van 'n hoë massamiddelpunt en 'n sagte suspensie.

Die 4 stadium semi-aktiewe suspensiestelsel ($4S_4$), wat tussen twee diskrete veer karakteristieke en twee diskrete demper karakteristieke kan skakel, het bewys dat hierdie kompromie oorkom kan word. Die sagte suspensieverstelling (sagte veer en lae demping) word vir ritgemak gebruik, terwyl die harde suspensieverstelling (stywe veer en hoë demping) vir hantering gebruik word. Die volgende vraag ontstaan dus: wanneer moet watter verstelling gebruik word? Die twee hoof bydraende faktore is die terrein profiel en die bestuurder se aksies.

Die ritgemak is hoofsaaklik afhanklik van die terrein waarop die voertuig ry. Sou die terrein geïdentifiseer kon word, kan sekere bestuurstyle verwag word vir daardie spesifieke omgewing. Die terreine wissel van rof en ongemaklik tot glad met hoë spoed maneuvers. Terreinklassifiseringsmetodes word voorgestel en getoets met data wat van die voertuig gemeet was op bekende soorte terreine. Goeie resultate is verkry met die terreinklassifiseringsmetodes. Vyf terreinsoorte is redelik akkuraat geïdentifiseer van data wat oor 'n tydspan van meer as 'n uur opgeneem is.

Hanteringsmaneuvers gebeur onverwags, die meeste van die tyd om 'n ongeluk te voorkom. Die $4S_4$ kan na die harde suspensieverstelling geskakel word om die hantering en die veiligheid van die voertuig te verbeter en ook die rolhoek van die voertuig te verlaag. Die besluit moet vinnig geneem word met die insittendes se veiligheid as prioriteit. Metodes is ondersoek om te bepaal wanneer die suspensie na die hanteringsmodus geskakel moet word, gebaseer op die kinematika van die voertuig. Die skakelstrategieë wat voorgestel word in die studie het die potensiaal, met 'n bietjie verfyning, om die ritgemak- teenoor hanteringsbesluit korrek te maak.

Acknowledgements

Soli Deo Gloria

- Dr. Petro Uys and Dr. Schalk Els for their wisdom and guidance
- Barend Uys, Carl Becker and Michael Thoresson for their support
- Mr. R.J. Grimbeek from the Statistics department
- My parents and family for believing in me
- The Mechanical and Aeronautical Engineering department at the University of Pretoria for this opportunity
- National Research Foundation for financial assistance



Table of contents

Summary	ii
Samevatting.....	iii
Acknowledgements.....	iv
Table of contents.....	v
List of symbols.....	vii
List of abbreviations.....	ix
List of figures.....	xi
List of tables.....	xv
1 Introduction.....	1-1
1.1 Problem statement.....	1-1
1.2 Scope.....	1-2
2 Background.....	2-1
2.1 Test Vehicle.....	2-1
2.2 Suspension system.....	2-2
2.3 Test Tracks.....	2-5
2.3.1 Belgian paving (BLG).....	2-6
2.3.2 Double lane change (DLC).....	2-6
2.3.3 Ride and handling track (RHT).....	2-7
2.3.4 City (CTY).....	2-7
2.3.5 Off-road track (ORT).....	2-8
2.4 Literature review.....	2-8
2.5 Conclusions from literature review.....	2-18
2.6 Data recording and processing.....	2-19
2.7 Filtering.....	2-23
2.8 Background conclusion.....	2-25
3 Terrain classification.....	3-1
3.1 Obstacle Detection.....	3-1
3.1.1 Method 1 (Not compensating for body pitch angle):.....	3-3
3.1.2 Method 2 (Vehicle body pitch angle compensated for):.....	3-4
3.2 Relative Roughness Indicator.....	3-6
3.3 Histogram of acceleration data.....	3-9
3.4 Fuzzy logic terrain classification.....	3-11
3.5 Self-Organising Maps.....	3-15
3.6 Statistical discrimination.....	3-25
3.7 Conclusion of Terrain classification methods.....	3-28
4 Ride comfort vs. Handling switching strategies.....	4-1
4.1 Benchmark switch.....	4-1
4.2 Comparison metrics.....	4-2
4.3 Single switch with delay vs. Hysteresis switch.....	4-4
4.4 Fast Fourier Transform analysis.....	4-5
4.5 Coherence.....	4-10
4.6 Fuzzy logic switching strategy.....	4-12
4.7 Polynomial prediction.....	4-14
4.8 Running Root Mean Square (RRMS) of the lateral acceleration.....	4-17
4.9 Conclusion of the Ride comfort vs. Handling switching strategies.....	4-22
5 Experimental results.....	5-1
5.1 Passenger response.....	5-1
5.2 Measurements.....	5-1
5.3 Test results.....	5-2

5.4	Conclusion of experimental results.....	5-10
6	Conclusions and Recommendations	6-1
6.1	Terrain classification.....	6-1
6.2	Switching strategies	6-2
	Bibliography and References	Bib/Ref-1
	Appendix A.....	A-1
A.2	Frequency Domain analysis (lateral acceleration).....	A-4
A.3	Frequency Domain analysis (yaw velocity).....	A-6
A.4	Coherence.....	A-9
A.5	Fuzzy logic.....	A-11
A.6	Polynomial prediction.....	A-14
A.7	RRMS of the lateral acceleration.....	A-17

List of symbols

a	:	Butterworth filtered signal coefficients, Hysteresis switch ON threshold value
b	:	Butterworth unfiltered signal coefficients, Hysteresis switch OFF threshold value
c_k	:	Constant associated with terrain k
C_{xy}	:	Coherence of the two signals, x and y
H_0	:	Static height of laser sensor [m]
H_i	:	Static height of laser sensor + suspension deflection [m]
i	:	Suspension unit i , index i
j	:	Index j
k	:	Index of terrain k
L	:	Distance travelled [m]
L_0	:	Initial laser measurement on a flat surface [m]
l_i	:	Actual laser measurement [m]
L_i	:	Laser measurement on a flat surface adjusted by the global pitch angle [m]
L_{nk}	:	Solution to the k^{th} discriminant function of the n^{th} observation
m	:	Single switch ON/OFF threshold value
M	:	Matrix of coefficients for the linear terms
n	:	Counter, n^{th} observation
N	:	number of terms, number of data points
P_{and}	:	Performance of the ON signal state compared to a benchmark [%]
P_{comb}	:	Objective function from the combination of P_{xor} , P_{and} and P_{nsw} [%]
P_{nsw}	:	Performance of the amount of switching in a signal compared to a benchmark [%]
P_{xor}	:	Performance of the ON and OFF signal state compared to a benchmark [%]
P_{xx}	:	Auto-correlation function of signal x
P_{xy}	:	Cross correlation function between two signals, x and y
P_{yy}	:	Auto-correlation function y
Q	:	Matrix of coefficients for the cross product terms
s_0	:	Benchmark switching signal
s_1	:	Proposed switching signal
t	:	Time [s]
T	:	Total time duration [s]
t_0	:	Start time [s]
T_n	:	Dominant terrain classification

t_L	:	Time after fixed distance was travelled [s]
v_n	:	Vector of the n^{th} observation
x	:	Signal, unfiltered signal
y	:	Signal, filtered signal
y_{rms}	:	Root Mean Square of signal x
z_i	:	Estimated road profile height at time step i [m]
\dot{z}_i	:	Vertical velocity of each suspension unit i [m/s]
\dot{z}_s	:	Vertical velocity measured by profilometer [m/s]
Θ_0	:	Angle between laser and vertical [°]
θ_i	:	Global pitch rotation of vehicle [°]

List of abbreviations

4S ₄	:	4 State Semi-active Suspension System
4WS	:	Four-Wheel Steering
Acc.	:	Acceleration [g]
ADAMS	:	Advanced Dynamic Analysis of Mechanical Systems
ANFIS	:	Artificial Neuro-Fuzzy Inference System
BLG	:	Belgian paving
CPU	:	Central Processing Unit
CTY	:	City traffic
DC	:	Direct Current
Disp.	:	Displacement [m]
DLC	:	Double lane change
DOF	:	Degrees of freedom
FFT	:	Fast Fourier Transform
FIS	:	Fuzzy Inference System
FMCW	:	Frequency Modulated Continuous Wave
GAP	:	Genetic Algorithm Predictor
GPS	:	Global Positioning System
GUI	:	Graphical User Interface
HMMWV	:	High Mobility Multi-purpose Wheeled Vehicle
IFFT	:	Inverse Fast Fourier Transform
IIR	:	Infinite Impulse Response
IMM	:	Interacting Multiple Model
IRI	:	International Roughness Index
Lat.	:	Lateral
LED	:	Light Emitting Diode
LF	:	Left front
LQG	:	Linear-Quadratic-Gaussian
LR	:	Left rear
meanSpd	:	Mean of vehicle Speed
ORT	:	Off-road track
PCA	:	Principal Component Analysis
PNN	:	Probabilistic Neural Network

QE	:	Quantization error
RF	:	Right front
RHT	:	Ride and handling track
RI	:	Roughness Indicator
RMS	:	Root Mean Square
rmsStrAng	:	Root mean square of the Steering Angle
RR	:	Right rear
RRI	:	Relative Roughness Indicator
RRMS	:	Running Root-Mean-Square
SOM	:	Self-Organising Map
stdStrAng	:	Standard deviation of the Steering Angle
SUV	:	Sports Utility Vehicle
TACOM	:	Tank-automotive and Armaments Command of the US Army
TE	:	Topographic error
UC	:	Unclassified terrain
UGV	:	Unmanned Ground Vehicle
Vel.	:	Velocity [m/s]
Vert.	:	Vertical

List of figures

Figure 1: The occurring percentage of each type of accident (Department of transport, 2004)	2-1
Figure 2: Test vehicle (Land Rover Defender 110)	2-2
Figure 3: 4S ₄ unit (Els, 2006a)	2-3
Figure 4: Gerotek Testing Facility (www.earth.google.com, 10/10/2006)	2-5
Figure 5: Belgian paving track	2-6
Figure 6: Land Rover with outriggers during Double lane change	2-6
Figure 7: Right hand drive vehicle path layout for the Double lane change (International Standards Organisation, 1999)	2-6
Figure 8: Ride and handling track (Google earth, 10/10/2006)	2-7
Figure 9: Roadmap between the University of Pretoria and Gerotek (MapSource, www.garmin.com)	2-8
Figure 10: Off-road track (Google earth, 10/10/2006)	2-8
Figure 11: Electronic and hydro-pneumatic components	2-19
Figure 12: Recorded data of all tests	2-21
Figure 13: GUI plotter	2-22
Figure 14: Frequency domain filter	2-23
Figure 15: Time domain filter	2-25
Figure 16: A four degree of freedom pitch plane vehicle model in Simulink	3-2
Figure 17: Detecting a triangular bump in the road using a laser distance meter	3-3
Figure 18: Method 1	3-4
Figure 19: Method 2	3-5
Figure 20: The measured parameters as well as the approximated road profile	3-5
Figure 21: Comparing the Relative Roughness Indicator (RRI) with the RRMS vertical acceleration	3-8
Figure 22: 3D Histograms of all the tests	3-9
Figure 23: Contour plots and ellipse approximations for each histogram	3-11
Figure 24: The superimposed range of accelerations for each test	3-11
Figure 25: FIS editor [MATLAB, fuzzy.m]	3-14
Figure 26: Comparison of terrain classification with Fuzzy logic	3-15
Figure 27: Cluster map of ALL_1 SOM with all the measured data as input variables	3-17
Figure 28: ALL_1 SOM with all the measured data as input variables	3-18
Figure 29: Performance of ALL_1 SOM with all the measured data as input variables	3-18

Figure 30: RIDE_1 SOM with RRI and vertical acceleration as input variables	3-19
Figure 31: Performance of RIDE_1 SOM with RRI and vertical acceleration as input variables	3-19
Figure 32: HAND_1 SOM with RMS lateral acceleration and vehicle speed as input variables	3-20
Figure 33: Performance of HAND_1 SOM with RMS lateral acceleration and vehicle speed as input variables	3-20
Figure 34: HAND_2 SOM with RMS lateral acceleration, steering angle and vehicle speed as input variables	3-21
Figure 35: Performance of HAND_2 SOM with RMS lateral acceleration, steering angle and vehicle speed as input variables	3-21
Figure 36: RIDE_HAND_1 SOM with RRI and RMS lateral acceleration as input variables	3-22
Figure 37: Performance of RIDE_HAND_1 SOM with RRI and RMS lateral acceleration as input variables	3-22
Figure 38: RIDE_HAND_2 SOM with RRI, RMS lateral acceleration and vehicle speed as input variables	3-23
Figure 39: Performance of RIDE_HAND_2 SOM with RRI, RMS lateral acceleration and vehicle speed as input variables	3-23
Figure 40: RIDE_HAND_3 SOM with RRI, RMS lateral acceleration, steering angle and vehicle speed as input variables	3-24
Figure 41: Performance of RIDE_HAND_3 SOM with RRI, RMS lateral acceleration, steering angle and vehicle speed as input variables	3-24
Figure 42: Comparing the Quadratic discriminant classification with the actual terrain	3-28
Figure 43: Steering angle vs. speed (Els 2006a)	3-29
Figure 44: Data used (top four graphs) to generate the Benchmark switch (bottom graph) Els (2006b)	4-2
Figure 45: P_{xor} flow diagram	4-3
Figure 46: P_{and} flow diagram	4-3
Figure 47: P_{nsw} flow diagram	4-3
Figure 48: Single switch with delay vs. Hysteresis switch	4-5
Figure 49: The FFT plots, Lateral acceleration and Benchmark comparison	4-6
Figure 50: Comparing the Benchmark switch with the Single switch and the Hysteresis switch	4-7
Figure 51: Optimization of ON and OFF threshold values for the Hysteresis switch (based on yaw velocity)	4-8
Figure 52: A comparison between the Benchmark switch and the Hysteresis switch (Yaw velocity frequency domain analysis)	4-9

Figure 53: Normalised steering angle and speed (maximum = 1, minimum = -1), Coherence and the comparison of the strategy with the Benchmark	4-10
Figure 54: A comparison between the Benchmark switch and the three possible coherence strategies	4-11
Figure 55: Fuzzy logic input and output membership functions	4-13
Figure 56: Comparison between the Benchmark switch and the Fuzzy logic switch	4-13
Figure 57: The process of determining the Polynomial prediction	4-15
Figure 58: Comparing the Least error mean and the Equal weight mean strategies to the Benchmark	4-16
Figure 59: Comparing the ON-switch delay, using polynomial prediction, with the Benchmark	4-17
Figure 60: Single switch optimization surfaces	4-19
Figure 61: Hysteresis switch optimization surfaces	4-20
Figure 62: Comparison of the Benchmark switch, Single switch and Hysteresis switch strategies	4-21
Figure 63: Passenger response button	5-1
Figure 64: Comparing the actual Single switch [$m = 0.24$, No delay] to the recalculated strategies (BLG)	5-3
Figure 65: Comparing the actual Single switch [$m = 0.24$, No delay] to the recalculated strategies (DLC)	5-4
Figure 66: Comparing the actual Hysteresis switch [$a = 0.225$, $b = 0.04$] to the recalculated strategies (DLC)	5-5
Figure 67: Comparing the actual Single switch [$m = 0.24$, No delay] to the recalculated strategies (RHT)	5-5
Figure 68: Comparing the actual Hysteresis switch [$a = 0.225$, $b = 0.04$] to the recalculated strategies (RHT)	5-6
Figure 69: Comparing the actual Hysteresis switch [$a = 0.225$, $b = 0.1$] to the recalculated strategies (RHT)	5-6
Figure 70: Comparing the actual Hysteresis switch [$a = 0.225$, $b = 0.04$] to the recalculated strategies (CTY)	5-7
Figure 71: Comparing the actual Single switch [$a = 0.24$, No delay] to the recalculated strategies (CTY)	5-8
Figure 72: Comparing the actual Single switch [$a = 0.24$, No delay] to the recalculated strategies (ORT)	5-8
Figure 73: Comparing the actual Hysteresis switch [$a = 0.225$, $b = 0.1$] to the recalculated strategies (ORT)	5-9

Figure 74: Frequency Domain analysis (lateral acceleration), Belgian paving	A-4
Figure 75: Frequency Domain analysis (lateral acceleration), Double lane change	A-4
Figure 76: Frequency Domain analysis (lateral acceleration), Ride and handling track	A-5
Figure 77: Frequency Domain analysis (lateral acceleration), City traffic	A-5
Figure 78: Frequency Domain analysis (lateral acceleration), Off-road track	A-6
Figure 79: Frequency Domain analysis (yaw velocity), Belgian paving	A-6
Figure 80: Frequency Domain analysis (yaw velocity), Double lane change	A-7
Figure 81: Frequency Domain analysis (yaw velocity), Ride and Handling Track	A-7
Figure 82: Frequency Domain analysis (yaw velocity), City traffic	A-8
Figure 83: Frequency Domain analysis (yaw velocity), Off-road track	A-8
Figure 84: Coherence, Belgian paving	A-9
Figure 85: Coherence, Double lane change	A-9
Figure 86: Coherence, Ride and handling track	A-10
Figure 87: Coherence, city traffic	A-10
Figure 88: Coherence, Off-road track	A-11
Figure 89: Fuzzy logic, Belgian paving	A-11
Figure 90: Fuzzy logic, Double lane change	A-12
Figure 91: Fuzzy logic, Ride and handling track	A-12
Figure 92: Fuzzy logic, city traffic	A-13
Figure 93: Fuzzy logic, Off-road track	A-13
Figure 94: Polynomial prediction, Belgian paving	A-14
Figure 95: Polynomial prediction, Double lane change	A-14
Figure 96: Polynomial prediction, Ride and handling track	A-15
Figure 97: Polynomial prediction, city traffic	A-15
Figure 98: Polynomial prediction, Off-road track	A-16
Figure 99: RRMS, Belgian paving	A-17
Figure 100: RRMS, Double lane change	A-17
Figure 101: RRMS, Ride and handling track	A-18
Figure 102: RRMS, city traffic	A-18
Figure 103: RRMS, Off-road track	A-19

List of tables

Table 1: Literature review summary (1)	2-17
Table 2: Literature review summary (2)	2-18
Table 3: Colour code	2-20
Table 4: Butterworth IIR filter coefficients	2-24
Table 5: Performance of SOM terrain classification [%]	3-25
Table 6: SOM terrain classification errors [%]	3-25
Table 7: Quadratic discriminant classification of training data	3-27
Table 8: Quadratic discriminant classification of testing data	3-27
Table 9: Quadratic discriminant method with histogram averaging	3-28
Table 10: Performance of the lateral acceleration frequency domain analysis using the Hysteresis switch strategy	4-7
Table 11: Performance of the lateral acceleration frequency domain analysis using the Single switch strategy	4-7
Table 12: Performance of the yaw velocity frequency domain analysis using the Hysteresis switch strategy	4-9
Table 13: Performance of Hysteresis switch [Coherence between: yaw velocity and lateral acceleration]	4-12
Table 14: Performance of Hysteresis switch [Coherence between: steer angle and lateral acceleration]	4-12
Table 15: Performance of Hysteresis switch [Coherence between: yaw velocity and steer angle]	4-12
Table 16: Performance of Fuzzy logic switch	4-13
Table 17: Performance of Polynomial prediction with Least error weighted mean method	4-16
Table 18: Performance of Polynomial prediction with Equal weighted mean method	4-16
Table 19: Performance of RRMS Lateral acceleration Single switch,	4-21
Table 20: Performance of RRMS Lateral acceleration Hysteresis switch,	4-21
Table 21: Performance of switching strategies (P_{xor})	4-22
Table 22: Performance of switching strategies (P_{and})	4-23
Table 23: Performance of switching strategies (P_{nsw})	4-24
Table 24: Overall results for all the strategies	4-25
Table 25: Hysteresis switch with lateral acceleration [a = 0.225, b = 0.04]	5-10
Table 26: Hysteresis switch with lateral acceleration [a = 0.225, b = 0.1]	5-10
Table 27: Single switch with lateral acceleration [m = 0.24, No delay]	5-10

1 Introduction

This thesis addresses the ride comfort versus handling decision for off-road vehicles operating under both off-road and on-road conditions. These vehicles are better known as Sports Utility Vehicles (SUV's). The problem statement will be given after which the scope of the study will be discussed.

1.1 Problem statement

The Sports Utility Vehicle (SUV) originated from military vehicles that travelled over rough terrain at relatively high speed. This implied that the vehicles needed large suspension movement to be able to absorb the energy from travelling over the terrain and high ground clearance to traverse large obstacles. Soldiers were used to rough conditions. Therefore ride comfort was not an important issue. Ride comfort of modern day vehicles are essential, especially when considering the prices paid by the owners. Today the SUV is marketed as both an on-road and off-road vehicle. This leads to a lethal combination of a soft suspension for ride comfort and a high centre of gravity due to the high ground clearance and the space needed for substantial suspension movement. This is the main cause of the high roll-over propensity of SUV's.

The main purpose of the suspension system is to attenuate the high frequency road excitation that is transmitted to the vehicle body. A soft suspension gives better ride comfort but worsens the handling ability of the vehicle. Designing a SUV with a passive suspension system, that will have both good ride comfort and handling capabilities, is almost impossible. There is always a compromise between the ride comfort and handling characteristics of a vehicle. Many solutions to this problem have been proposed. The two main approaches are: active and semi-active vehicle suspension systems.

Theoretically the vehicle can be isolated extremely well from the road input by using an active suspension system. This means that there are actuators that connect the vehicle body to the axles and wheels. These actuators force the wheels to follow the terrain profile in order to keep the vehicle body level. In reality this is not as simple as it seems. Enough energy must be generated or stored on the vehicle to power these actuators. Also the terrain input must be known before travelling over it, in order to apply the right amount of force at each actuator. If incorrect inputs are

given to the actuators the ride comfort and/or handling abilities may be worsened compared to a passive suspension system.

The semi-active suspension system may not be as effective as the active suspension system, but it is a lot cheaper, because energy is only required to activate the valves or electrical switches. These switches enable the control system to change the characteristics of the vehicle to either have better ride comfort or better handling. Once a decision is made whether a ride comfort (soft suspension) or handling (hard suspension) mode is needed, the vehicle reacts to terrain inputs in the same way as a vehicle with the same passive suspension characteristics would. It is therefore not essential to know the exact terrain profile that the vehicle is travelling over.

The 4 State Semi-active Suspension System ($4S_4$) has been developed at the University of Pretoria, South Africa. The $4S_4$ is a semi-active suspension that can switch between a soft and a stiff spring characteristic, as well as between low and high damping. Switching is achieved through hydraulic valves within 50 to 100 milliseconds. The idea behind the $4S_4$ is to switch between a “ride comfort mode” (soft spring and low damping) and a “handling mode” (stiff spring and high damping), thus presently using only two of the four possible states. Identifying the moment when the switching between these two settings (ride comfort and handling) should occur, is of the utmost importance for safety and comfort of the occupants. This study is directed at developing a suitable method to make the ride comfort vs. handling decision from observations made with instrumentation on the vehicle. Proposed ideas were evaluated on a SUV fitted with the $4S_4$ suspension system and various sensors.

1.2 Scope

The aim of the study is to find a method for determining when the occupants of a vehicle would require the suspension to be switched to ride comfort or handling mode. Possible methods could include optical, sonar and mechanical terrain scanning devices for determining the road roughness and/or obstacles. Alternatively onboard sensors that measure the vehicle’s kinematic behaviour from certain terrain and driver inputs can be used. Observations include vertical acceleration, lateral acceleration, roll velocity, yaw velocity, suspension displacements, kingpin steering angle and vehicle speed.

To determine the viability of different observation and processing methods on which the ride comfort vs. handling decision can be based, five tests that are representative of different driving conditions are analysed. The resulting switching signal is compared to an ideal switching strategy

defined by an expert vehicle test engineer. This strategy takes the mechanical and electronic limitations of the system into account to produce a signal that will result in a safe and comfortable driving experience for the occupants. The test tracks on which the tests were conducted include a standard Belgian paving track, a long level road for the Double lane change tests, a ride and handling track comparable to mountain pass driving and an off-road track for 4×4 vehicles. All of these tracks were situated at the Gerotek (www.gerotek.co.za) testing facility. Normal city driving was also investigated on the public road between the University of Pretoria and Gerotek.

Post processing of the measured data consists of filtering and determining statistical characteristics (root mean square, coherence, histograms, etc.). Several programming methods are considered such as Fuzzy logic, Self-Organising Maps and logical if-then algorithms.

2 Background

Sports Utility Vehicles (SUV's) are involved in many accidents on the road today because of their multi-purpose functionality. The safety of these vehicles can be improved by using different suspension settings for different applications. The following sections discuss a test vehicle and the test tracks that were used to quantify the performance of a SUV equipped with the locally developed suspension ($4S_4$) under various road conditions. Literature is reviewed for solutions to similar problems. A brief description of the data logging system that was used to record the measurements is presented and some filtering techniques that were used are explained.

2.1 *Test Vehicle*

Figure 1 shows the 2003 road accident statistics for South Africa. These statistics only include accidents where the vehicle or driver was responsible for the crash. Therefore no pedestrian related accidents were taken into account.

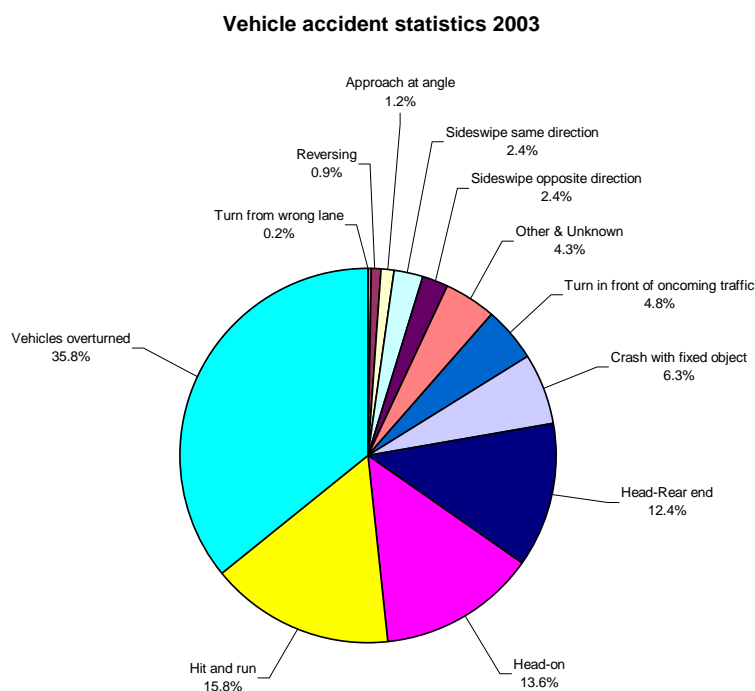


Figure 1: The occurring percentage of each type of accident (Department of transport, 2004)

More than a third of the accidents involved vehicle turnover or rollover. According to the South African Department of Transport (**Department of transport, 2004**) trucks, buses and minibuses have the highest fatal crash rate. All these vehicles have a high centre of gravity and relative soft

suspension, which in turn results in higher rollover propensity. Although SUV's are not mentioned as a vehicle class on its own, these vehicles can also be characterised by their high centre of gravity and soft suspension.



Figure 2: Test vehicle (Land Rover Defender 110)

Previous studies have indicated that the safety of SUV's could be improved by replacing the passive suspension system with a semi-active suspension system (Els, 2006a). The Land Rover Defender 110 (Figure 2) can be categorised as a SUV, but is biased towards off-road rather than on-road capabilities. An additional advantage to this vehicle is that most of the chassis and body panels are flat and rectangular, which simplifies the modifications and additions that are needed to accommodate the $4S_4$ suspension system. Because of its interior size and simplicity all the electronic, hydraulic and pneumatic equipment can easily be mounted onto the vehicle.

SUV's are required to be off-road vehicles as well as everyday city cars. The $4S_4$ suspension system allows the vehicle to be excellent in both scenarios.

2.2 Suspension system

The function of the suspension system of a vehicle is to isolate the driver and the passengers from high frequency road disturbances, for example: potholes and other uneven surfaces. This will be referred to as "ride comfort". Generally the softer the suspension the better the ride comfort. However vehicles do not only travel in straight lines. When the steering wheel is turned, there will

be a greater load transfer to one side of the vehicle. A harder suspension will result in less vehicle body roll. Changing the direction of the vehicle suddenly at relatively high speeds will be referred to as "handling". These two extreme states, ride comfort and handling or hard and soft suspension, provide a problem for design engineers. Both ride comfort and handling criteria are equally important in most vehicles. For a passive suspension a compromise between these two states is the only option. The result is that the spring and damping characteristics are set for a specific purpose. Racing cars need stiffer suspension to handle high speed cornering, but have terrible ride comfort qualities. Busses on the other hand need soft suspension to ensure that the passengers are comfortable, but this forces the driver to make turns at much lower speeds than other cars.

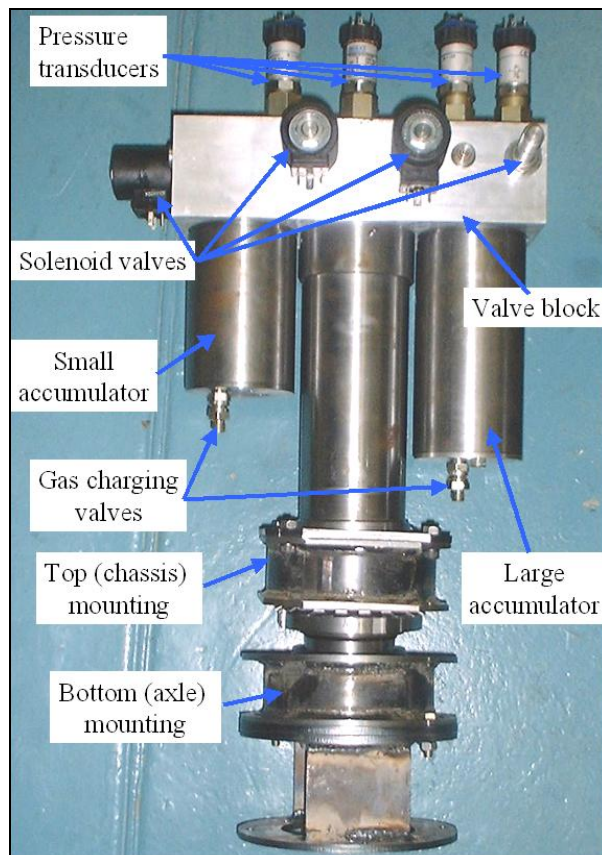


Figure 3: 4S₄ unit (Els, 2006a)

The Tank-Automotive and Armaments Command of the US Army (TACOM) proposed a revolutionary hydro-pneumatic suspension system (**Eberle & Steele, 1975**) allowing the driver to alter the characteristics of the suspension system using manual valves. This proposal was proven and implemented on a SUV by **Els (2006a)**. This system has two discrete spring stiffness characteristics, which are directly proportional to the gas volume controlled by switching hydraulic valves. There are also two discrete damping states, which are controlled by restricting the flow of oil by switching hydraulic bypass valves. This results in a combination of four states that each of the four suspension struts could be set to. A reservoir stores additional oil that could be pumped into

each suspension strut or be bled back to the reservoir. This allows the driver to adjust the ride height and therefore the centre of gravity. This system will be referred to as the 4 State Semi-active Suspension System ($4S_4$). Figure 3 shows one of the suspension units developed by **Els (2006a)**.

Mathematical optimisation was done by **Els, et al., (2006)** to obtain the best suspension characteristics for both ride comfort and handling. This was achieved by modelling the test vehicle in MSC, ADAMS (www.msc-africa.co.za) as accurately as possible. The optimization algorithm Dynamic Q, developed by **Snyman (2005)**, was used to minimize the vertical acceleration for ride comfort and the body roll angle for handling. After this was achieved the suspension struts were designed by **Els (2006a)** and built. The $4S_4$ suspension units were modelled in Simulink (www.mathworks.com) by **Theron and Els (2005)** and validated against experiments that tested the suspension units in tension and compression at various frequencies. It was then possible to simulate the behaviour of the vehicle with the new suspension before conducting actual tests. The test vehicle was modified slightly and the $4S_4$ was installed. When the vehicle was set to the handling mode, the average roll angle was reduced by more or less 70% (**Els 2006a**) but the ride comfort is not noticeably better compared to the standard vehicle. The reason for this is that the damping in the soft mode is the same as on the baseline vehicle. High flow valves are needed, but are expensive. The next prototype of the suspension system will solve this problem. Furthermore the ride height can also be adjusted to about 100 mm below and above the standard vehicle's ride height. This can improve the safety of the vehicle significantly (**Els 2006a**). If the selection of the ride comfort vs. handling mode is based on human decision, different people could choose different strategies at different times during the same driving manoeuvre over the same terrain. This will also imply that the driver has to consider one more issue while concentrating on all the other driving tasks. Therefore the decision should preferably be made objectively and automatically without the driver needing to worry about it.

It is critical that the right decision should be made at the right time. From a safety point of view, if the control strategy should change from handling to ride comfort at a critical time, it will almost certainly cause an accident.

For this study the ride height is kept to the same height as the standard test vehicle. Lowering the ride height does improve the vehicle's handling ability but it is beyond the scope of this study. The effects of rapid longitudinal acceleration and deceleration (braking) were also left out of the equation. The vehicle was instrumented with a wide variety of instruments to measure some of the kinematic parameters of the vehicle. The data was used to classify which suspension setting would

suit the situation the best. The valves that control the gas volume and the oil flow in the suspension units have a fairly slow response time (50 to 100 *ms*). A decision is made based on the operating conditions and is not based on classical proportional control theory. There are only two settings, (hard and soft suspension) and therefore a bipolar (ON/OFF) mode selection control was used.

Five tests were investigated by **Els (2006a)** to quantify the vehicle's capabilities before and after the $4S_4$ suspension were installed. These five tests were chosen to be representative of the vehicle's typical operating conditions.

2.3 Test Tracks

All the tests, except the city traffic, were performed at the Gerotek Testing Facilities (www.gerotek.co.za) outside Pretoria in South Africa (see Figure 4). This is a world class test facility with a number of tracks that enable vehicle engineers and test drivers to test their vehicles on standardised road surfaces. These test tracks are discussed in the following sections.



Figure 4: Gerotek Testing Facility (www.earth.google.com, 10/10/2006)

2.3.1 Belgian paving (BLG)



Figure 5: Belgian paving track

The Belgian paving is a straight horizontal road, approximately 100 m long and 4 m wide (see Figure 5). The surface consists of irregular sized bricks or cobble stones. The vehicle is driven in a straight line over the track at a constant speed. This tests the vehicle's ability to attenuate the high frequency excitations from the road for better passenger ride comfort.

2.3.2 Double lane change (DLC)



Figure 6: Land Rover with outriggers during Double lane change

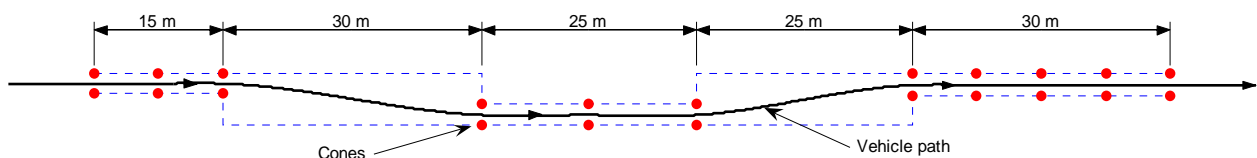


Figure 7: Right hand drive vehicle path layout for the Double lane change (International Standards Organisation, 1999)

This severe lane-change manoeuvre is a standardised accident avoidance test (**International Standards Organisation, 1999**). The test surface is a flat, smooth concrete road. Traffic cones are

placed in specified positions to guide the driver so that the test is repeatable. The driver needs to change lanes quickly to one side of the road and then back again. This tests the vehicle's handling characteristics. Figure 6 shows the test vehicle during the Double lane change. Notice the large amount of body roll angle that the vehicle has at that moment. Outriggers are fitted to the vehicle to prevent rollover. The standardised layout of the test is shown in Figure 7.

2.3.3 Ride and handling track (RHT)



Figure 8: Ride and handling track (www.earth.google.com, 10/10/2006)

The Gerotek Ride and handling track consists of sharp corners, steep hills and valleys (see Figure 8). This track's surface is not as smooth as the long straight track used for the Double lane change. This simulates mountain pass driving and is also used to test the vehicle's handling capability. Tests were done at high speeds, pushing the vehicle to its limits.

This track is 4.2 km long with 13 left and 15 right turns. The maximum gradient is 15% and the track is used for tests on all wheeled vehicles including extra heavy vehicles, off-road vehicles and motorcycles (www.gerotek.co.za, 03/11/2006).

2.3.4 City (CTY)

City driving was tested in normal traffic conditions. The road between the University of Pretoria and the Gerotek testing facility was used (see Figure 9). These are normal South African tarred roads, complete with potholes and patches of new tar covering old potholes.

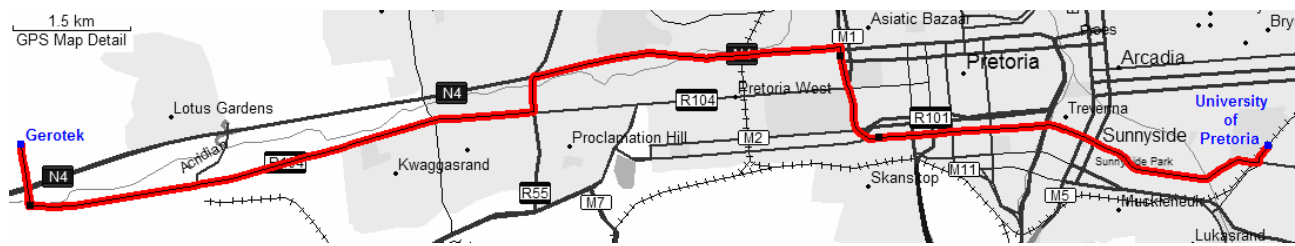


Figure 9: Roadmap between the University of Pretoria and Gerotek (MapSource, www.garmin.com)

2.3.5 Off-road track (ORT)



Figure 10: Off-road track (www.earth.google.com, 10/10/2006)

The Gerotek Off-road track is exclusively for off-road vehicles (see Figure 10). The track has various sections of rocky terrain as well as steep hills and valleys. Concrete was used to fix the track features for the purpose of repeatable tests. The amount of discomfort is extreme and therefore the vehicle is driven slowly over this terrain. The high ground clearance and large suspension movement enables 4×4 SUV's to be tested for extreme manoeuvrability on this track. This track is 2.6 km long and 4 m wide with a maximum gradient of 52%. The applicable vehicles are limited to vehicles with a front and rear overhang of not more than 1.5 m, approach and departure angles of at least 40°, a hump radius of less than 10 m, a ground clearance of more than 200 mm and a turning circle of less than 20 m diameter (www.gerotek.co.za, 03/11/2006).

A literature review on the ride comfort vs. handling decision will be presented now.

2.4 Literature review

Publications on the control of vehicle suspension systems were surveyed to gain better insight to possible methods for making the ride comfort versus handling decision.

Els (2006a) investigated the ride comfort vs. handling compromise for off-road vehicles in a PhD with the same title. Any passive suspension system poses a compromise because the ride comfort and handling criteria lie on opposite sides of the design spectrum. The 4 State Semi-active Suspension System ($4S_4$) was proposed to eliminate this compromise by changing the suspension to the appropriate driving mode. Four prototypes were designed, manufactured, tested and mathematically modelled. Suspension characteristics were optimized for the ride comfort and handling settings. The second set of prototypes were installed on a Land Rover Defender 110 and tested extensively to quantify the improvements in both driving modes. Several strategies for making the decision between the two driving modes were investigated. The requirements were that the switching should happen automatically, should be fail safe and should use easily measurable parameters. The following concepts were considered:

- Frequency analysis of accelerations
- Lateral acceleration
- Lateral acceleration vs. vertical acceleration
- Steering angle vs. speed
- Pitch and roll velocity vs. acceleration
- Vehicle height, throttle position and brake application

Finally a strategy that compared the moving RMS of the lateral and vertical accelerations was implemented with great success. The following recommendations for improving the strategy were given:

- The time required for the system to switch from the ride comfort mode to the handling mode should be reduced.
- The switching thresholds should be optimized.
- Terrain identification should be investigated in order to improve the performance of the some of the other strategies.

Trent and Green (2002) used a model-based genetic algorithm predictor (GAP) that was developed to estimate the propensity for vehicle rollover. The mathematical model was based on a Jeep Cherokee (1997) SUV and is discretised at 100 Hz. The genetic algorithm predicted that the simulation would undergo rollover, 400 ms in advance. This supplies enough time to activate active anti-roll algorithms and systems such as differential braking and/or active suspension control. The genetic algorithm predicts the rollover by calculating whether the tyre deflection will exceed a specified roll threshold.

The University of Tokushima developed a model of an active suspension system for passenger cars, using linear and Fuzzy logic controls. (**Yoshimura, et al., 1999**) The model is described by a nonlinear system with four degrees of freedom, subject to irregular excitation from a road surface. The active control is the sum of two kinds of control. The former is obtained by vertical acceleration of the vehicle body as the principal source of control, and the latter is obtained by using Fuzzy logic control as the complementary control. In the derivation of fuzzy control rules, linear combinations of the vertical and angular velocities and displacements of the vehicle body are denoted as the input variables. The fuzzy control rules are determined by minimizing the mean squares of the time responses of the vehicle body, under certain constraints on the acceptable relative displacements between the vehicle body and the suspension components, and the tyre deflections. In particular, emphasis is placed on the minimization of the vertical and angular acceleration of the vehicle body from the viewpoint of passenger ride comfort. The simulation results verified that the proposed active suspension system is very effective in the vibration isolation of the vehicle body. No method for improving the handling of the vehicle was mentioned.

A Neuro-Fuzzy controller was designed by **Foda (2001)** to improve damping and ride quality of a semi-active suspension system using a quarter-car model. The simulations show that the controller improves both the ride quality and the suspension travel in terms of vehicle acceleration and dynamic tyre loading. The neural network learns rules and deduces conclusions. The controller structure is simple (seven rules) so that real-time implementation is possible. The handling of a vehicle can not be modelled with a quarter-car model and is therefore not addressed.

Rao and Prahlad (1995) used a quarter-car to model the active suspension system of a vehicle. The simulation was controlled with fuzzy-logic-based control to enhance ride comfort faced with unknown road terrains. This is achieved by controlling the vertical acceleration to an acceptable level. Bell-shaped membership functions with respect to the Fuzzy logic control system were used. The flex, spread and centre of these functions associated with the linguistic variables were by fine-tuned by adjusting the parameters through trial and error. The simulations proved that the Fuzzy logic controller reduced the vehicle vibration and gave reasonably good responses. It was also observed that the controller is able to take care of the wider variations in the plant parameters from their nominal values. Again it was not possible to improve the handling of the vehicle using a quarter-car model.

Neural networks were efficiently trained to identify the dynamics of a nonlinear pneumatic suspension and were also trained to work as a nonlinear controller on high-speed railway vehicles

by **Nagai, et al. (1997)**. The neural network was trained using an actual experimental setup. It consisted of one input layer with 4 neurons, two hidden layers with 5 neurons each and one output layer with 1 neuron. The performance of the neural network controller was compared to that of the conventional linear quadratic controller. It was found that the neural network controller consumed less energy while providing better performance in the low frequency range. Typical railway disturbances are below 5 Hz.

Research on an emulator for human driving behaviour that uses a self-organising fuzzy rule-based system referred to as a fuzzylot is presented by **Pasquier, et al. (2001)**. A human driver is used to drive a simulation of a motor vehicle. The fuzzy neural network processes the driver input data, which it clusters, identify fuzzy variables and extract the fuzzy rule-base. There are a number of methods to automatically generate fuzzy rules from numerical data. A rule selection phase is used to delete the rules that have zero weights to all consequences. The autopilot is able to drive the vehicle on the same route that the human driver drove. This proves the self-organising capabilities of the neural network, the adaptability of the fuzzy rule-based system and the application possibilities to a real-world problem.

A Fuzzy logic based controller was used to control a body-suspension-wheel simulation model by **AL-Holou, Joo and Shaout (1995)**. The controller used two inputs: body velocity and suspension velocity. The control signal is a function of the inputs signals and is determined from the fuzzy rule-base. The controller showed major improvements over the passive suspension and minor improvement over the Skyhook method. This can be improved upon by using an adaptive fuzzy control method, which changes the input and output membership functions iteratively. An adaptive control method is said to improve both ride quality and road handling.

The design of Fuzzy controllers for semi-active suspension generated through the genetic algorithm with a local improvement mechanism is presented by **Hashiyama, Furuhashi and Uchikawa (1995)**. The algorithm's effectiveness is demonstrated by generating fuzzy controllers for a semi-active suspension system. The scheme for designing a Fuzzy logic controller is generally as follows:

- Define input and output variables
- Set parameters for each variable's membership functions
- Describe fuzzy rules
- Tune membership function parameters
- Modify the fuzzy rules

The design of the Fuzzy logic controller involves a lot of trial and error. Fuzzy neural networks are used to overcome these difficulties by identifying the control rules from measured data. It can be difficult to obtain the actual data in advance. Using genetic algorithms it was possible to determine the number of fuzzy rules, membership function parameters and the fuzzy rules. Thus the 5 steps of the fuzzy controller design were automated.

Wu and Xu (1999) proposed a damping fuzzy controller for a seven D.O.F. vehicle model with semi-active suspension. The fuzzy controller parameters were determined using a local improvement genetic algorithm. The genetic algorithm is based on the mutation of mating bacteria. Stronger genes are passed down through the generations, which ensure the survival of the strongest fuzzy rules. The fitness function is constantly evaluated and guides the optimization process. This random method can obtain the optimal fuzzy controller parameters if enough evaluations are performed.

A Fuzzy logic controller that controls an intelligent semi-active continuously adjustable damper suspension system was developed by **Nicolas, et al. (1997)**. Two strategies are considered: driver actions/responses and vehicle dynamics. The main advantage of the fuzzy control is the lower number of sensors needed to achieve the same results as compared to other control algorithms (e.g. Skyhook). The controller consists mainly of 3 parts:

- Input pre-processing: Sensor signal processing and filtering.
- Fuzzy Inference System (FIS): Data is fuzzified into linguistic variables.
- Post-processing: Determines the damping value to be applied.

The fuzzy system received the following data:

- Vehicle velocity vs. steering angle
- Vehicle velocity vs. steering speed
- Vehicle velocity vs. longitudinal acceleration
- Vehicle velocity vs. longitudinal deceleration
- Vehicle velocity vs. vertical acceleration

The Fuzzy logic controller is well suited for the suspension system because it is highly non-linear, it is difficult to simulate adequately, the control improvements are quite subjective, it is able to deal with the compromise between vehicle handling and comfort and it is very difficult to define a performance index based only on objective criteria. The fuzzy controlled suspension has lower

oscillation and settling time than the soft damper setting. It also produces better comfort for passengers than the hard damper setting.

An invention by **Kyrtsos (1998)** utilizes a method and apparatus for detecting a rollover condition by analysing the forces acting on the vehicle. The patent involves three accelerometers and a controller that compares the data received. A safety device is actuated if a potential rollover is detected. There will be fluctuations in the measurements due to the irregular road input. The measurements need to be averaged over a certain time period. If the period is too short the controller may be too sensitive and if the period is too long the system may not respond quickly enough or not at all. The data must be compared to a predetermined threshold value. This value has to be altered when certain conditions are changed. (e.g. weight, temperature, etc.) The difference between the standard deviation of the data from two accelerometers is also compared with a predetermined value. The third accelerometer is used to account for the effect of the road conditions.

Fault detection in a modern automation process was incorporated using intelligent control, thereby improving the reliability of complex control systems (**Tyan, Wang, Bahler, 1996**). Some methods to achieve this are: Parameter estimation, state observation, statistical likelihood ratio tests, rule-based expert system reasoning, pattern recognition and artificial neural networks. This paper describes a method that uses pattern recognition, an artificial neural network for fault diagnosis through a back propagation learning algorithm and using Fuzzy logic for fault control by keeping track of the parameter changes in a dynamic system. The test case used was a magnetic levitation vehicle (MLV). There are four distinct phases in the neural fault diagnosis and fuzzy fault control scheme.

- Process control and state observer: Determining the system's dynamic behaviour and estimate inaccessible states.
- Neural fault diagnosis: The class and cause of the malfunction is determined
- Fuzzy fault control: Derives a series of actions and analyses the consequences of the current fault.
- Actions: An appropriate action is taken based on the analyses above.

It was shown that the neural network classifier accomplishes a fairly accurate classification when track disturbance irregularities are present. This paper demonstrated the concept of a “diagnostic doctor” for dynamic systems.

It is important for a high-speed unmanned ground vehicle (UGV) to sense changing terrain conditions and modify its control strategy and motion planning algorithms to complete the specified operation as efficiently as possible. **Iagnemma and Dubowsky (2002)** proposed three methods for terrain characterisation and identification. These methods include:

- Vision based classification of the path ahead – Visual data consists of colour, geometric shapes, textures and distinguishing between soil and vegetation.
- Terrain parameter identification from a wheel-terrain interaction analysis – This entails physical parameters such as cohesion, internal friction angle and shear deformation modulus to classify terrain for example loose soil, muskeg, rock, etc. The parameters are calculated using simplified equations of terramechanics.
- Auditory wheel-terrain contact signatures for terrain classification – Potential low cost, low complexity additional sensors.

The UGV associates the data collected from all the sensors with a certain terrain type and is thus also able to learn. This database can then be used for predictive motion planning and advanced feedback control. The terrain parameters were estimated with good accuracy using limited computational resources.

A vibration-based terrain classification algorithm was proposed by **Iagnemma, Brooks and Dubowsky (2004)** for planetary rovers. Through empirical observations it was established that different terrain properties results in unique vibration patterns. An accelerometer was used to record the high-frequency vibrations. The algorithm uses principal component analysis (PCA) to distinguish between terrain classes and consists of two steps: an *a priori* analysis and an on-line classification.

Data was collected on two different types of terrain for the *a priori* analysis. The log power spectral densities of each was calculated and stored in matrices containing the spectral content for a segment of data and the variation in spectral content at a given frequency as a function of time. PCA was then used to discriminate between the two terrain types. During the on-line classification the vibrations are measured and the terrain is classified according to the *a priori* analysis. The results showed that this type of sensing could be used for quick, efficient and robust classification of terrain. This type of terrain identification can be improved by combining it with a vision-based method.

Tsunashima, Murakami and Miyata (2005) developed an estimation algorithm to determine the state of a vehicle and the road condition. This could enable a vehicle to achieve effective control for example: four-wheel steering (4WS) and stability. The state of the vehicle is determined from

inexpensive sensors measuring different parameters. The Interacting Multiple Model (IMM) method was proposed to respond to variations in road conditions in order to estimate the side-slip angle and the friction coefficient. A bicycle vehicle model was used to perform a Double lane change at 50 *km/h*. The road had three sections with three different friction coefficients. These friction coefficients were estimated very closely to the actual coefficients. The IMM estimator correctly determined the vehicle and road state simultaneously from lateral accelerations and yaw rate measurements.

Braghin, et al. (2005) proposed a method for estimating tyre contact parameters such as kinematic conditions (e.g. side-slip angle), dynamic properties (e.g. vertical load and contact area) and adhesion characteristics (e.g. surface roughness). Accelerometers are fixed to the liner of the tyre and sends data with radio signals to a central computing unit. To determine if this method would be able to discriminate between different roughness and adherence conditions, tests were performed on roads with different textures and wetness characteristics. The Root Mean Square (RMS) of the radial acceleration signal, was not able to give a unique roughness parameter for the different road tests, but does indicate to some extent a difference in the road surface. A speed independent roughness parameter is needed to correctly classify the road type.

According to **Marzbanrad, et al. (2004)**, vehicle suspension control can be improved by using a sensor to measure the road irregularities at some distance in front of the vehicle. Road roughness could be measured with an ultrasonic sensor. A simulation was done with a four degree-of-freedom (DOF) half-car model driving over a road with random irregularities. A method similar to the Kalman filter and Linear-Quadratic-Gaussian (LQG) controller was used to estimate the state variables. The mean square values of the body acceleration, tyre deflection, and suspension rattle spaces were used to optimize the suspension system. The performance of the control system improves, as the preview time is increased but only up to a certain point. The control system was improved even with a short preview time. The preview method can also lower power consumption of an active suspension unit.

Donahue (1998) used a fully active suspension system with preview control to improve ride comfort when driving at higher speeds over rough terrain. The system was implemented on a HMMWV military vehicle with commercially available hardware. Two types of range finding units were considered: Frequency Modulated Continuous Wave (FMCW) radar and a modulated infrared LED (Light Emitting Diode) optical sensor. The optical sensor detected small road irregularities better than the radar but the radar had a longer preview range. The radar sensors were mounted in

front of the vehicle. Trigonometric relations were used to extract the road profile in front of each tyre. The vehicle's heave, pitch and roll also affected the measurements and were adjusted using a modified Kalman filter. The data was then stored in a buffer, ready for the control system to use. The preview controller did not perform as well as was expected. Some possible causes for this were:

- Bad synchronization between the digital road data and the actual road.
- Compounded distance error when driving long distances.

Schurter and Roschke (2000) present an alternative for modelling a magnetorheological damper. Conventional modelling involves nonlinear differential equations that take a substantial amount of CPU time to solve. Takagi-Sugeno-Kang developed the Artificial Neuro-Fuzzy Inference System (ANFIS) and uses a hybrid learning algorithm for mapping input data to output data. The fuzzy model was trained using data obtained from solving the non-linear differential equations. It was shown that the ANFIS was able to accurately characterise the dynamic behaviour of the damper. It is stated that the fuzzy model execution is approximately 10 000 times faster than the mathematical model. Important steps in developing the fuzzy systems are the following:

- Collect enough training and checking data from the target model.
- Use ANFIS to create the fuzzy model that relates inputs to outputs.
- Validate the process by comparing outputs of the fuzzy model and the target model.

Advantages of Fuzzy logic over conventional arithmetic methods:

- The difficulties of modelling and analysing complex systems are reduced.
- Qualitative aspects of human experience can be incorporated in the mapping laws.

The US army developed an unmanned ground vehicle (**Sadhukhan, Moore and Collins, 2004**). Internal sensors and a Probabilistic Neural Network (PNN) are used to identify the terrain type. This aids the control system to navigate the vehicle autonomously. Vibration and wheel slip were identified as the main characteristics for discriminating between different terrain types. An ADAMS model and a miniature model were used to collect vertical acceleration data. The FFT of the data were used to classify the terrain using a pattern recognition algorithm. Three terrain types at four different speeds were very accurately identified. The algorithm was able to do real-time terrain classification and was computationally inexpensive. Future work will include wheel slip measurements that will increase the set of terrain types that can be classified. Table 1 and Table 2 summarises the results obtained from the literature study. Before any of these and other methods can be applied to the vehicle equipped with the $4S_4$, information about the system is needed in the

form of measurements from sensors, recorded under normal driving conditions. The next segment describes this in more detail.

Article	Test Vehicle	Test method	Road surface	Objective	Algorithm	Results	Conclusion
AL-Holou, N., Joo, D. S., Shaout, A., 1995, The development of Fuzzy Logic based controller for semi-active suspension system	Quarter-car model with semi-active suspension	Simulation	Sinusoidal	To improve ride quality and road handling using a fuzzy logic controller.	Fuzzy Logic controller (Input: Body velocity, Suspension velocity)	The fuzzy logic controller improves the body acceleration, however it has a greater tyre deflection than the skyhook controller.	A fuzzy logic adaptive control method will improve the tyre deflection which changes the input and output membership functions iteratively.
Hashiyama, T., Furuhashi, T., Uchikawa, Y., 1995, Design of Fuzzy controllers for semi-active suspension generated through the Genetic Algorithm	Quarter-car model with semi-active suspension	Simulation	Unknown	An alternative method for designing fuzzy controllers using genetic algorithms.	Fuzzy Logic controller designed using genetic algorithms (Input: Displacement, Velocity, Acceleration, Jerk)	The performance index showed that the method is feasible.	The design of the fuzzy controller can be automated by using genetic algorithms.
Tyan, C., Wang, P. P., Bahler, D. R., 1995, An application on intelligent control using neural network and Fuzzy Logic	Magnetic Levitation vehicle	Simulation	Train track	To do fault detection on a dynamic system and take action to correct it.	Neural network & Fuzzy logic	It was shown that the neural network classifier accomplishes a fairly accurate (93.85%) classification when track disturbance irregularities are present.	This paper demonstrated the concept of a "diagnostic doctor" for dynamic systems.
Rao, M.V.C. & Prahlad, V., 1997, A tuneable Fuzzy Logic controller for vehicle-active suspension systems	Quarter-car model with active suspension	Simulation	Pseudo-random road profile	To develop a tuneable fuzzy logic controller for an active suspension system.	Fuzzy Logic controller (Input: Suspension displacement and velocity)	It was found to bring down the suspension acceleration and displacement to a reference level.	The controller is able to take care of wider variations in the plant parameters.
Nagai, M., Moran, A., Tamura, Y. & Koizumi, S., 1997, Identification and control of nonlinear active pneumatic suspension for railway vehicles, using Neural Networks	Railway vehicles with active pneumatic suspension	A suspension system, with air spring and pneumatic actuator	Random disturbances (Railway)	To analyze the performance of neural networks for the identification and optimal control of active pneumatic suspensions of high-speed railway vehicles.	Neural Networks (Inputs: Pressure, acceleration, displacement)	The neuro-control provided better performance and energy efficiency than the linear quadratic control in the low frequency range	Neural networks can identify the nonlinear dynamic properties of a pneumatic suspension.
Nicolas, C.F., Landaluz, J., Castrillo, E., Gaston, M., Reyero, R., 1997, Application of Fuzzy Logic control to the design of semi-active suspension systems	Quarter-car model, Renault R-11, SEAT-VW Cordoba GTI, Land Rover Discovery	Simulation and real vehicle tests	Normal road and step input	To implement fuzzy logic control strategies for semi-active suspension systems by using driver input data and vehicle dynamics data.	Fuzzy Logic controller	Minimal difference between Fuzzy and Skyhook, but Fuzzy uses less sensors. Fuzzy also has lower oscillations and settling time than soft susp. and greater comfort than hard susp.	Fuzzy Logic is well suited for the highly non-lin., difficult to simulate, subjective control, compromise between handling and comfort. Has excellent performance with a low cost sensor system.
Yoshimura, T., Nakaminami, K., Kuriimoto, M., Hino, J., 1998, Active suspension of passenger cars using linear and fuzzy-logic controls	Half-car model with active suspension	Simulation	Irregular excitation from road	To Investigate the effect of Linear and/or Fuzzy Logic control on the active suspension.	Linear and Fuzzy-Logic controls (Lin. input: Vertical accelerations, F.L. input: Vertical and rotary velocities and displacements)	Linear and Fuzzy Logic controls improve vertical acceleration, velocity and displacements compared to passive suspension or Linear control.	Considering the rotary effect gives a slight improvement in the control. A combination of Linear and Fuzzy Logic control gives the best suspension performance
Kyrtsos, T., 1998, Roll-over detector for vehicles, U.S. Patent: 6225894	Commercial trucks	Real vehicle tests	-	To determine a method for detecting a roll-over condition	-	-	Rollover can be detected by analysing the forces acting on the vehicle. The forces are calculated from measured accelerations.
Donahue, M. D., 1998, Implementation of an active suspension, preview controller for improved ride comfort	Quarter-car model and actual vehicle	Simulations and vehicle tests	Rough terrain	To improve ride comfort for a vehicle with fully active suspension using preview control.	Preview control and Kalman filtering	The predictive controller with preview did not perform as well as was expected.	The preview data and the actual road should be synchronised.
Wu, Y., Xu, B., 1999, Study on the damping Fuzzy control of semi-active suspension	7 DOF vehicle ride model with semi-active suspension	Simulation	Random road excitation	Parameter identification of Fuzzy controllers with a local improvement Genetic Algorithm	Damping Fuzzy controller with Genetic Algorithm	The ride performance index is decreased with increase in genetic generations	With the proposed fitness function and the GA method, the optimal fuzzy controller parameters can be obtained.
Schurter, K. C. & Roschke, P.N., 2000, Fuzzy modelling of a Magnetorheological damper using ANFIS	(Magnetorheological Damper)	Simulation	Gaussian random noise	To model a Magnetorheological damper using ANFIS.	ANFIS	A multiple input/single output fuzzy inference system was created to characterise the damper.	The ANFIS model is considerably faster to analyse than the mathematical model.
Foda, S.G., 2001, Neuro-Fuzzy control of a semi-active car suspension system	Quarter-car model with band-limiting semi-active suspension	Simulation	Step input, Pulse input, Humps	To design a Neuro-Fuzzy controller for a semi-active suspension system.	Neuro-Fuzzy controller (Language: MATLAB SIMULINK and Fuzzy Toolbox)	Vertical accelerations and displacements are well damped.	The controller enhanced ride performance by damping the body ride and suspension work space responses for different road profiles.
Pasquier, M., Quek, C., Toh, M., 2001, Fuzzylot: a novel self-organising fuzzy-neural rule-based pilot system for automated vehicles	Simulator with steering wheel and pedals	Real-time simulation with human driver input and autopilot output	Virtual road with right and left bends	To do research on intelligent vehicle technologies for routing, navigation and control.	Self-organising Fuzzy rule-based system	Simulator data is fed into a fuzzy neural network, which clusters the input, identifies fuzzy variables and extracts the fuzzy rule-base.	The fuzzy rule-base emulates the human driver and can be used to successfully control the vehicle on the same route.
Trent, V. and Greene, M., 2002, A Genetic Algorithms predictor for vehicular rollover	Simulation model based on a Jeep Cherokee (1997)	Simulation of constant radius test	Flat	To predict vehicle rollover with Genetic Algorithm Predictor.	Genetic Algorithm Predictor (GAP), (Input: Tyre deflection)	Is able to predict rollover 0.4s in advance.	Gives enough time to activate active stability systems (differential braking, adjustable suspension)
Iagnemma, K., Dubowsky, S., 2002, Terrain estimation for high-speed rough-terrain autonomous vehicle navigation	Unmanned Ground Vehicle	Simulation and wheel tests	Rough: Vegetation, loose soil, packed soil	To identify and classify terrain	Motion planning control strategy	The algorithm produced reasonable estimations of cohesion and internal friction angle.	The terrain parameters were estimated with good accuracy using limited computational resources.
Iagnemma, K., Brooks, C. & Dubowsky, S., 2004, Visual, tactile, and vibration-based terrain analysis for planetary rovers	Planetary Rover	Wheel test	Gravel and sand	To identify and classify terrain	Principal Component Analysis for terrain classification	This method was able to discriminate between two different terrain types.	The results showed that this type of sensing could be used for quick, efficient and robust classification of terrain.

Table 1: Literature review summary (1)

Article	Test Vehicle	Test method	Road surface	Objective	Algorithm	Results	Conclusion
Marzbanrad, J., Ahmadi, G., Zohoor, H., Hojjat, Y., 2004, Stochastic optimal preview control of a vehicle suspension	Half-car model with passive or active suspension	Simulation	Random road excitation	To improve the suspension control of a vehicle by using a sensor to measure road irregularities some distance in front of the vehicle.	Customised Kalman filter & Linear-Quadratic-Gaussian controller	Acceleration responses are decreased using the optimal preview control. The control system improves with the increase of preview time.	The performance index and the mean-square responses are reduced when using the preview control over randomly irregular roads.
Sadhukhan, D., Moore, C., Collins, E., 2004, Terrain estimation using internal sensors	Unmanned Ground Vehicle, ADAMS model	Simulation and vehicle test	Grass, gravel, sand	To enable the UGV to autonomously navigate over various terrain types at different speeds.	Probabilistic Neural Network	The FFT of the vertical acceleration data were used to train a pattern recognition algorithm to classify the terrain.	The algorithm identified the three terrain types accurately at four different speeds.
Tsunashima, H., Murakami, M. & Miyata, J., 2005, Vehicle and road state estimation using interacting multiple model approach	Bicycle model	Simulation	Road with various friction coefficients	To determine the friction coefficients to achieve effective control	Interacting Multiple Model, Extended Kalman Filter	The friction coefficients were accurately estimated by the IMM method	The IMM estimator correctly determined the vehicle and road state simultaneously from lateral accelerations and yaw rate measurements.
Braghin, F., Brusarosco, M., Cheli, F., Cigada, A., Manzoni, S., Mancosu, F., 2005, Measurement of contact forces and patch features by means of accelerometers fixed inside the tire to improve future car active control	Tyre testing apparatus and car	Wheel test and vehicle test	Roads with different roughness and wetness conditions	To determine tyre contact forces and contact patch features.	Terrain classification from RMS radial acceleration	Side slip angle and vertical contact forces were accurately estimated. Surface roughness does not give good results.	Currently trying to find a less disperse and speed independent surface roughness parameter.
Els, P.S., 2006, The ride comfort vs. handling compromise for off road vehicles	Land Rover Defender 110 and ADAMS simulation model	Simulation and vehicle tests	Rough and smooth test tracks	Improve handling capabilities as well as ride comfort	Running RMS lateral acceleration vs. vertical acceleration for decision control	Handling capabilities were improved and ride comfort were maintained over rough terrain	Handling manoeuvres can be detected using RRMS lateral acceleration but further optimization is required

Table 2: Literature review summary (2)

2.5 Conclusions from literature review

Many of the proposed strategies are only tested on simulation models and not validated with real vehicles. Most of the literature focussed on obtaining better ride comfort and not trying to improve the vehicle's handling capability. There was not much literature found on terrain classification and only modest success of a true classifier was discovered. Neural Networks and Fuzzy logic were the most common methods that were used for control. Vehicle body accelerations, velocities and suspension displacements were regularly used as input signals to the control system.

From the literature it was concluded that the following possibilities should be investigated further:

- Terrain classification
- Neural Networks
- Fuzzy logic
- RRMS accelerations
- Probability statistics

2.6 Data recording and processing

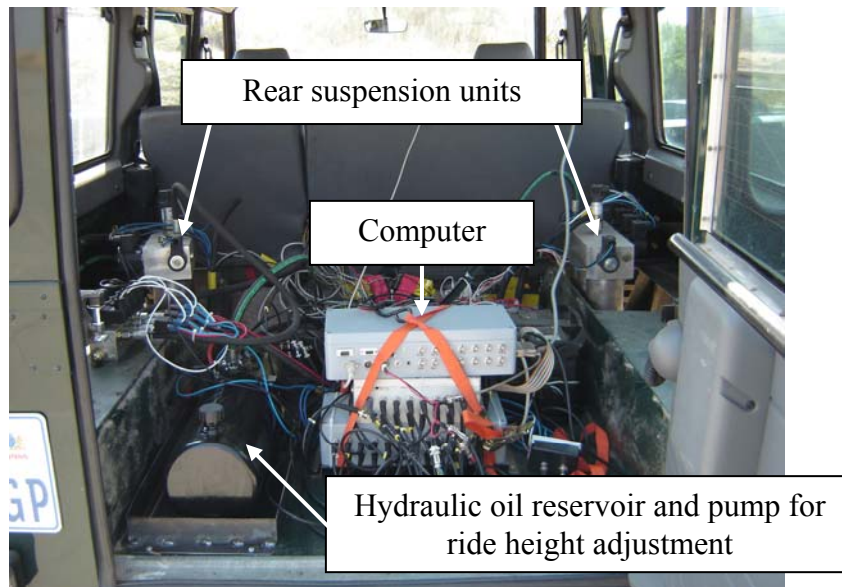


Figure 11: Electronic and hydro-pneumatic components

A PC104 form factor computer (**Ampro CoreModule 420**, www.ampro.com) computer as well as an input/output board (**Diamond-MM-AT**, www.diamondsystems.com) was used to record various time dependant data (see Figure 11). Programs (**Els, 2006a**) written in Turbo Pascal were used in a real-time operating system (MS-DOS) to log all the data. The following parameters were measured because they sufficiently describe the kinematic behaviour of the vehicle:

Vertical acceleration [g]

Lateral acceleration [g]

Displacement of each suspension unit [mm]

Yaw velocity [$^{\circ}/s$]

Roll velocity [$^{\circ}/s$]

Kingpin angle [$^{\circ}$]

Vehicle speed [km/h]

Vertical accelerations, suspension unit displacements, kingpin angle and vehicle speed can be used to determine the level of ride comfort, while lateral acceleration, yaw and roll velocity, kingpin angle and vehicle speed can be used to establish the degree of handling manoeuvres that the vehicle is experiencing.

All the measurements are stored as voltage readings in a binary file. The main reasons are for simplicity, speed and using the hard drive space more efficiently. It also has the advantage that if a calibration error occurred, it could easily be changed without repeating the test. These files were later converted to matrices using programs written in MATLAB (www.mathworks.com). The raw data was then multiplied with the correct calibration factors to obtain practical measurements. Unfortunately the data still contained signal drift and noise that had to be addressed.

The measured data contains many imperfections. Because the sensors are mounted on the vehicle body, it is clear that the engine vibration has a significant effect on the measurements at higher frequencies ($+20 \text{ Hz}$). In post-processing, filters with different cut-off frequencies were used to reduce unwanted noise on the signals. The best results were found with an ideal 3 Hz low-pass filter. Another problem was determining when the sensors were at their zero values. The best way of reducing this problem would be to start recording the data when the vehicle is stationary and horizontal. However in some tests the vehicle was already in motion before the recording of the data started. Adding to this problem was the fact that some of the sensors are sensitive to drift. This means that the signal has relatively high amplitude and low frequency content for example from temperature fluctuations. The mean was subtracted from signals that had a constant mean value throughout the duration of the test for example vertical acceleration. For signals such as the lateral acceleration and the suspension unit displacements a different strategy was used. The maximum of a histogram from these measurements indicated the position where the signal spent most of its time. For example, the section before and after the Double lane change is performed is longer than the manoeuvre itself. These sections are displayed as a peak on the histogram of that particular signal and represent the zero values of these signals. Another method similar to this would be to subtract the mean of a section from the whole signal where it is known to be zero.

Throughout the text the colour code in Table 3 is used, unless specified otherwise. Figure 12 shows all channels that were recorded on all the test tracks.

Belgian Paving (BLG):	Green
Double Lane Change (DLC):	Blue
Ride and Handling Track (RHT):	Red
City Traffic (CTY):	Magenta
Off-Road Track (ORT):	Yellow

Table 3: Colour code

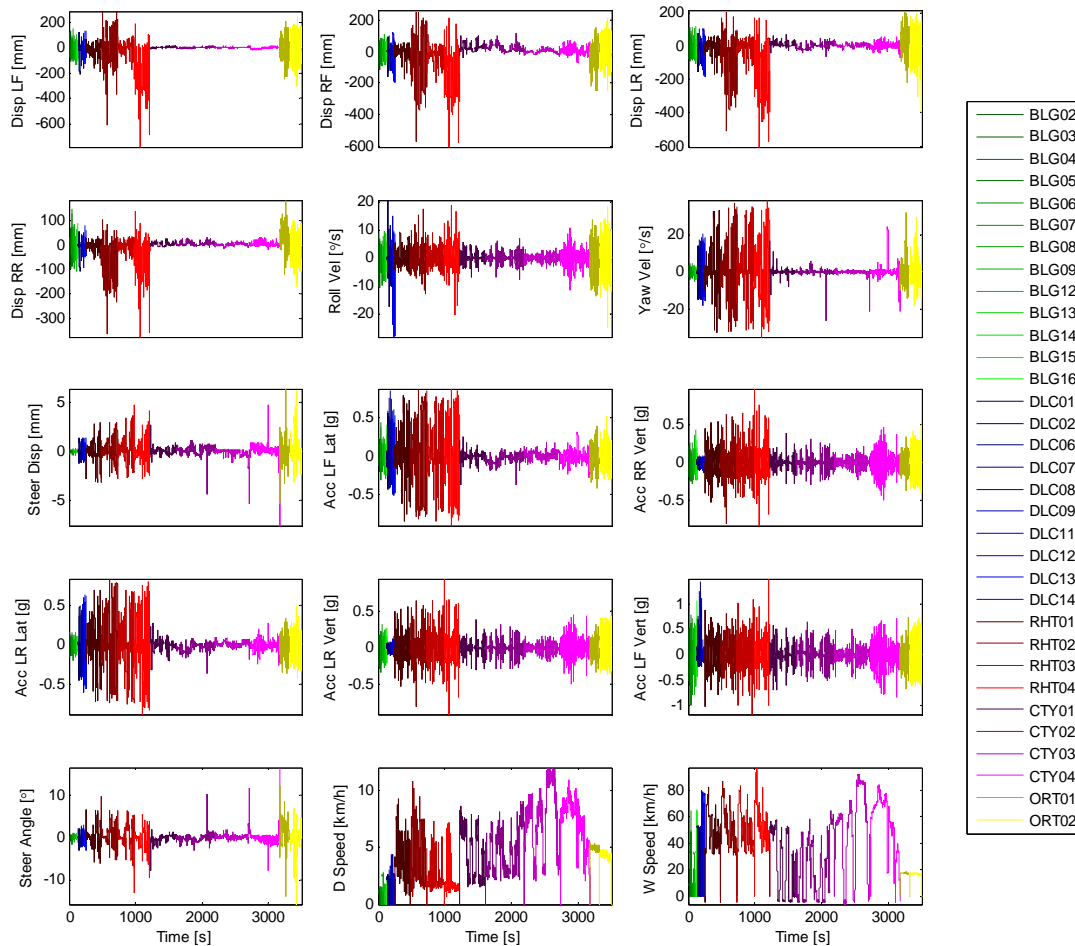


Figure 12: Recorded data of all tests

The following information was recorded:

Channels 1 to 4 contain the displacement of each suspension strut.

- Suspension displacement left front (Disp LF) [mm]
- Suspension displacement right front (Disp RF) [mm]
- Suspension displacement left rear (Disp LR) [mm]
- Suspension displacement right rear (Disp RR) [mm]

Gyros were used to obtain the vehicle's roll and yaw velocities

- Body roll velocity (Roll Vel) [$^{\circ}/s$]
- Body yaw velocity (Yaw Vel) [$^{\circ}/s$]

A cord displacement meter was attached to the vehicle's steering arm. However this did not work as well as kingpin angle measurement.

- Steering displacement (Steer Disp) [mm]

Three tri-axle accelerometers were used to obtain the lateral and vertical accelerations of the vehicle body.

- Body lateral acceleration left front (Acc LF Lat) [g]

- Body vertical acceleration right rear (Acc RR Vert) [g]
- Body lateral acceleration left rear (Acc LR Lat) [g]
- Body vertical acceleration left rear (Acc LR Vert) [g]
- Body vertical acceleration left front (Acc LF Vert) [g]

A rotational potentiometer was directly attached to the vehicle's kingpin to measure the turning angle of the wheel.

- Kingpin angle on left front wheel (Steer Angle) [°]

Optical tachometers on the driveshaft and the left rear wheel were used to measure the speed of the vehicle. Once again the wheel speed did not measure as well as the driveshaft speed.

- Vehicle speed measured from left rear wheel (W Speed) [km/h]
- Vehicle speed measured from the driveshaft (D Speed) [km/h]

A graphic user interface (GUI) was developed to quickly view recorded data to make sure that all the sensors worked and all the channels were reading correctly. This was used to check certain statistical properties of the data and was also able to filter out the unwanted frequency content.

Figure 13 shows a picture of the GUI with raw and filtered lateral acceleration data.

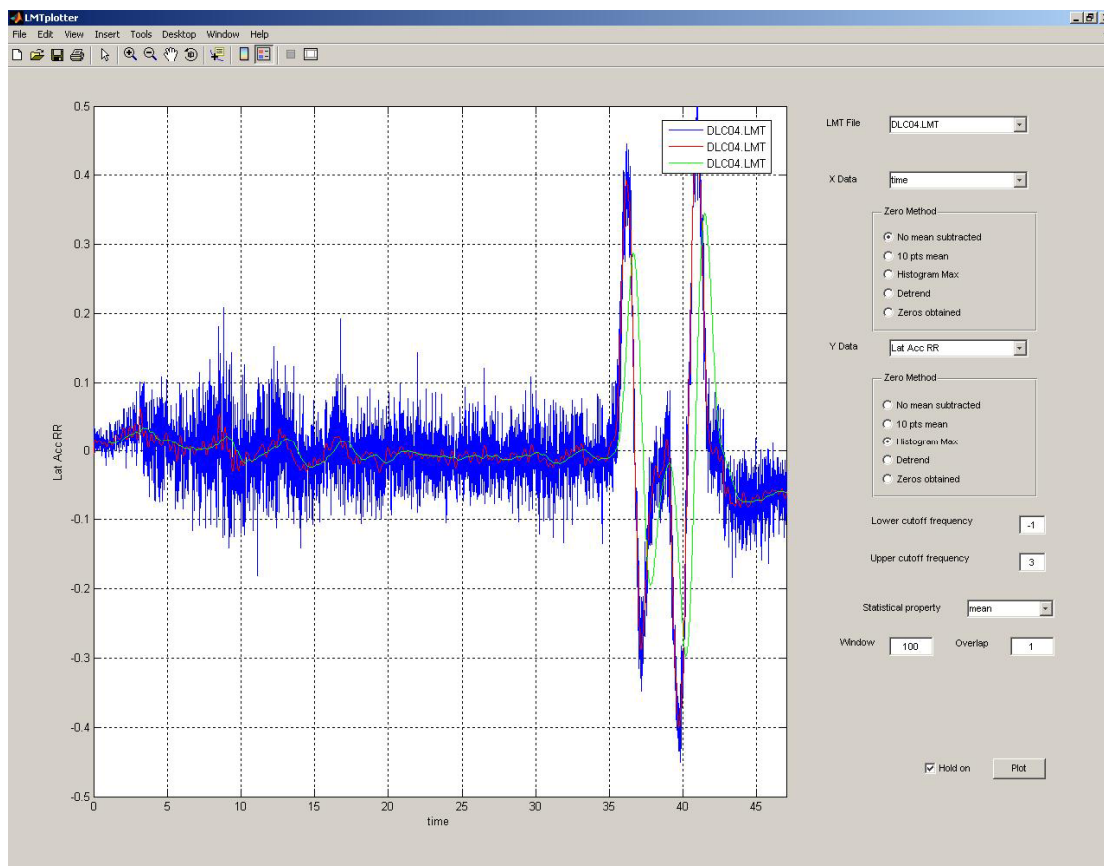


Figure 13: GUI plotter

Filtering the data was an important step in the process. Two techniques were used and are discussed in the next section.

2.7 Filtering

Electronic signals contain noise and it is sometimes necessary to reduce the high frequency content to be able to analyse the data properly. This is done by filtering out the unwanted frequencies. There are mainly two ways of digitally filtering discretized data namely: Frequency domain and time domain filtering. Another option is analog filtering and is done before sampling takes place using various electronic components.

Frequency domain filtering is done by first calculating the Fast Fourier Transform (FFT) of a signal. Then a weighting curve is used to set the amplitude of the unwanted frequencies equal to zero, after which the Inverse Fast Fourier Transform (IFFT) is calculated. This is an ideal filter that changes the amplitude of the signal at different frequencies. This cannot be done in real time and will therefore have a delay.

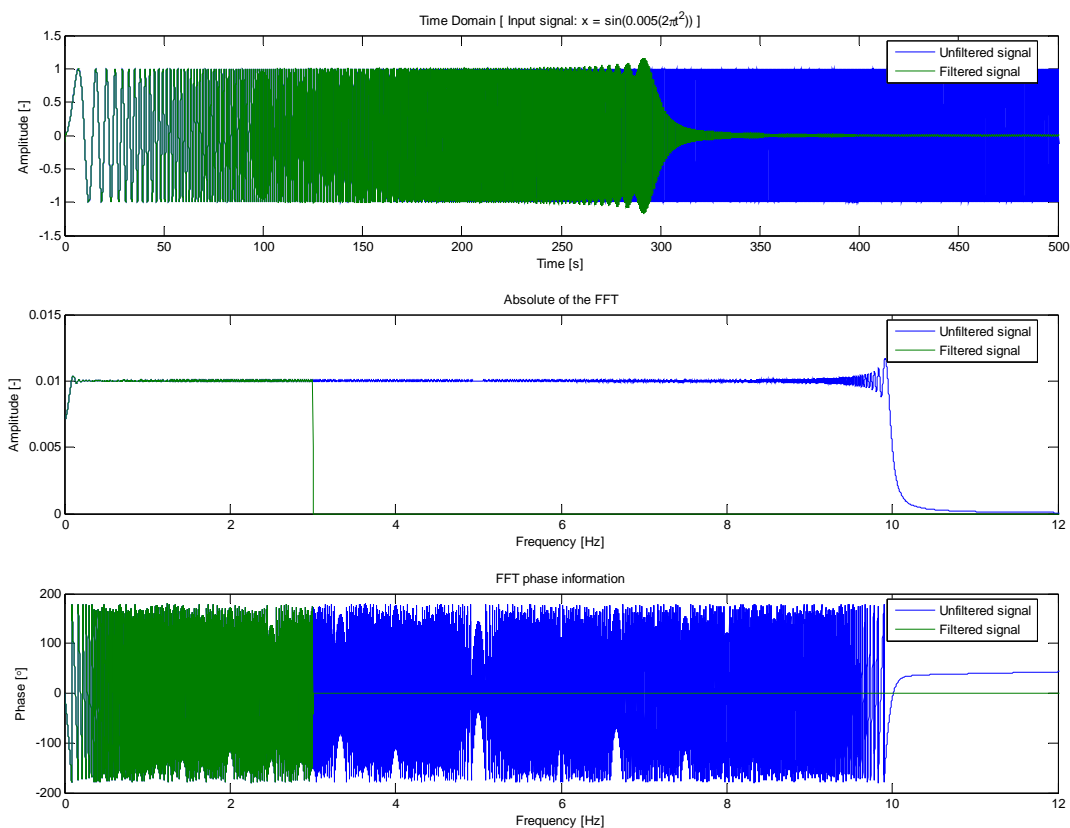


Figure 14: Frequency domain filter

The advantage of frequency based filtering over time domain filtering is that very specific frequencies can be totally eliminated and there is no phase lags as a result of the ideal filter. The disadvantage of this technique is that a large amount of data points are needed to calculate an acceptable FFT that contains enough information to successfully filter out the unwanted frequency content. The calculation is computationally intensive and takes a relatively long time to calculate. Figure 14 shows an unfiltered chirp signal and the same signal after a 3 Hz ideal frequency domain low-pass filter was applied to it. Notice the sharp cut-off at 3 Hz on the FFT plots.

Time domain filtering can be calculated in real-time as each data point is received. An example of this type of filter is a Butterworth Infinite Impulse Response (IIR) filter. The following equation is used to calculate the next point in the filtered signal:

$$y_n = \frac{1}{a_1} [b_1 x_n + b_2 x_{n-1} + \dots + b_{N+1} x_{n-N} - a_2 y_{n-1} - \dots - a_{N+1} y_{n-N}] \quad \text{Eq. 1}$$

Where y is the filtered signal and x is the unfiltered signal

Variable n is a counter and $2N+1$ is the number of terms that is used by the filter

Vectors, a and b , are predetermined constants from the Butterworth MATLAB (www.mathworks.com) functions: *buttord.m* and *butter.m*. These 26 coefficients are shown in Table 4.

#	a [x 100]	b [x 1E-9]
1	0.010000	0.000372
2	-0.105028	0.004466
3	0.506414	0.024564
4	-1.482242	0.081878
5	2.932981	0.184226
6	-4.133225	0.294762
7	4.253322	0.343889
8	-3.220241	0.294762
9	1.780215	0.184226
10	-0.700768	0.081878
11	0.186443	0.024564
12	-0.030101	0.004466
13	0.002230	0.000372

Table 4: Butterworth IIR filter coefficients

The same signal as in Figure 14 was filtered using a 3 Hz low-pass Butterworth filter and is shown in Figure 15. The absolute of the FFT shows that the correct frequencies are being filtered out but does not have such a sharp cut-off frequency as the previous filter did. Unfortunately the filter also produces a phase lag, which means that the filtered signal is delayed with respect to the raw data.

The conclusion can now be made that both these filtering methods result in a delay of the actual measured signal.

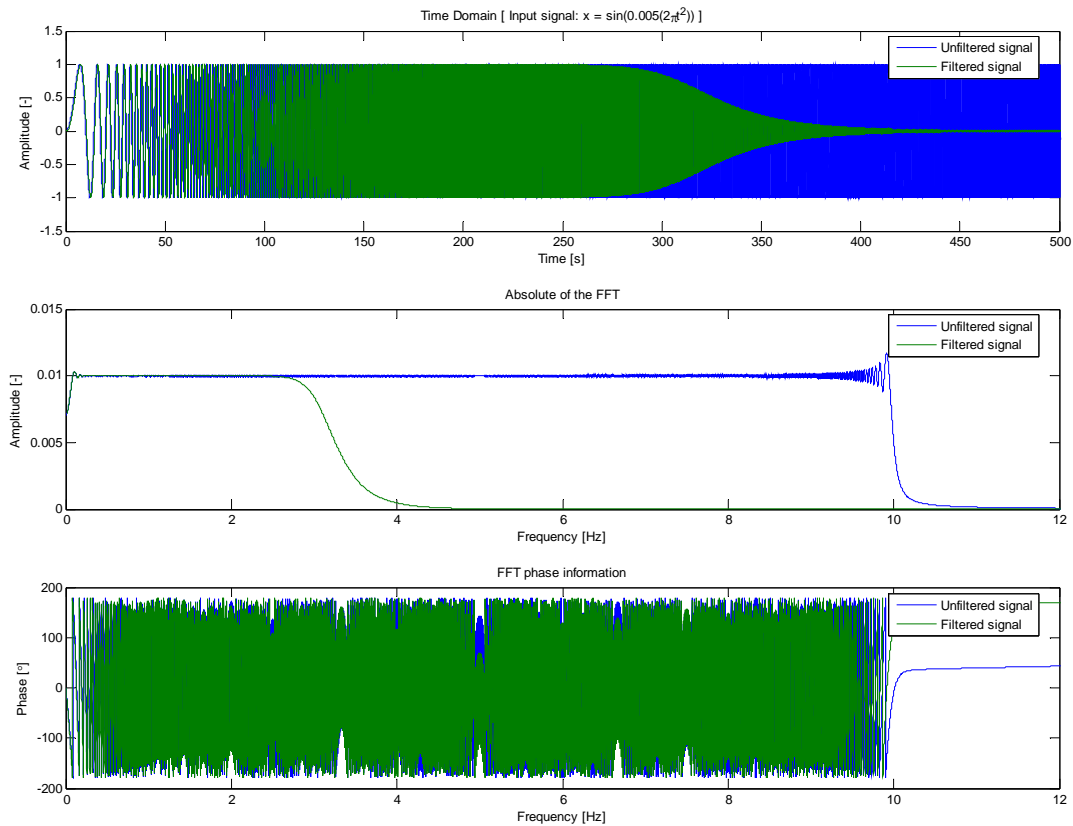


Figure 15: Time domain filter

2.8 Background conclusion

The data obtained from the measurements were processed using different methodologies. There were two main objectives that needed to be addressed: terrain classification and the ride comfort vs. handling switching strategy. The literature survey showed that very little work has been done to solve the ride comfort vs. handling decision process. The vehicle that was used in this study is equipped with a computer that is able to receive and store measured data from sensors and perform basic control strategies for switching the hydraulic and pneumatic valves. This enables the vehicle to be in a ride comfort mode over relative rough terrain and in a handling mode when severe manoeuvres are being performed. Five test tracks were used to represent the typical terrain and driving styles that are normally used with a SUV. Chapter 3 will focus on the terrain classification of these five test tracks. Chapter 4 investigates different methods for determining the ride comfort versus handling decision, while chapter 5 looks at experimental results obtained by some of these strategies. Finally conclusion are drawn in chapter 6 based on all the methods that were discussed in this thesis.

3 Terrain classification

Whether ride comfort or handling is required, mainly depends on the type of terrain that a vehicle is travelling over. Identification of the terrain can be used to improve the ride comfort by adjusting the suspension to soft springs and soft dampers. In this chapter several ideas for detecting or classifying the terrain that the vehicle is travelling on, are investigated. These ideas range from obstacle detection using “preview” sensors to Fuzzy logic, Self-Organising Maps (SOM’s) and statistical methods.

3.1 Obstacle Detection

Ride comfort is primarily influenced by the roughness of the terrain and the ability of the vehicle to attenuate these excitations. However if an "intelligent" vehicle can recognise the terrain or an obstacle that is in front of it, it could enhance the control needed for vehicle stabilising (e.g. semi-active suspension). A preview of the road ahead can be achieved by either “looking” (e.g. laser distance sensor) or “listening” (e.g. sonar) for a deviation to the norm of the road profile (**Iagnemma and Dubowsky, 2002**). Sonar can be influenced by ambient noise. On the other hand laser sensors are influenced by the colour of the terrain surface and lighting conditions. Laser sensors were chosen for the following proposal because of their simplicity, but the concept should work for any other non-contact distance measuring device.

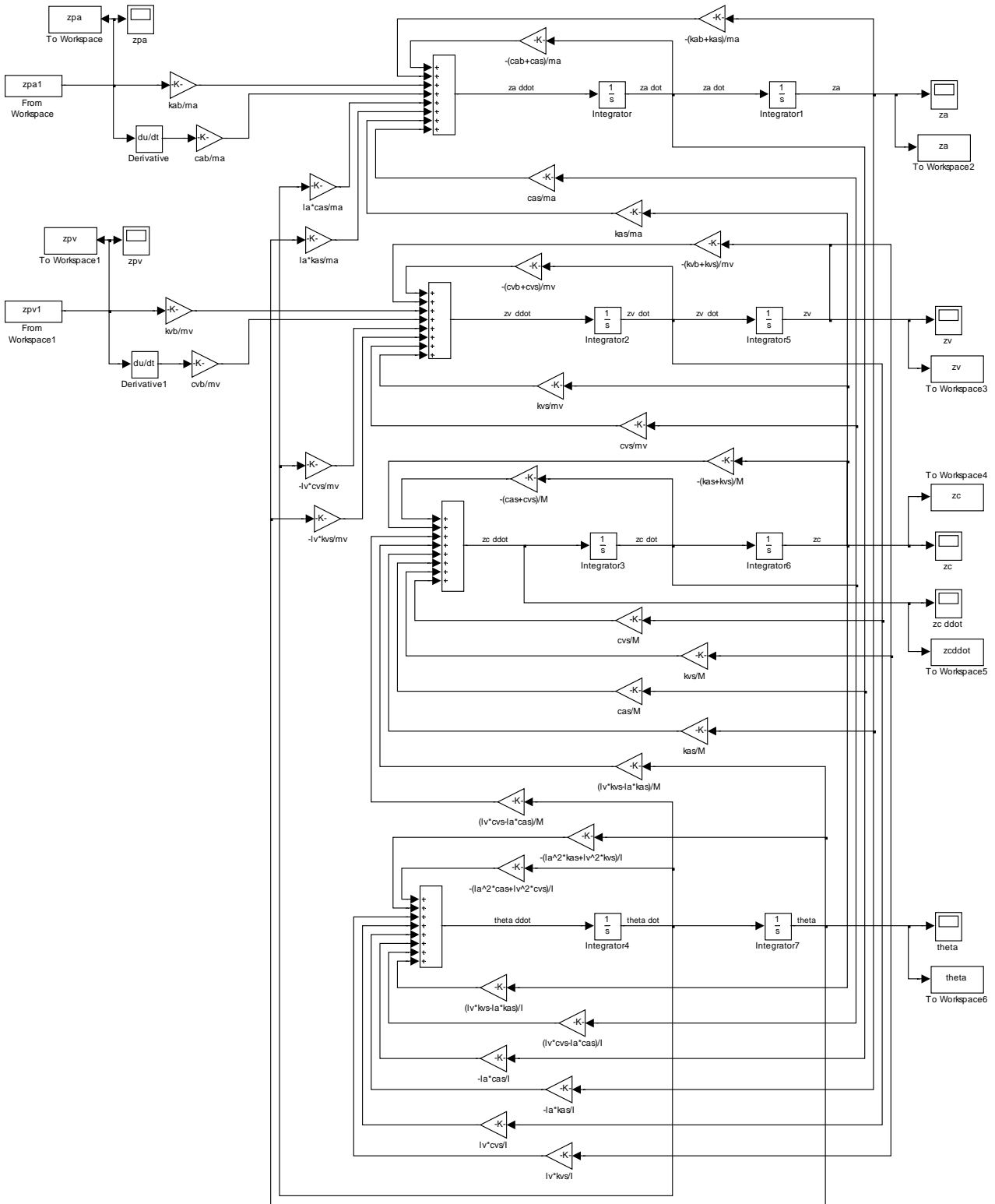


Figure 16: A four degree of freedom pitch plane vehicle model in Simulink

A four degree of freedom pitch plane vehicle model of the Land Rover test vehicle was built in Simulink (www.mathworks.com) as indicated in Figure 16. The four degrees of freedom are: vertical translation of the unsprung mass in the front (front wheels and axle) and the rear (rear wheels and axle), vertical translation and pitch rotation of the sprung mass (vehicle body).

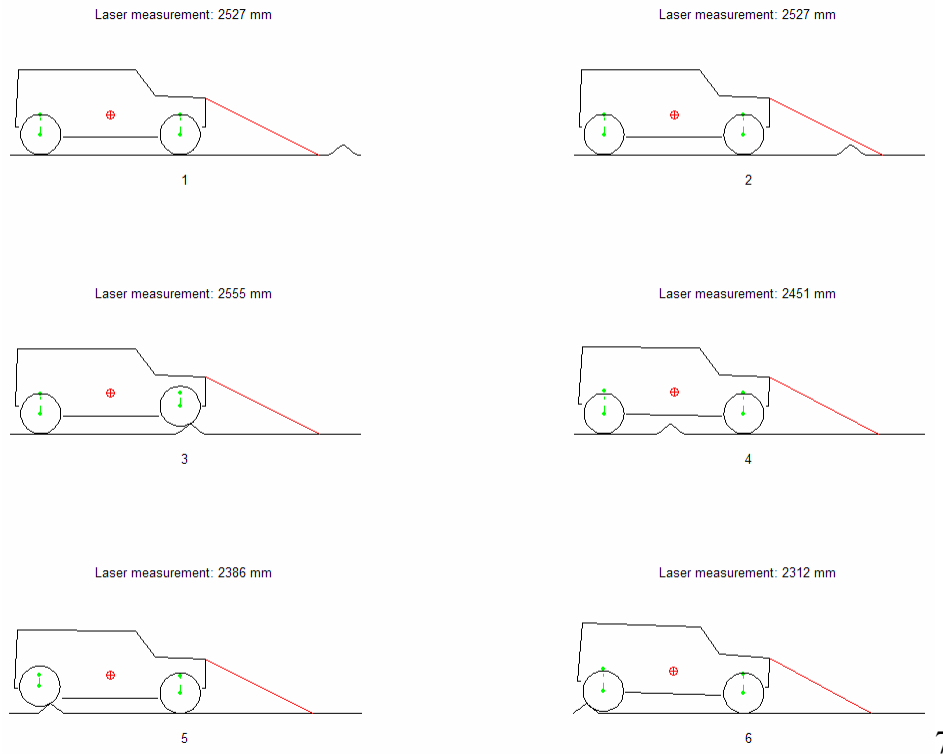


Figure 17: Detecting a triangular bump in the road using a laser distance meter

Any road profile at any speed can be simulated by this model. A Runge-Kutta solver with a fixed time step of 0.05 s was used to calculate the dynamics of this mass-spring-damper model. The model was not validated because it was only used to prove the concept of road preview. Figure 17 shows six frames of the vehicle model driving over a triangular bump in the road at 20 km/h . Preview information was obtained with two methods, one ignoring and another including the vehicle body pitch angle.

3.1.1 Method 1 (Not compensating for body pitch angle):

With reference to Figure 18, the following equations can be formulated.

$$\cos(\Theta_0) = \frac{z_i}{L_0 - l_i} = \frac{H_0}{L_0} \dots \text{Similar triangles} \quad \text{Eq. 2}$$

$$z_i = \frac{H_0(L_0 - l_i)}{L_0} \quad \text{Eq. 3}$$

Where

H_0 : Static height of laser sensor [m]

L_0 : Laser measurement on a flat surface [m]

l_i : Actual laser measurement [m]

z_i : Estimated profile height at time step i [m]

Θ_0 : Angle between laser and vertical [$^\circ$]

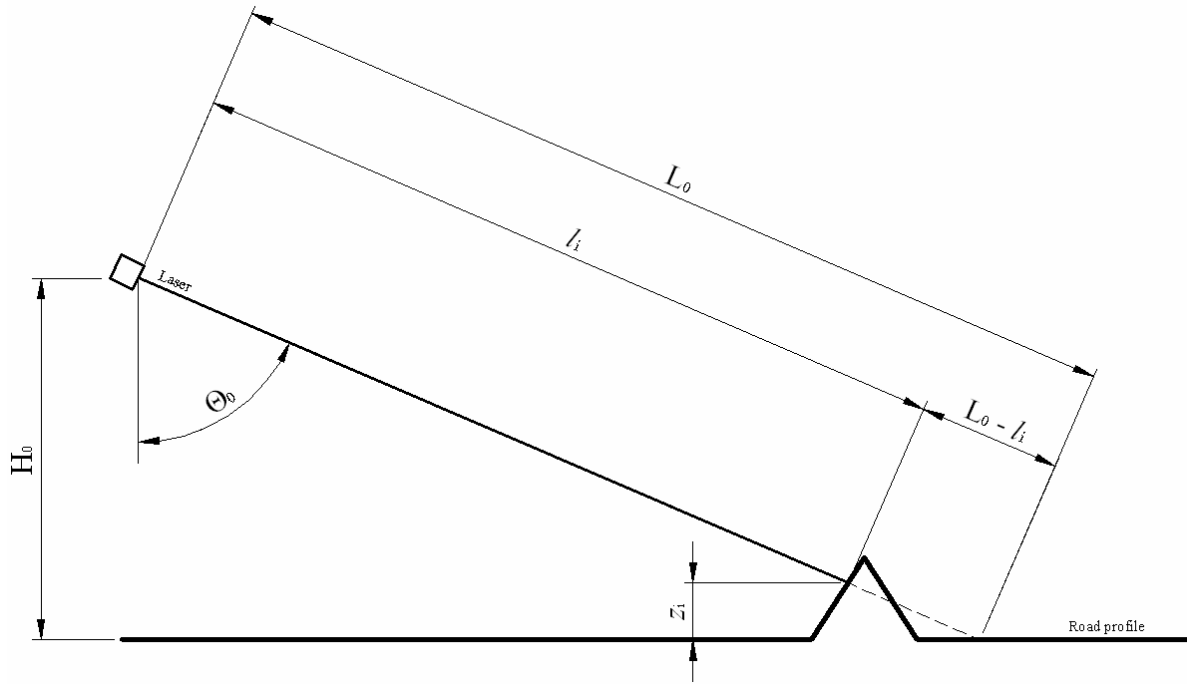


Figure 18: Method 1

3.1.2 Method 2 (Vehicle body pitch angle compensated for):

From Figure 19, the following equations can be formulated.

$$\cos(\Theta_0 + \theta_i) = \frac{z_i}{L_i - l_i} = \frac{H_i}{L_i} \dots \text{Similar triangles} \quad \text{Eq. 4}$$

$$z_i = \frac{H_i(L_i - l_i)}{L_i} \quad \text{Eq. 5}$$

Where

H_i : Static height of laser sensor + suspension deflection [m]

L_i : Laser measurement on a flat surface adjusted by the global pitch angle [m]

l_i : Actual laser measurement [m]

z_i : Estimated profile height at time step i [m]

θ_i : Global pitch rotation of vehicle [°]

Θ_0 : Angle between laser and vertical [°]

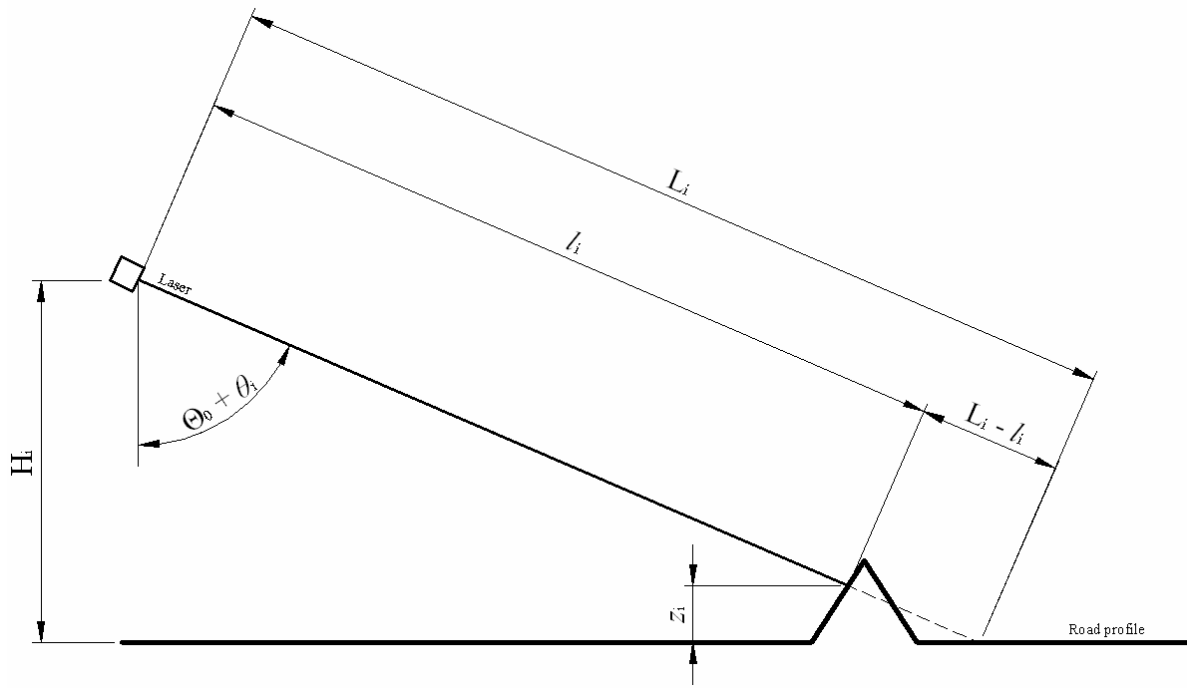


Figure 19: Method 2

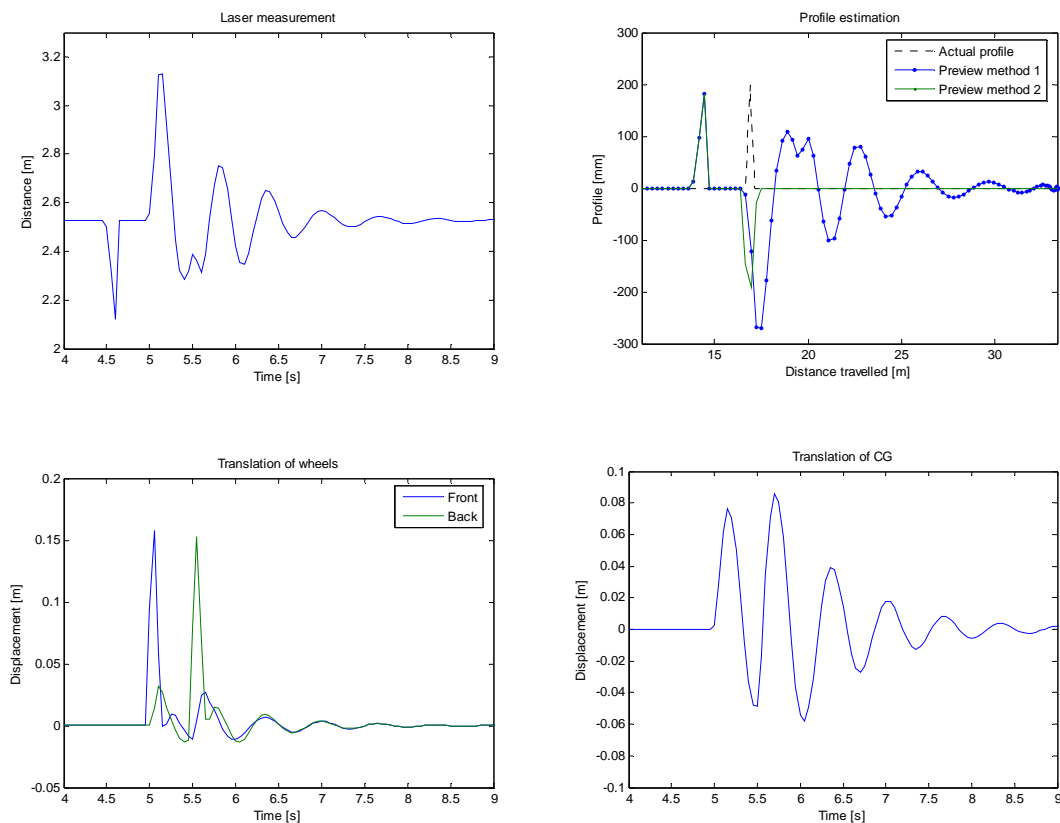


Figure 20: The measured parameters as well as the approximated road profile

Figure 20 indicates the results obtained from the implementation of the two simple profile preview methods using the same laser measurement. The top left graph in this figure gives the distance that was measured. The top right graph indicates the actual terrain profile, as well as the estimated

preview profile. The bottom two graphs show the vertical translation of the unsprung masses and the sprung mass respectively. Both methods detected the bump 0.5 s before the first wheel made contact with the obstacle. The preview time is directly related to the vehicle speed. The switching delay of the hydraulic and pneumatic valves for the semi-active suspension system is at worst 0.1 s. This would be equal to the preview time for the current setup at 100 km/h.

The first method oscillates after the vehicle travels over the bump. For the same reason the second method displays a ditch after the bump at about a distance of 17 m but does not have the oscillations of the first method. This method is more expensive because it requires determining the global pitch angle of the vehicle. The ditch that is displayed in the graph can also be eliminated if the global position of the laser sensor is known, but global positioning systems (GPS) are not that accurate yet. This is a simplified and ideal model that does not take the vehicle roll angle into consideration. It merely provides the control system for the semi-active suspension a split second preview of what the road profile will be.

This method had some similarities with the technology used for high speed profiling of roads to determine the road roughness. The next section explores the possibility of using the suspension displacements to determine the relative road roughness.

3.2 *Relative Roughness Indicator*

Road profiling systems are used to validate the calculated response of a mathematical vehicle model to the response of an actual vehicle. It is also used to measure the roughness of road surfaces. To ensure good quality roads, they must be built to a certain standard. The International Roughness Index (IRI) is a standardised method for computing the road roughness from measurements by most profilometers.

A quarter-car model is used to calculate the suspension deflection from the measured road input. The accumulated suspension motion is then divided by the distance travelled. The result is a dimensionless parameter (m/km) called the IRI. This index is linearly proportional to the roughness of the road. (<http://www.umtri.umich.edu>, 01/13/2005) The following equation (Eq. 6) was used to calculate the IRI (Sun, 2001).

$$IRI = \frac{1}{L} \int_0^T |\dot{x}_s(t)| dt \quad \text{Eq. 6}$$

Where

- L : Distance travelled [m]
- T : Total duration of measurement [s]
- t : time [s]
- \dot{x}_s : Vertical velocity measured by profilometer [m/s]

The relative roughness of the five test tracks used in the current study differ considerably. The proposed relative roughness indicator is based on the International Roughness Index (IRI), which is used to determine the quality of the road. Instead of using a quarter-car-model to calculate the wheel displacement, it is measured at each suspension unit. The total suspension motion is accumulated over a fixed travelled distance. Large displacements indicate a relatively rough terrain. When the vehicle travels over a specific terrain the soft suspension will also produce larger displacements than the hard suspension setting. The integration of the suspension motion, when the vehicle is standing still for a long period of time, can cause large accumulation errors as can be seen in the first graph of Figure 21. It is clearly visible in the city traffic sections, where stopping at traffic lights caused the high peaks with the IRI calculation. However the exact roughness index is not of importance, only the relative roughness between the different terrains is essential. The second graph in Figure 21 shows the Relative Roughness Indicator (RRI). This was achieved by dividing the calculated roughness by the amount of time that it took to complete the specific distance that needed to be travelled. The RRI was calculated every 5 m from the past 10 m that was travelled. The average displacement of the four suspension units was used in Eq. 7 to calculate the RRI.

$$RRI = \frac{\left[\frac{1}{L} \int_{t_0}^{t_L} \left(\sum_{i=1}^4 \dot{x}_i(t) \right) / 4 dt \right]}{(t_L - t_0)} \quad \text{Eq. 7}$$

Where

- L : Distance travelled [m]
- t_0 : Start time [s]
- t_L : Time after fixed distance was travelled [s]
- t : time [s]
- i : Suspension unit i , with $i = [1, 2, 3, 4]$
- \dot{x}_i : Vertical velocity of each suspension unit i [m/s]

This means that when the vehicle is not moving, it can not be experiencing rough terrain and has a low roughness value regardless of the suspension motion. The difference between the ride comfort and the handling tests are obvious. It is also interesting to note that the ride and handling track (red) has rough sections. The first and third Ride and Handling Track (RHT) tests were done with the hard suspension setting. The second and fourth Ride and Handling Track (RHT) test was done with a soft suspension and switching only to the handling mode where sharp cornering took place (RRMS strategy, **Els, 2006a**). These two tests have a higher RRI because of the softer suspension setting that were enabled most of the time. The third graph in Figure 21 shows the time history of the Running Root Mean Square (RRMS) of the vehicle's vertical acceleration, which is commonly used to quantify ride comfort. The RRI is a much better indication of terrain roughness than the IRI and the vertical acceleration. From the evidence presented in this paragraph, it is quite clear that the relative displacements of the suspension units were unique for the different terrain types. The following section focuses on the measured accelerations that are perpendicular to the driving direction (lateral and vertical acceleration).

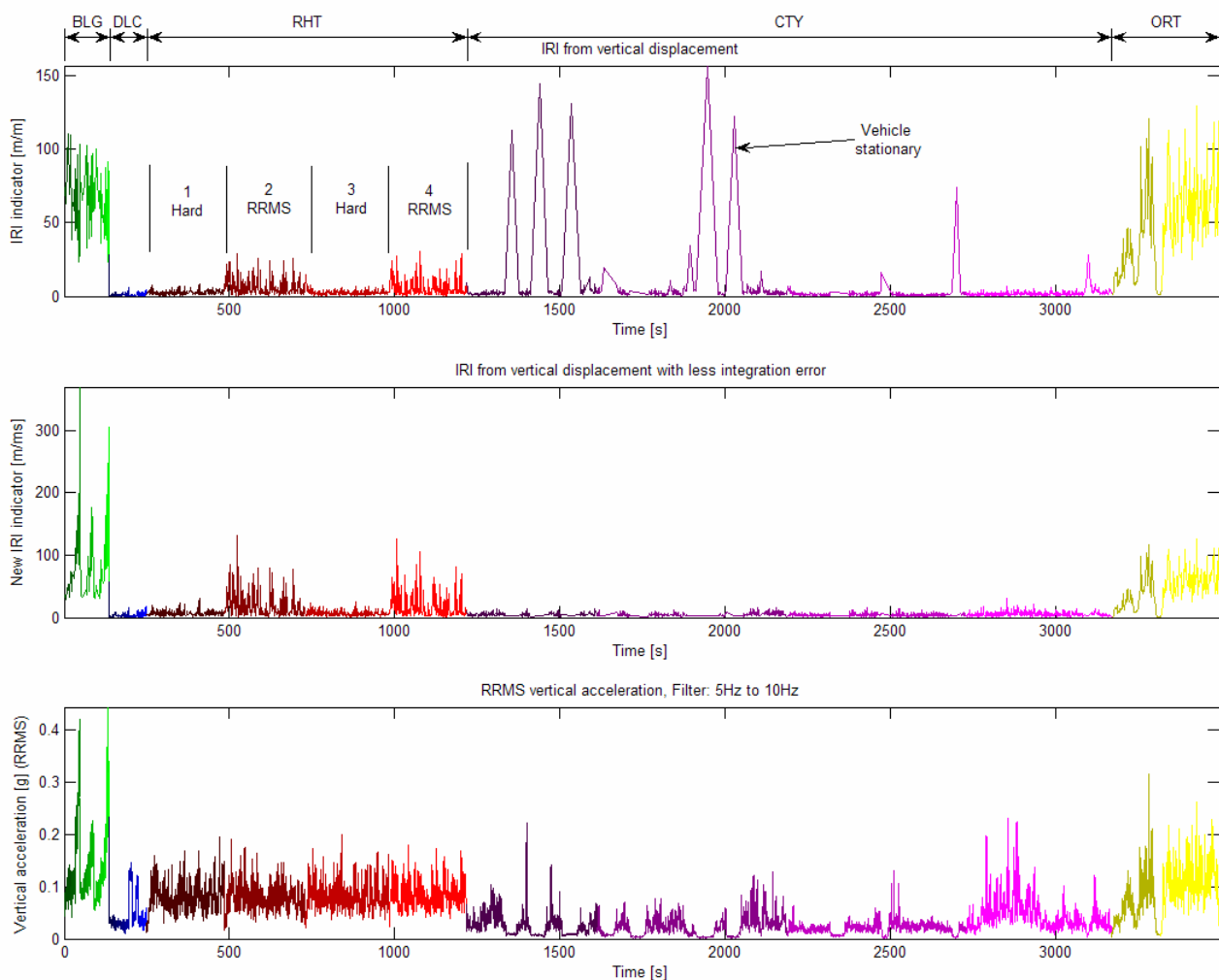


Figure 21: Comparing the Relative Roughness Indicator (RRI) with the RRMS vertical acceleration

3.3 Histogram of acceleration data

A histogram shows the range and distribution of data. This is done by grouping the data according to their numeric range into intervals called bins (MATLAB, www.mathworks.com). The number of data points encountered in each bin is counted. The amount in each bin will give an indication of the time that the signal spent in a certain range.

Figure 22 displays six histograms of lateral vs. vertical acceleration data. Because the amount of data differed for each test the histograms were normalised by dividing with the maximum value. It is assumed that the shape of each surface will stay more or less the same with larger data sets. The grey surface shows the histogram of all the tests, while the rest are colour coded according to Table 3. Contour plots of these surfaces were produced and can be seen in Figure 23. The total area inside the outer most contour line represents 90% of all the data. The area between each contour line represents 10% of the data. Ellipses were fitted around each contour plot to approximate the maximum range of each test.

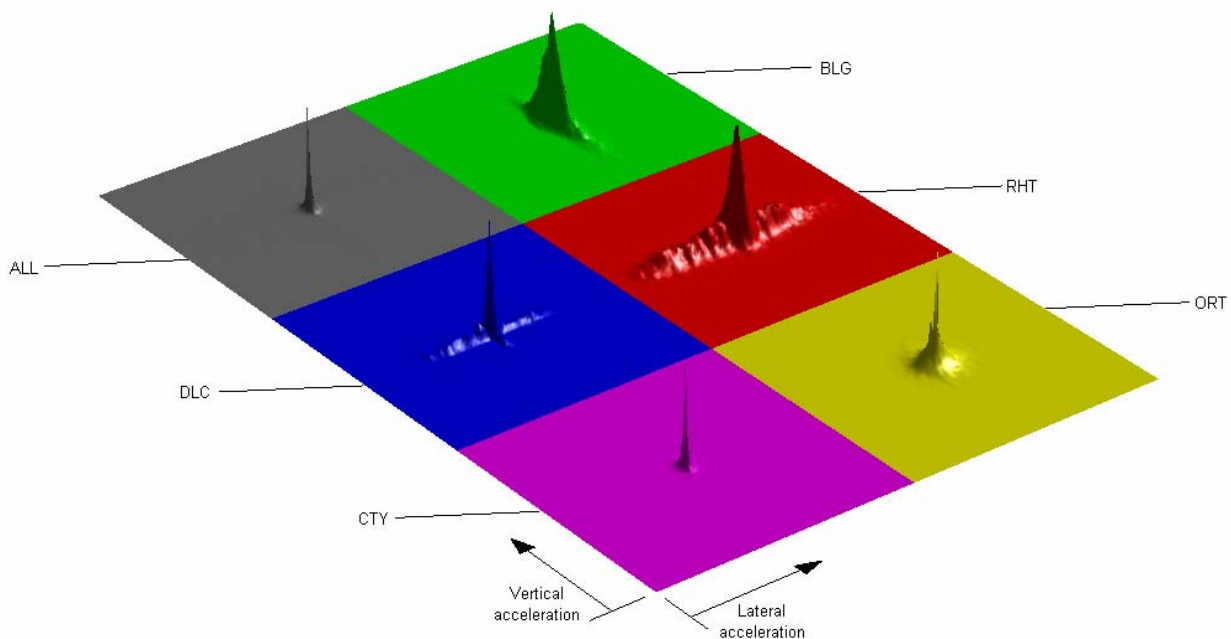


Figure 22: 3D Histograms of all the tests

In Figure 24 these approximations are superimposed. This graph shows that each terrain has a different acceleration signature. However there is too much overlap between the different tests and it would be difficult to clearly identify the terrain and/or handling manoeuvre at any given point in time. Another problem is that the vehicle reaches these extremities for only short periods of time.

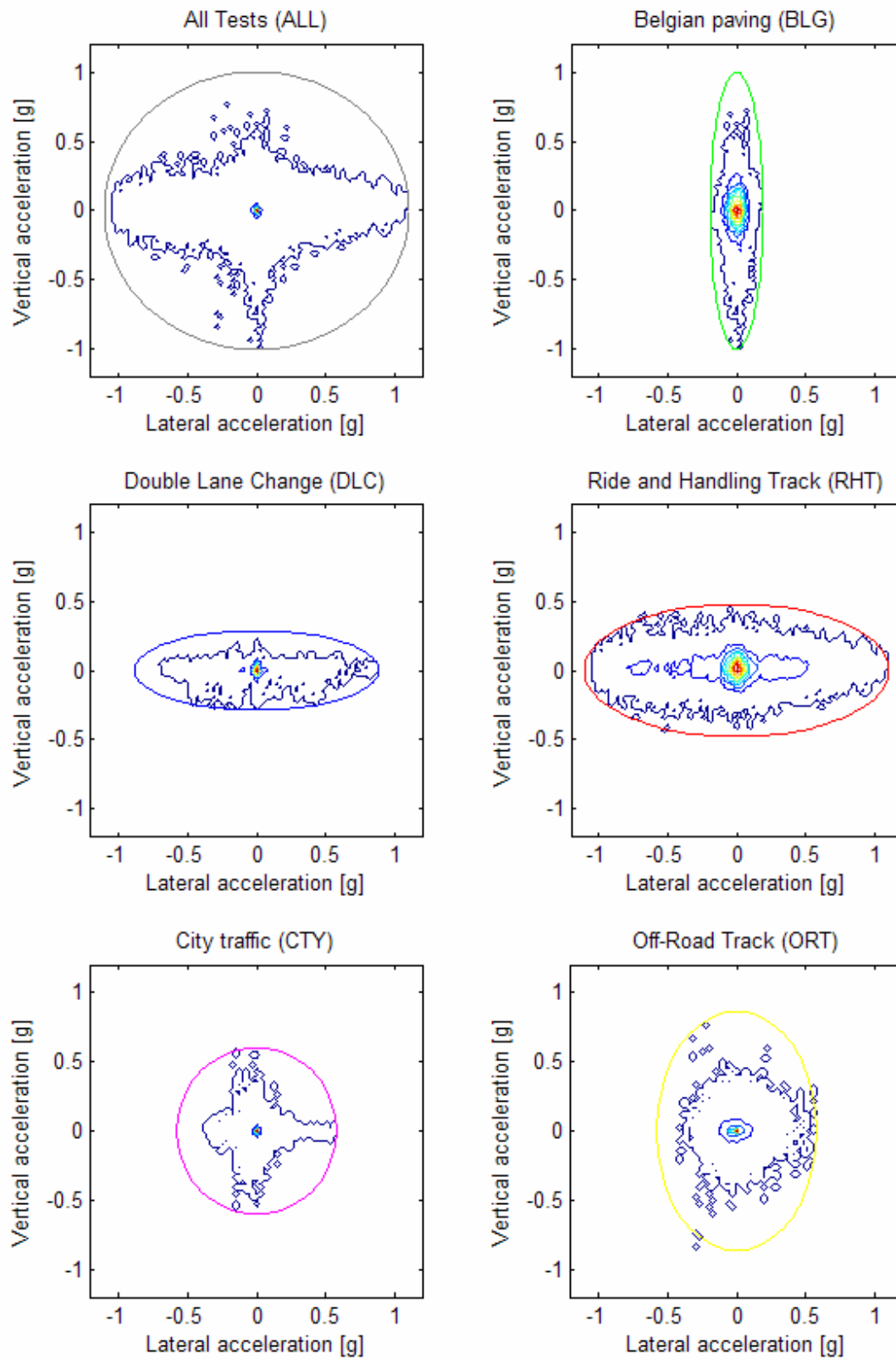
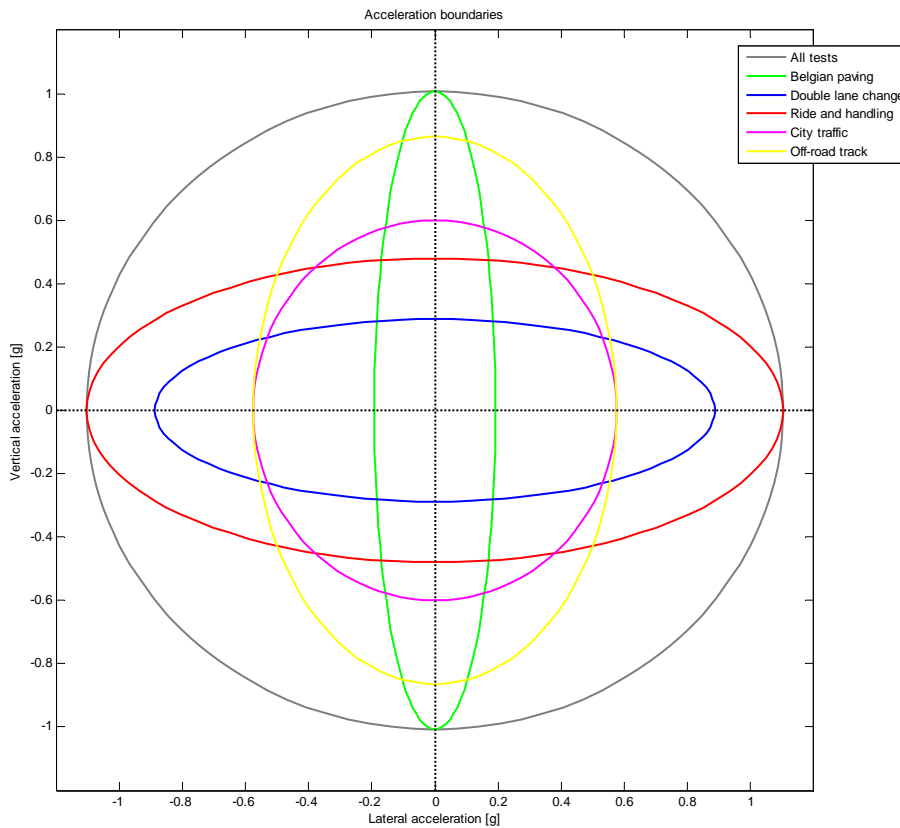


Figure 23: Contour plots and ellipse approximations for each histogram

Figure 24: The superimposed range of accelerations for each test

The lateral acceleration can be related to the driver's actions. The vertical acceleration is due to the terrain roughness. The following section uses Fuzzy logic with the relative road roughness as well as the driver's input to determine the terrain that the vehicle is travelling over.

3.4 Fuzzy logic terrain classification

Fuzzy logic is an algorithm that can be used to map input space data to an output space result. Fuzzy logic is an extension to multi-valued logic. The theory of fuzzy sets states that objects can be classified using membership functions. The membership of the object to a specific class is calculated as a matter of degree. Linguistic variables are used to define the fuzzy rules that govern the output of the algorithm.

For example:

IF vehicle Speed is high AND Steer angle is low
 THEN suspension is soft
 IF vehicle Speed is high AND Steer angle is high
 THEN suspension is hard

When solving problems, Fuzzy logic bases its decision on significance rather than precision. There are many applications for Fuzzy logic due to its speed, low cost and simplicity. (**Fuzzy logic Toolbox, 2005**)

When using the Fuzzy logic toolbox in MATLAB (www.mathworks.com), there are 11 standard types of membership functions to choose from and the user can also define functions. Changing their parameters stretches and shifts the membership functions. There are therefore an infinite number of possibilities to construct the Fuzzy Inference System (FIS). The following is one possibility. Weight functions are used to map the input space to the output space. The following input variables were used:

- Roughness Indicator (RI, also referred to as Relative Roughness Indicator (RRI))
- Standard deviation of the Kingpin steering angle (stdStrAng)
- Root Mean Square of the Kingpin steering angle (rmsStrAng)
- Mean Speed (meanSpd)

These parameters were chosen because they are directly related to the terrain input (RI) and the driver's actions (Kingpin steering angle and speed of the vehicle). The standard deviation of the steering angle indicates the range of the steering inputs while the RMS indicates the magnitude.

The output variable was defined as the degree that the input data matched a certain terrain profile based on the set of rules it was given.

The following rules were based on logical deduction and the knowledge that was gained by studying the data:

- If (RI is high) and (stdStrAng is low) and (rmsStrAng is low) then (Terrain is BLG)
- If (RI is low) and (stdStrAng is medium) and (rmsStrAng is medium) and (meanSpd is high) then (Terrain is DLC)
- If (RI is medium) and (stdStrAng is high) and (rmsStrAng is high) and (meanSpd is high) then (Terrain is RHT)
- If (RI is low) and (stdStrAng is low) and (rmsStrAng is medium) and (meanSpd is high) then (Terrain is CTY)
- If (RI is high) and (stdStrAng is high) and (rmsStrAng is high) and (meanSpd is low) then (Terrain is ORT)

There is however a large number of rules that can still be added. Figure 25 shows the process that was followed to generate the Fuzzy Inference System (FIS). All the input data were first normalised to ensure that all the variables had the same significance. A thousand data points from each of the 5

terrains were taken to test the FIS. Figure 26 shows the result of the output. The terrain that was classified the best was the Belgian paving (BLG) because the test was only done in a straight line and therefore the stdStrAng and the rmsStrAng was low. This was therefore the only rule that was necessary to correctly identify the test. It is definitely clear that the difference between the handling and ride comfort tests were distinguished but the decision between these extremes cannot be based on these results. The FIS can be improved by doing formal optimization on all the parameters.

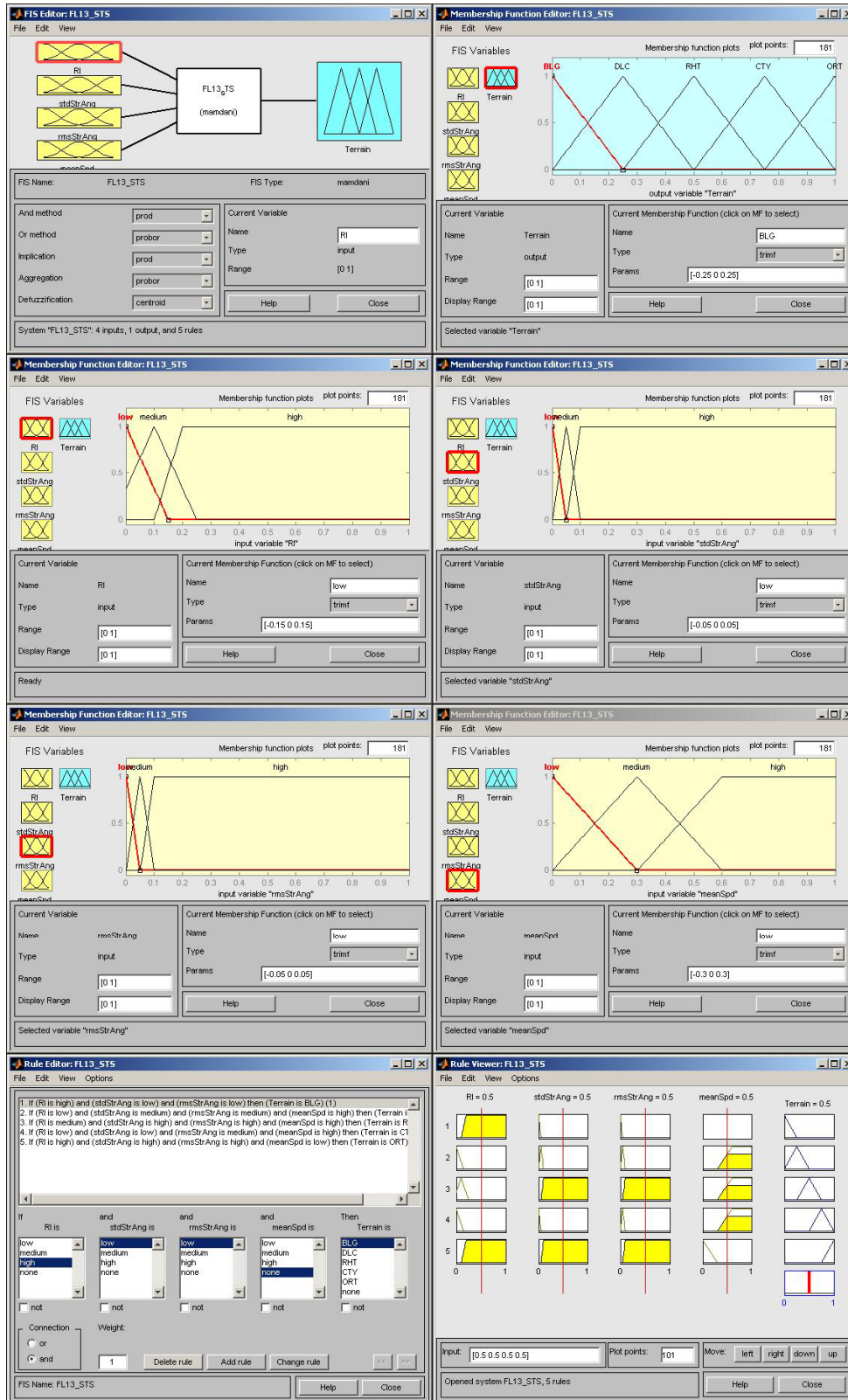


Figure 25: FIS editor [MATLAB, fuzzy.m]

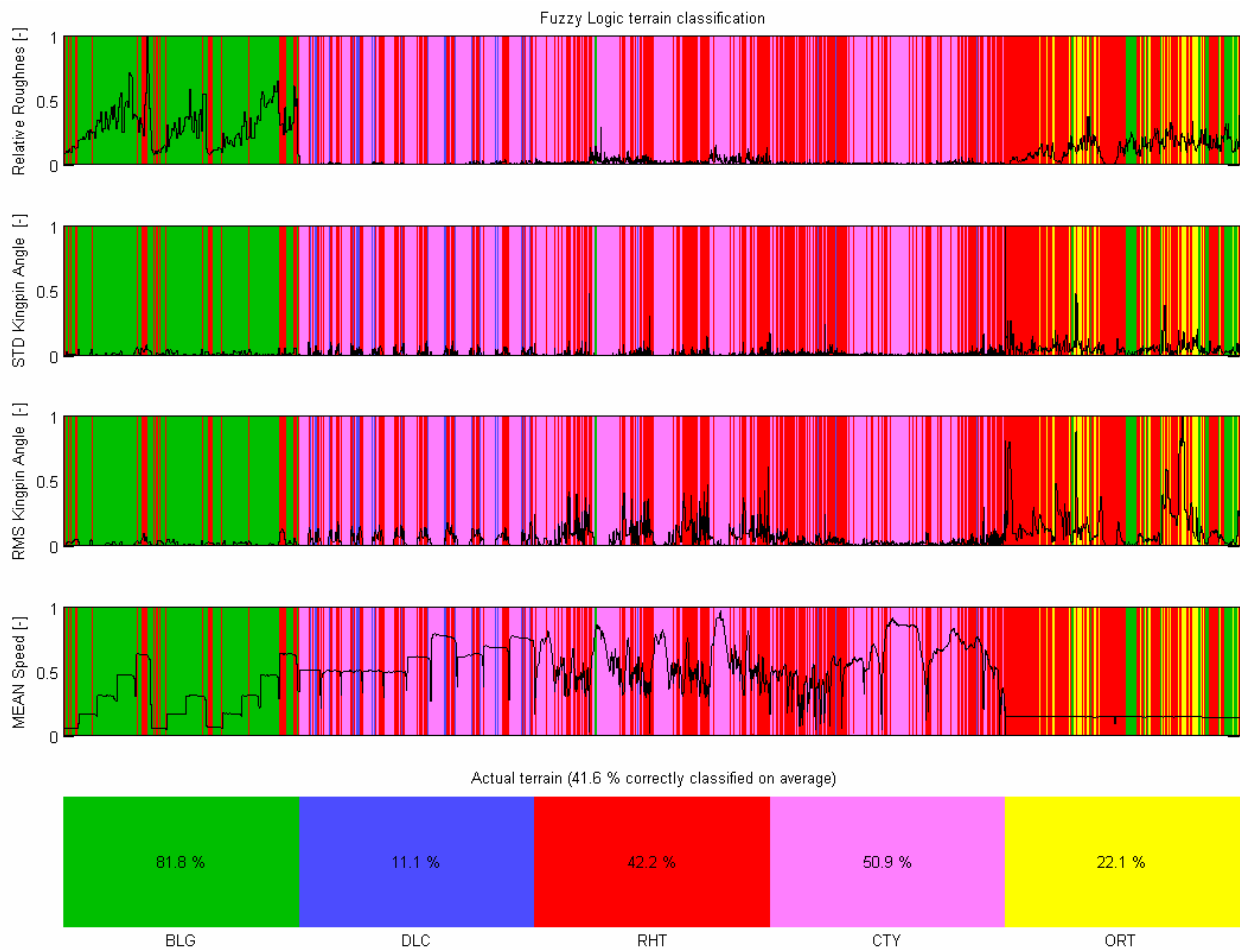


Figure 26: Comparison of terrain classification with Fuzzy logic

Closely related to Fuzzy logic is Artificial Neural Networks. Self-Organising Maps is one type of neural network that was used in an attempt to classify the terrain in the next section.

3.5 Self-Organising Maps

Artificial Neural Networks (ANN's) have many similarities to the human brain. Each sensory input the human brain receives (visual, auditory, etc.), is mapped into a corresponding area of the cerebral cortex. **Kohonen (2001)** formulated the principle of topographic map formation (**Negnevitsky, 2002**). The principle states that a particular feature of the input pattern corresponds to the spatial location of an output neuron.

Self-Organising Maps (SOM's) can produce topology preserving maps of any feature space. Self-organisation is achieved by stochastically presenting input features to the neurons, which then arranges them into a map. Topology preservation means that neighbouring neurons represent neighbouring regions in the input feature space. The SOM is a high-dimensional scaling method that projects the input feature data to a low-dimensional display. It converts complex, non-linear

statistical relationships from high-dimensional input data to a one- or two-dimensional grid. Similar vectors from the input feature space are projected to neurons that are topologically close to each other. If a SOM is applied correctly, it can be a highly effective tool to visualise high-dimensional data on a two dimensional grid. The SOM learns without supervision, which means the data is automatically arranged onto the map. SOM's were initially intended for data visualization but it is now more commonly used for data classification.

There are many applications where the SOM has been successfully implemented such as process analysis, monitoring, diagnostic methods, etc. in the industrial, medical and telecommunications industries. **(Kohonen, 2001)**

A Self-Organising Map (SOM) can be called an intelligent multi-dimensional histogram. All the measurements that were taken were stored in a matrix of vectors. Each column in the matrix is called a variable and each row index represents a point in time. All the variables are first normalised to ensure that the SOM is not biased towards some variables. The training of the SOM is done by clustering similar row vectors together giving them a unique bin index on a predetermined map, the cluster map. The SOM is an artificial neural network that can be stored and reused without the need of a huge database to compare variables with. Neural networks have the disadvantage that they can only give an output if the input values are relatively close to what it was trained with. In other words it can not do what it was not trained to do.

Two thousand linearly spaced data points from each test was used to train the SOM. Different combinations of variables were used to try and determine the best training dataset. The whole dataset was then used to test the SOM. The size of the training dataset is about 3% of the total dataset's size.

Terrain Classification

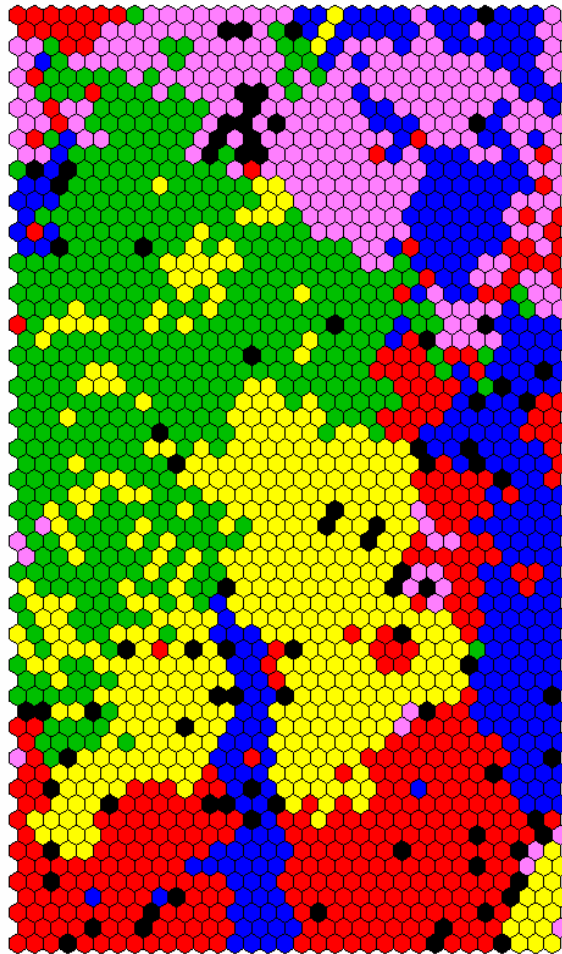


Figure 27: Cluster map of ALL_1 SOM with all the measured data as input variables

Figure 27 to Figure 41 shows the SOM's and their performance of correctly classifying the terrain. The terrain classification maps use the colour codes depicted in Table 3. The U-matrix and other variable maps use a scaled colour code where blue indicates low values and red indicates high values. The U-matrix shows the cluster boundaries as high values (light blue to red), while the cluster itself is shown as low values (dark blue). This is an indication of the "distance" between neighbouring cells, which is why there are more cells in the U-matrix than in the other maps. If cells are close to each other (dark blue) it means that they contain similar data and are clustered together.

Figure 28 indicates the SOM with all 14 measurements used as input variables. The terrain classification of the SOM is compared to the actual terrain in Figure 29. The percentage of correctly classified terrain types is 77.1% on average and the percentage of unclassified terrain is 1.1%.

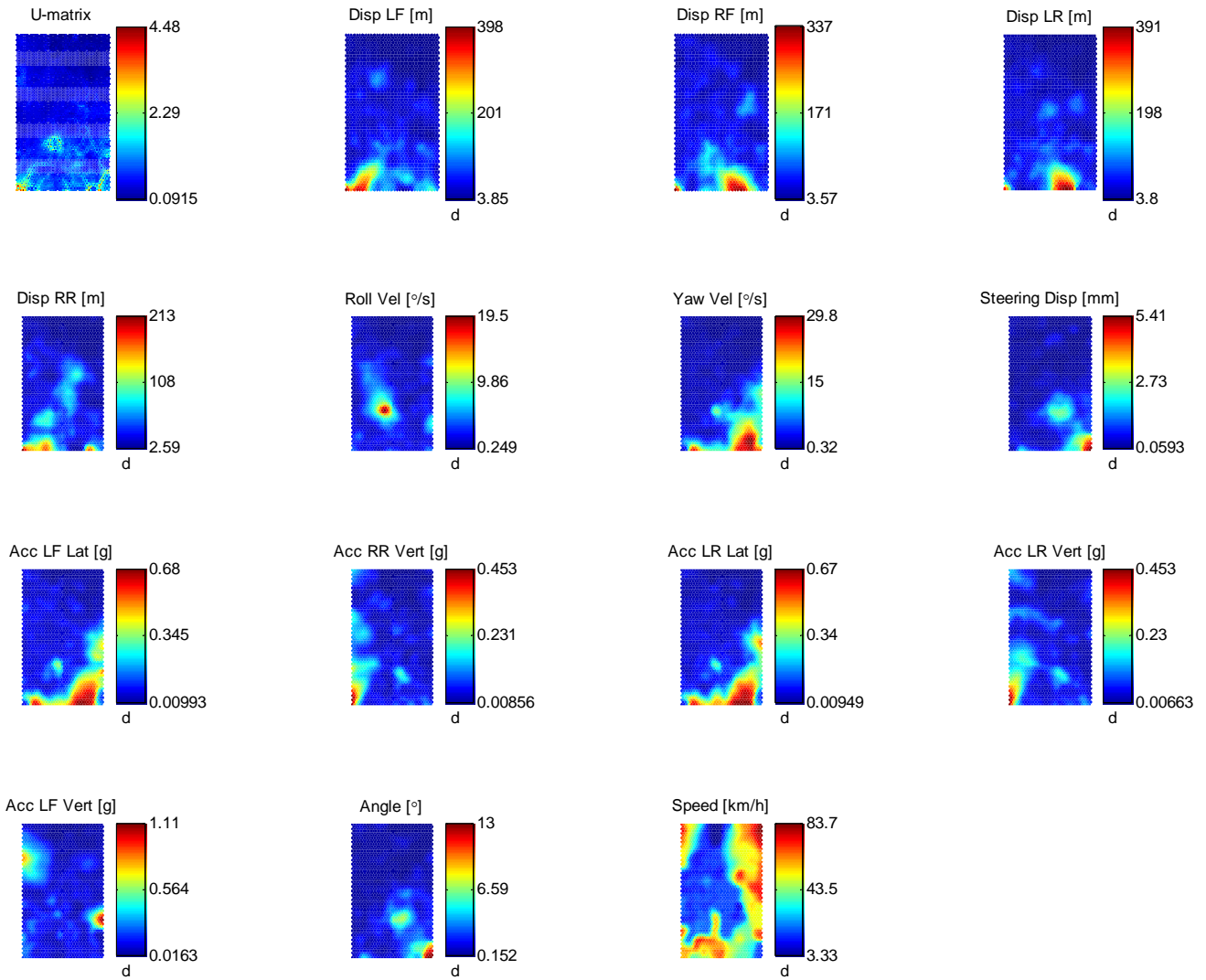


Figure 28: ALL_1 SOM with all the measured data as input variables

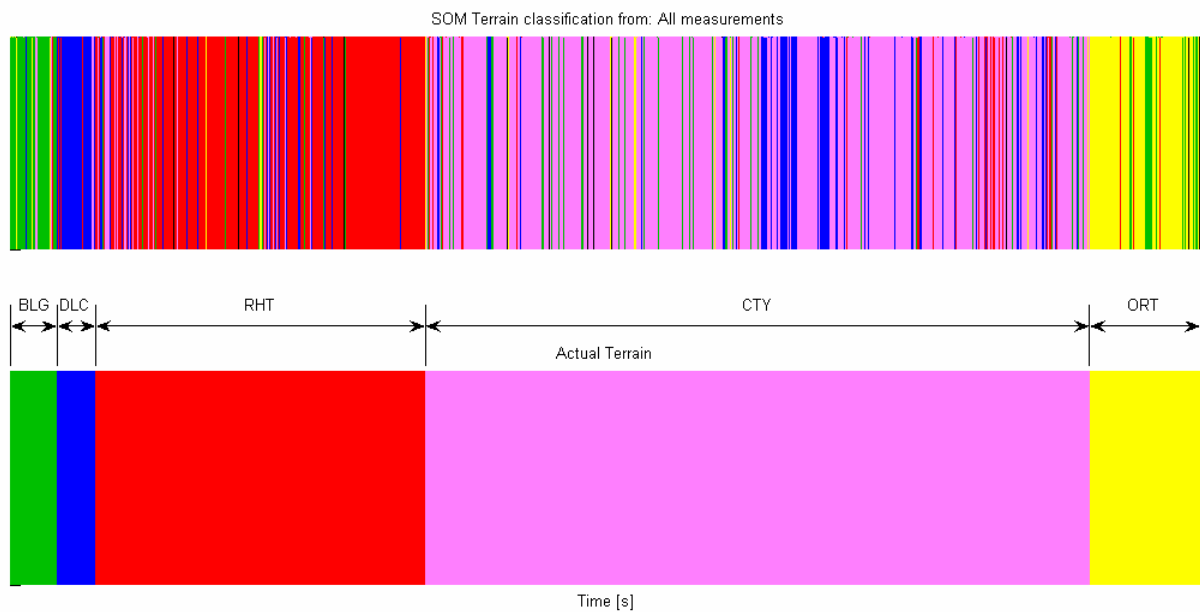


Figure 29: Performance of ALL_1 SOM with all the measured data as input variables

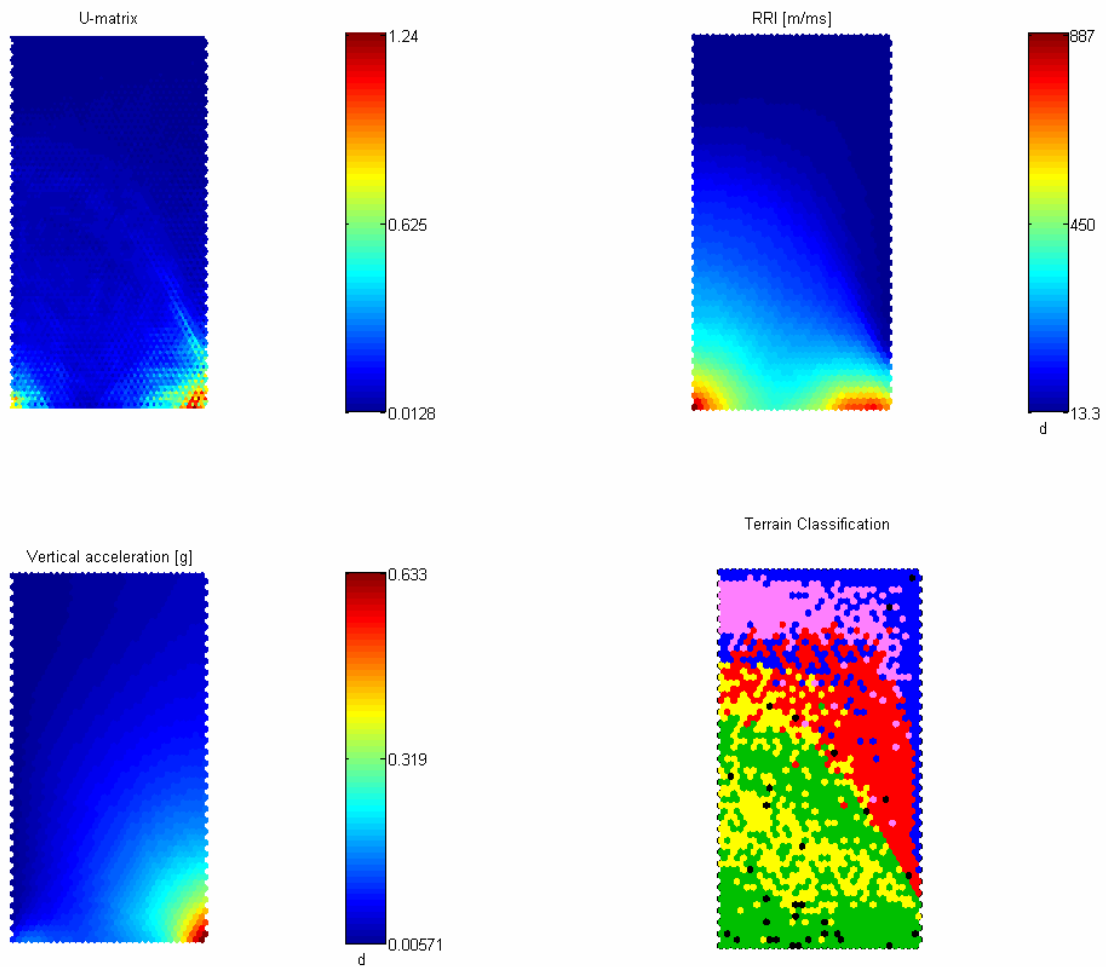


Figure 30: RIDE_1 SOM with RRI and vertical acceleration as input variables

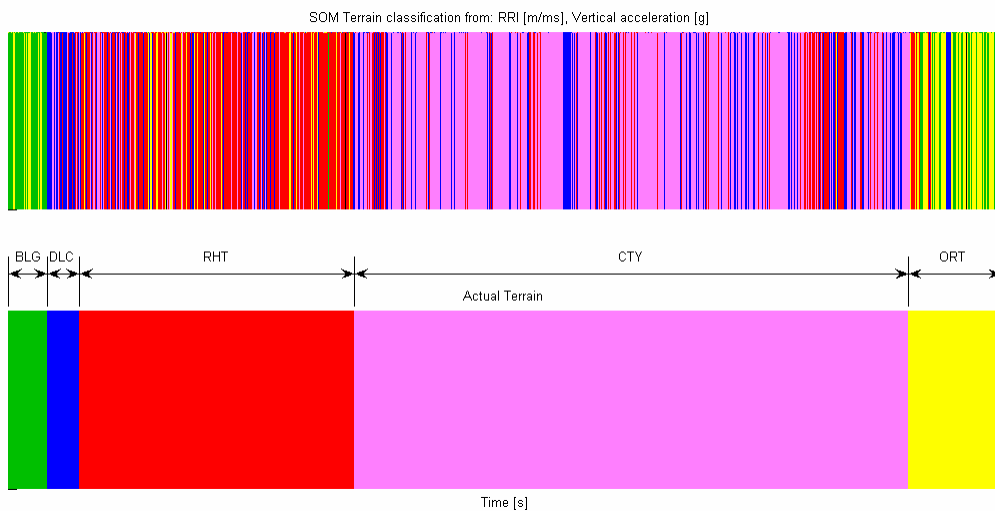


Figure 31: Performance of RIDE_1 SOM with RRI and vertical acceleration as input variables

Figure 30 shows the results when using the RRI and the vertical acceleration as input to the SOM. The percentage of correctly classified terrain types is 63.2% on average and the percentage of unclassified terrain is 0.41% (see Figure 31).

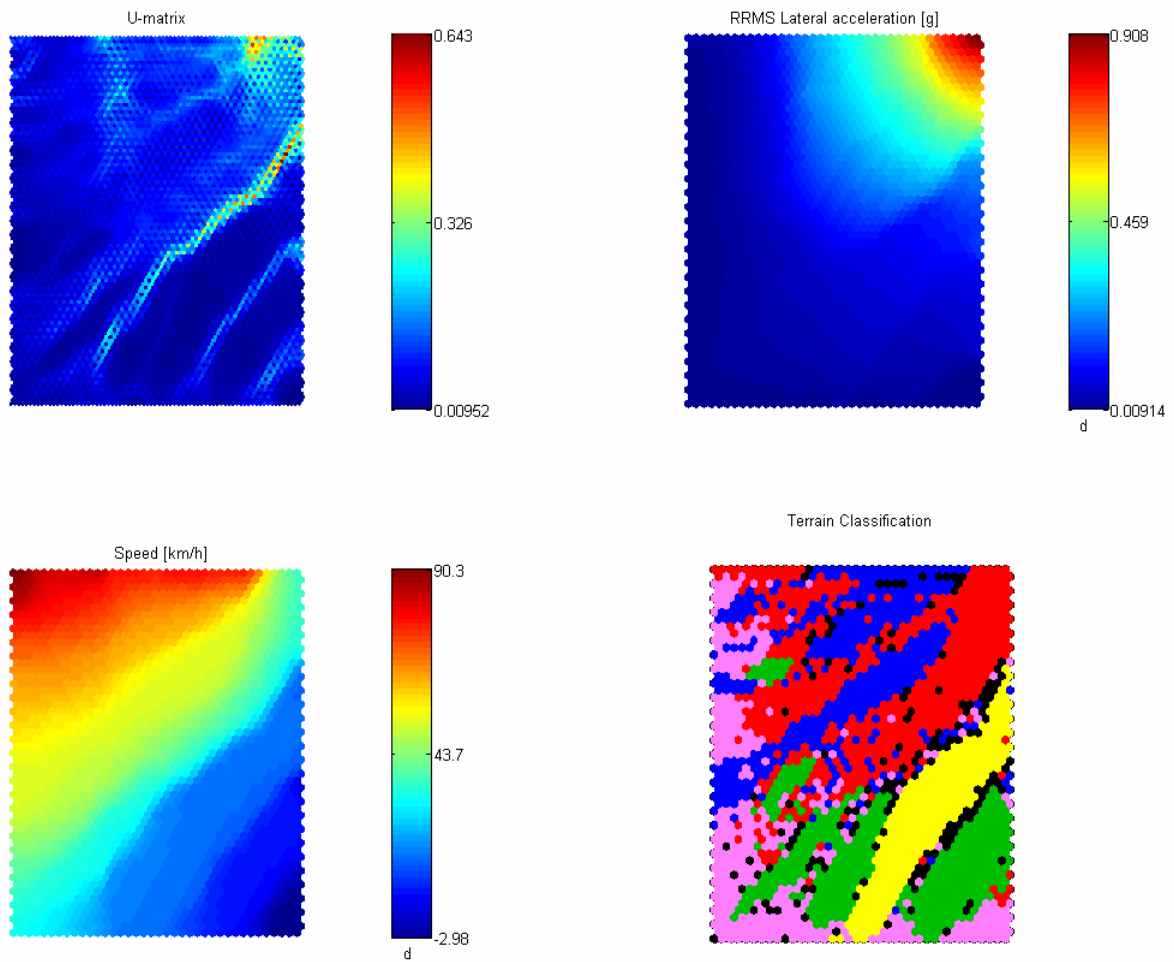


Figure 32: HAND_1 SOM with RMS lateral acceleration and vehicle speed as input variables

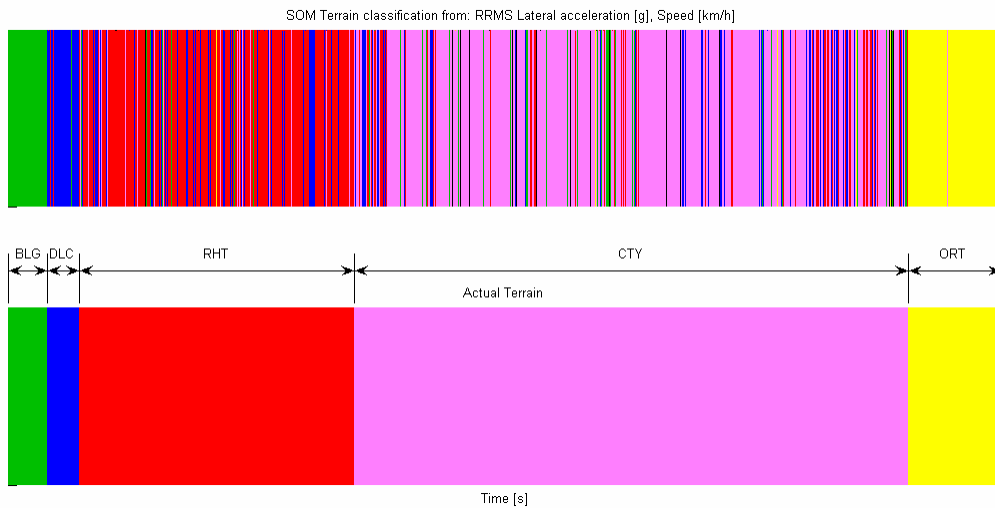


Figure 33: Performance of HAND_1 SOM with RMS lateral acceleration and vehicle speed as input variables

Figure 32 indicates the results achieved by using RRMS lateral acceleration and speed as input variables. The percentage of correctly classified terrain types is 77.1% on average and the percentage of unclassified terrain is 2.1%. (see Figure 33)

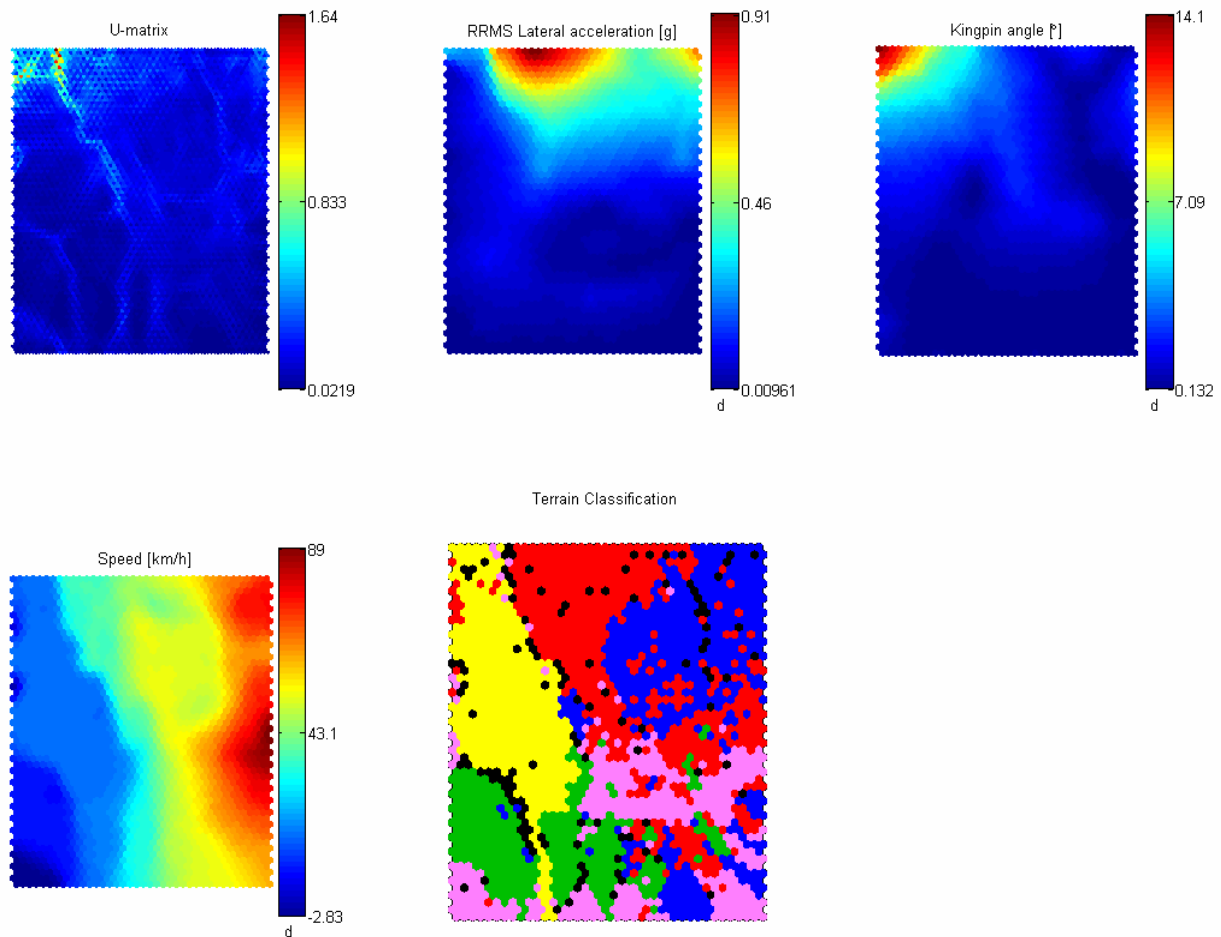


Figure 34: HAND_2 SOM with RMS lateral acceleration, steering angle and vehicle speed as input variables

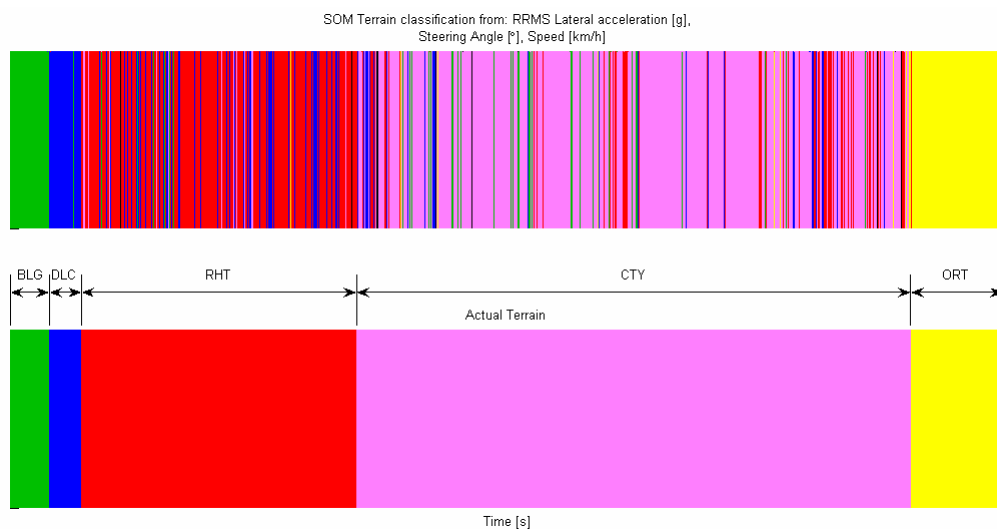


Figure 35: Performance of HAND_2 SOM with RMS lateral acceleration, steering angle and vehicle speed as input variables

This analysis used the RRMS lateral acceleration, kingpin angle and the speed of the vehicle and is shown in Figure 34. The percentage of correctly classified terrain types is 78.9% on average and the percentage of unclassified terrain is 1.3% (see Figure 35).

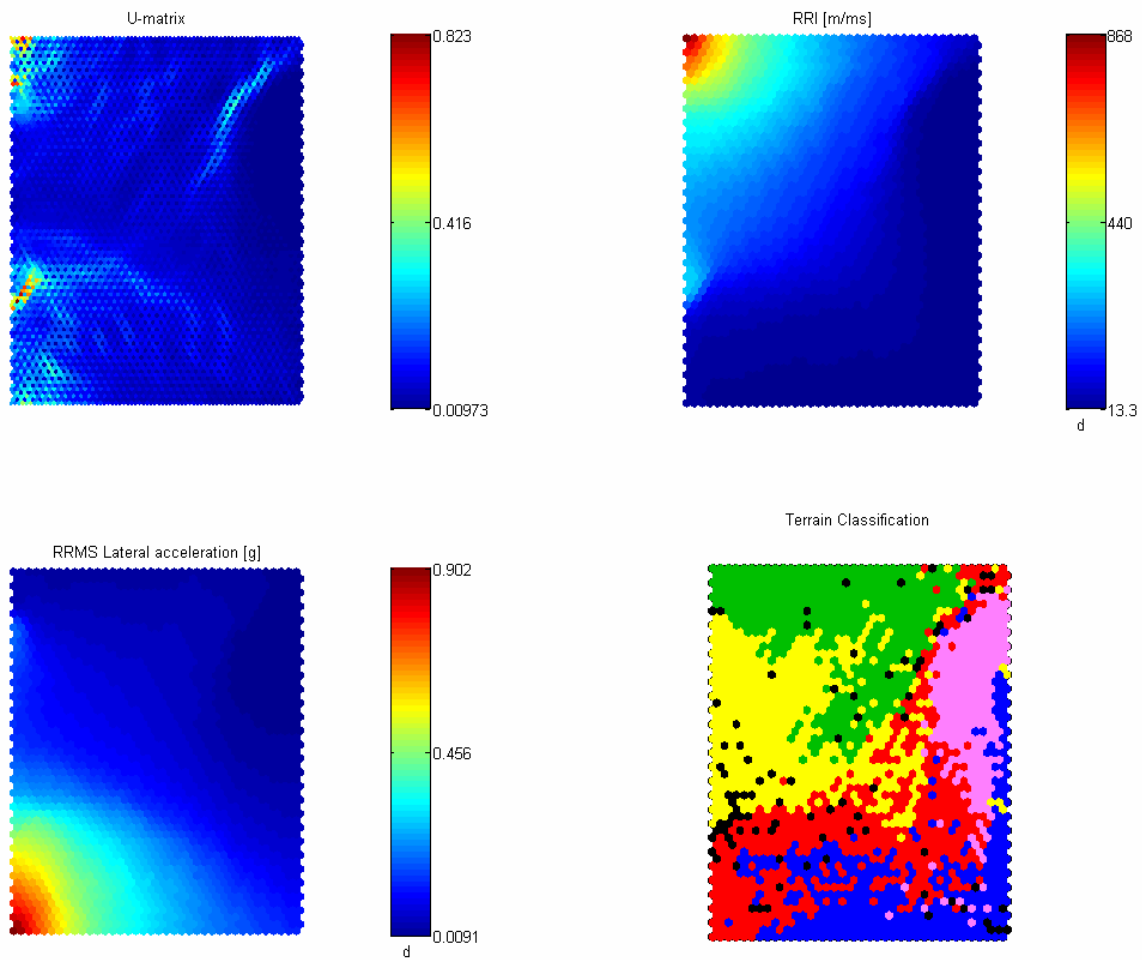


Figure 36: RIDE_HAND_1 SOM with RRI and RMS lateral acceleration as input variables

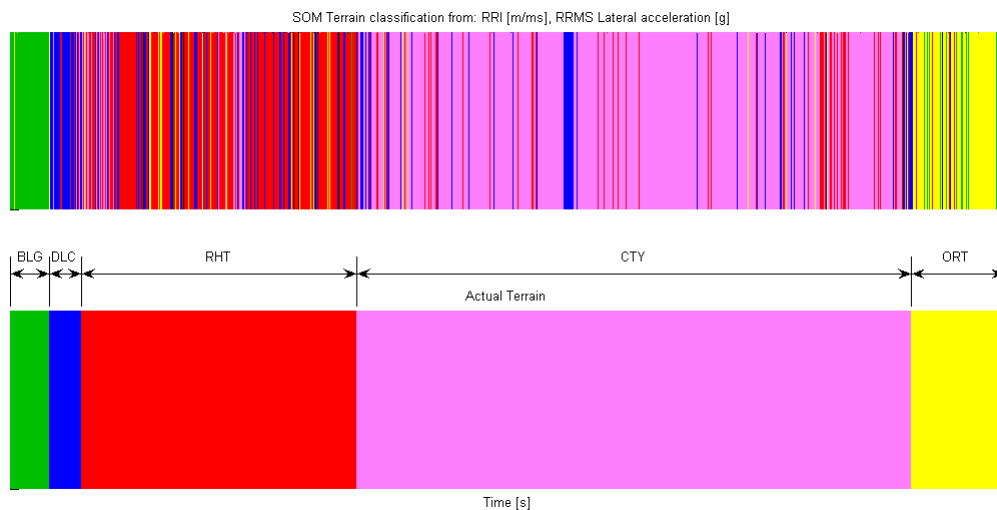


Figure 37: Performance of RIDE_HAND_1 SOM with RRI and RMS lateral acceleration as input variables

A combination of ride comfort and handling parameters (RRI and RRMS lateral acceleration respectively) were used in Figure 36. The percentage of correctly classified terrain types is 76.2% on average and the percentage of unclassified terrain is 0.96% (see Figure 37).

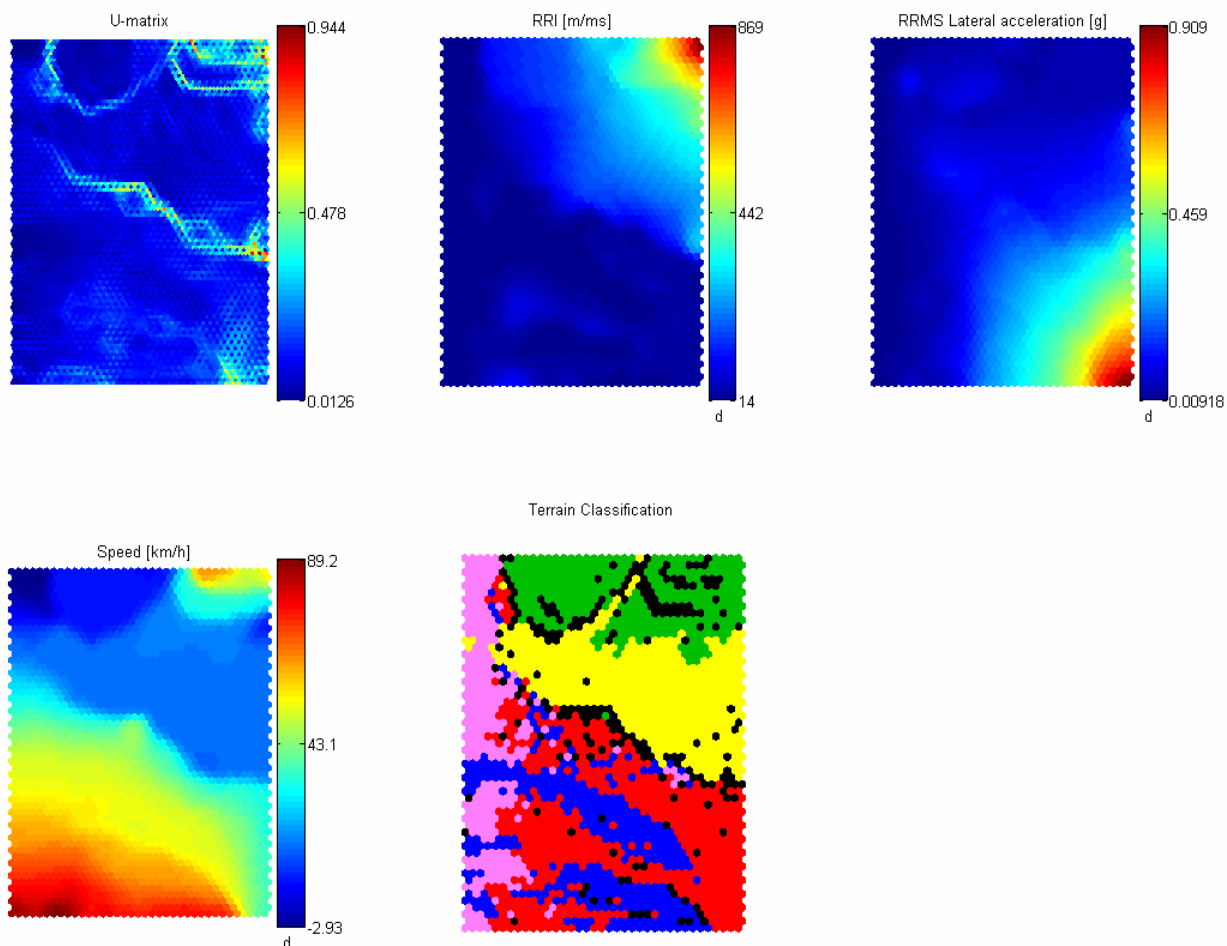


Figure 38: RIDE_HAND_2 SOM with RRI, RMS lateral acceleration and vehicle speed as input variables

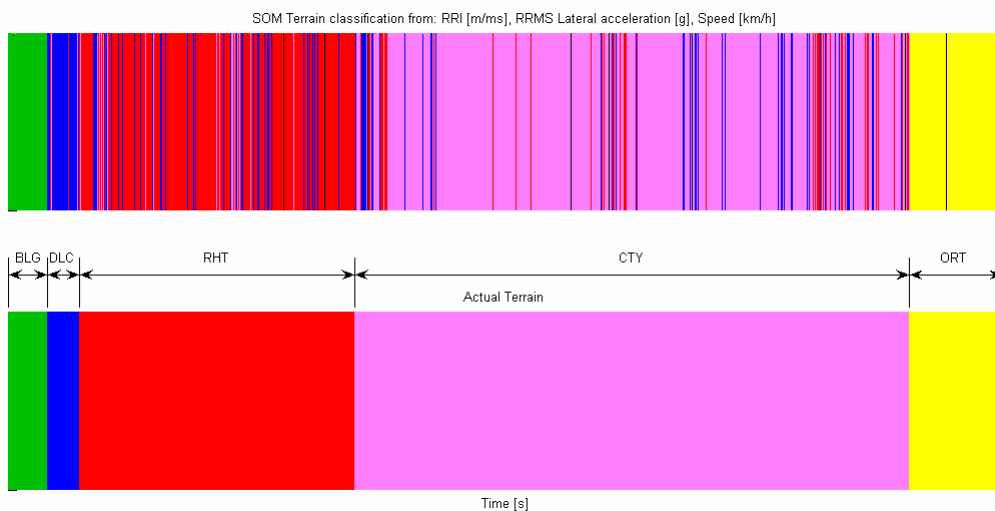


Figure 39: Performance of RIDE_HAND_2 SOM with RRI, RMS lateral acceleration and vehicle speed as input variables

Figure 38 displays the result obtained by applying the RRI, RRMS lateral acceleration and speed to a SOM. The percentage of correctly classified terrain types is 83.7% on average and the percentage of unclassified terrain is 1.0% (see Figure 39).

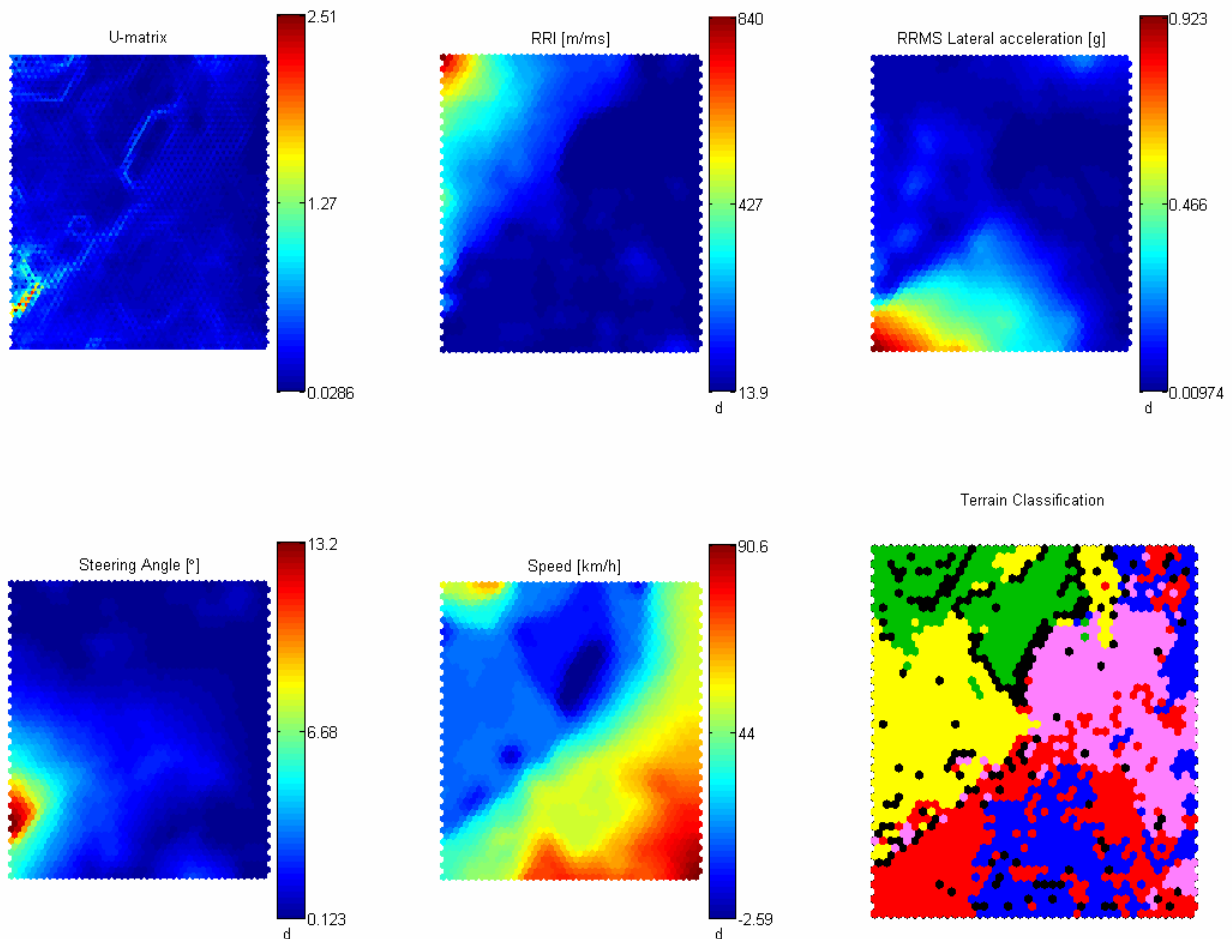


Figure 40: RIDE_HAND_3 SOM with RRI, RMS lateral acceleration, steering angle and vehicle speed as input variables

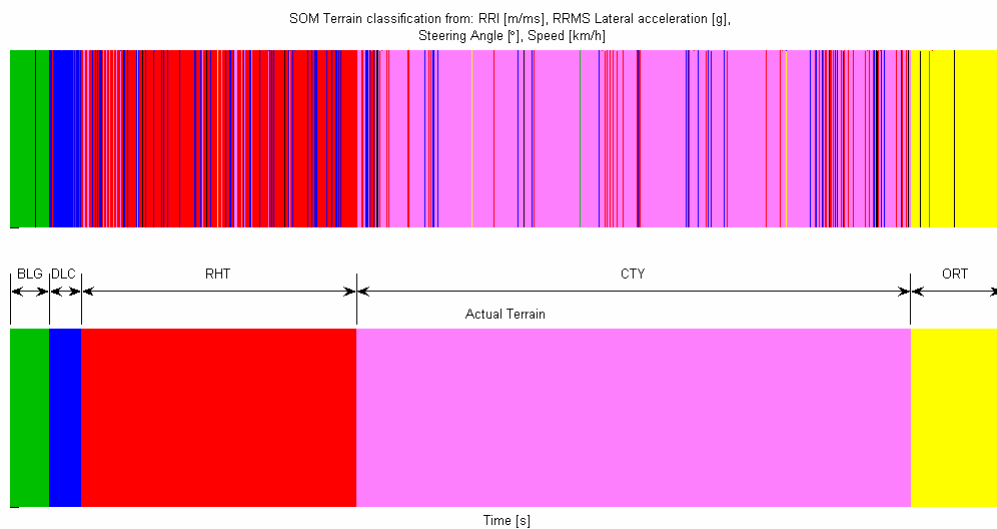


Figure 41: Performance of RIDE_HAND_3 SOM with RRI, RMS lateral acceleration, steering angle and vehicle speed as input variables

The steering angle is added to this analysis shown in Figure 40. The percentage of correctly classified terrain types is 84.6% on average and the percentage of unclassified terrain is 1.4% (see Figure 41).

Table 5 lists the performance of the SOM's for a specific test and in the last column all the tests combined. The Belgian paving is classified correctly in most of the algorithms. Using purely the vertical acceleration and the relative roughness as classifiers in the RIDE_1 SOM produced the worst results of all. While combining the ride comfort and handling data produced the best result as seen in the last two rows of the table.

SOM	Description	Figures	BLG	DLC	RHT	CTY	ORT	ALL
ALL_1	14 measurements	28 & 29	83.0	91.7	78.3	75.5	76.0	77.1
RIDE_1	RRI & vert. acc.	30 & 31	75.3	59.5	63.3	65.7	43.5	63.2
HAND_1	RRMS lat. acc. & speed	32 & 33	96.7	89.1	72.4	73.8	98.4	77.1
HAND_2	RRMS lat. acc., speed & steer angle	34 & 35	96.1	91.4	70.4	78.2	96.4	78.9
RIDE_HAND_1	RRI & RRMS lat. acc.	36 & 37	94.8	69.0	62.2	82.7	73.1	76.2
RIDE_HAND_2	RRI, RRMS lat. acc. & speed	38 & 39	98.7	91.5	79.4	82.2	96.5	83.7
RIDE_HAND_3	RRI, RRMS lat. acc., speed & steer angle	40 & 41	98.3	92.2	76.4	85.5	95.4	84.6

Table 5: Performance of SOM terrain classification [%]

Table 6 gives the percentage of errors that occurred for each SOM. The SOM cannot classify data that it was not trained with. The UC column shows the percentage of unclassified data. The SOM algorithm tests the map by feeding it the same data that it was trained with. This produces the quantization (QE) and topographic (TE) errors. The quantization error indicates the accuracy of the output that was generated. The topographic error is a measure of the probability that the correct cell was chosen for the input data. The lowest percentage of data that was not classified by a SOM was that produced by RIDE_1. This however does not redeem it from its poor classification's performance.

SOM	Description	Unclassified terrain	Quantization error	Topographical error
ALL_1	14 measurements	1.1	109.0	4.0
RIDE_1	RRI & vert. acc.	0.4	2.9	2.9
HAND_1	RRMS lat. acc. & speed	2.1	2.0	10.1
HAND_2	RRMS lat. acc., speed & steer angle	1.3	7.4	4.5
RIDE_HAND_1	RRI & RRMS lat. acc.	1.0	1.8	19.9
RIDE_HAND_2	RRI, RRMS lat. acc. & speed	1.0	5.8	4.9
RIDE_HAND_3	RRI, RRMS lat. acc., speed & steer angle	1.4	13.0	4.8

Table 6: SOM terrain classification errors [%]

From these tables it appears that the parameters: RRI, RRMS lateral acceleration, speed and steer angle would be the best choice for identifying the terrain type. This means that the SOM needs both ride comfort and handling features to classify the terrain correctly.

3.6 Statistical discrimination

The last attempt at terrain classification was done by using a purely statistical approach. A quadratic discriminant function based on the assumption of normality was suggested and implemented by

Grimbeek (2006) at the University of Pretoria. The total data set consisted of 11 measurements and 395 214 observations from 5 different terrain types altogether. It was not possible to have an equal amount of data for each terrain type due to the length of the respective tests (Belgian paving: 100 *m* long, Ride and Handling Track: 4200 *m* long). A “test” data set was obtained by systematically using a 1000 observations from each one of the terrain data sets. The balance of 390 214 observations was used as the “training” data set. There are a total of 390 coefficients that was determined by the SAS program (www.sas.com) from the training data set. The following equations are used to classify the terrain:

$$L_{nk} = c_k + \sum_{i=1}^{11} M_{ki} v_{ni} + \sum_{i=1}^{11} \sum_{j=1}^{11} Q_{kij} v_{ni} v_{nj} \quad \text{Eq. 8}$$

$$\text{If: } \max_{1 \leq k \leq 5} (L_{nk}) = L_{nk}$$

$$\text{Then: } T_n = k, \text{ where } k = [1, 2, 3, 4, 5] \quad \text{Eq. 9}$$

Where

n is the n^{th} observation

k is the current discriminant function for terrain k , $k = [1, 2, 3, 4, 5]$

c_k is a constant associated with terrain k

M is a matrix of coefficients for the linear terms

Q is a matrix of coefficients for the cross product terms

v_n is a vector of the n^{th} 11 measurements that were taken

i and j are indexes, $i = j = [1, 2, 3, \dots, 10, 11]$

L_{nk} is the solution to the k^{th} discriminant function of the n^{th} observation

T_n is the index k that gives the maximum of L_{nk} ,

$T_n = 1$: Belgian paving

$T_n = 2$: Double lane change

$T_n = 3$: Ride and handling track

$T_n = 4$: City traffic

$T_n = 5$: Off-road track

The training data set was used to estimate the coefficients for the five likelihood discriminant functions, a function for each terrain type. These discriminant functions were applied to the “test” data to categorise the observations into one of the five terrain types. The results can be seen in Table 7 and Table 8. The original printout of the results can be seen in the appendix A.1.

Terrain	1	2	3	4	5	Total
1	90.71	0.94	0.17	3.66	4.51	100
2	0.64	81.45	2.03	15.88	0	100
3	2.01	2.24	93.84	0.14	1.77	100
4	1.56	2.41	1.99	92	2.02	100
5	6.29	0.01	0.79	3.39	89.51	100
Total	3.78	3.36	34.36	40.96	17.54	100

Table 7: Quadratic discriminant classification of training data

Terrain	1	2	3	4	5	Total
1	90.2	1.1	0.2	3.7	4.8	100
2	0.3	81.6	2.2	15.9	0	100
3	2.1	2.5	93.4	0.2	1.8	100
4	2	2.4	2	91.8	1.8	100
5	6.3	0	0.4	2.7	90.6	100
Total	20.18	17.52	19.64	22.86	19.8	100

Table 8: Quadratic discriminant classification of testing data

The total percentage of misclassification was 10.5% this means that 527 out of 5000 observations were classified into a different terrain type than the one it originated from (**Grimbeek, 2006**).

Table 7 shows the percentage of the correctly classified observations from the training data. Table 8 shows a similar trend for the testing data set. The performance of the classification is more or less the same for each terrain type except for the Double lane change. The reason for this can be found when looking at the misclassified observations that are not on the diagonal. The Double lane change was misclassified as city traffic for 15.9% of the time. This clarifies the slightly worse performance of this method when the Double lane change is classified. The city traffic and the Double lane change have many similarities, especially when comparing the section just before the lane change manoeuvre is performed to normal city driving in a straight line.

Figure 42 shows the results from applying the equations (Eq. 8 and Eq. 9) on a data set containing 5000 observations of each terrain type. The results shown in the bottom graph was obtained by calculating the histogram of a moving window (100 observations) to eliminate spurious classification of a similar terrain types. The maximum of this histogram indicates the dominant classified terrain. This method however has a 0.5 s delay when moving from one type of terrain to another. At this stage this is not such a big problem and this method improves the accuracy of identifying the correct terrain significantly (see Table 9)

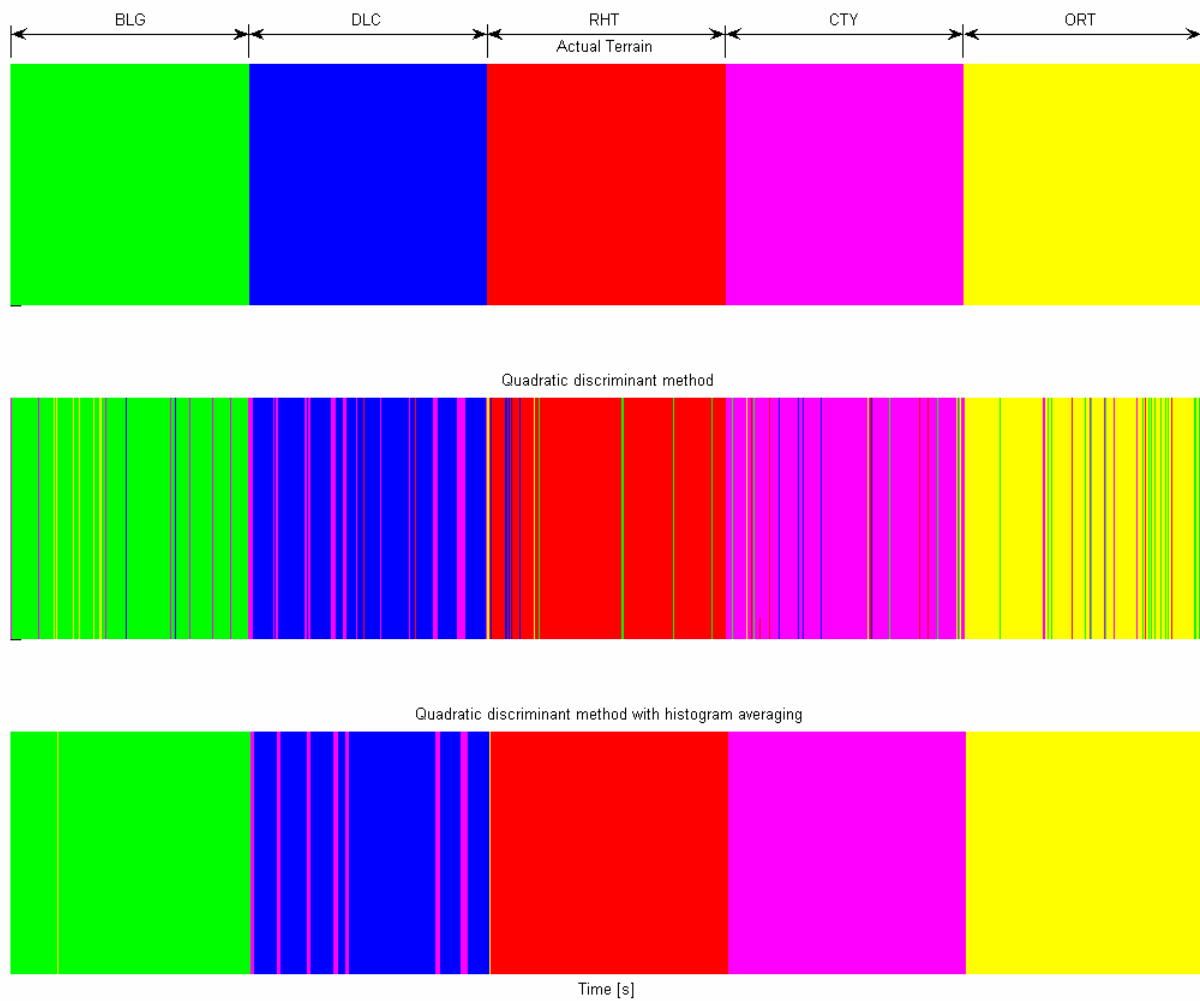


Figure 42: Comparing the Quadratic discriminant classification with the actual terrain

Terrain	1	2	3	4	5	Total
1	99.44	0.00	0.00	0.00	0.56	100
2	0.92	85.70	0.00	13.38	0.00	100
3	0.00	0.74	98.48	0.00	0.78	100
4	0.00	0.00	1.44	98.56	0.00	100
5	0.00	0.00	0.00	1.04	98.96	100
Total	20.07	17.29	19.98	22.60	20.06	100

Table 9: Quadratic discriminant method with histogram averaging

The conclusions drawn from all the results that were obtained from the various terrain classification methods can now be summarised.

3.7 Conclusion of Terrain classification methods

The main reason for classifying the terrain is to improve certain ride comfort vs. handling decision based strategies. An example of this is the speed vs. steer angle strategy investigated by Els (2006a). Figure 43 shows the boundaries of the speed and steering angles for three known terrain

types. If the terrain can be classified in real-time, different parameters for each terrain can be used in a decision making strategy to get the optimum results in each situation.

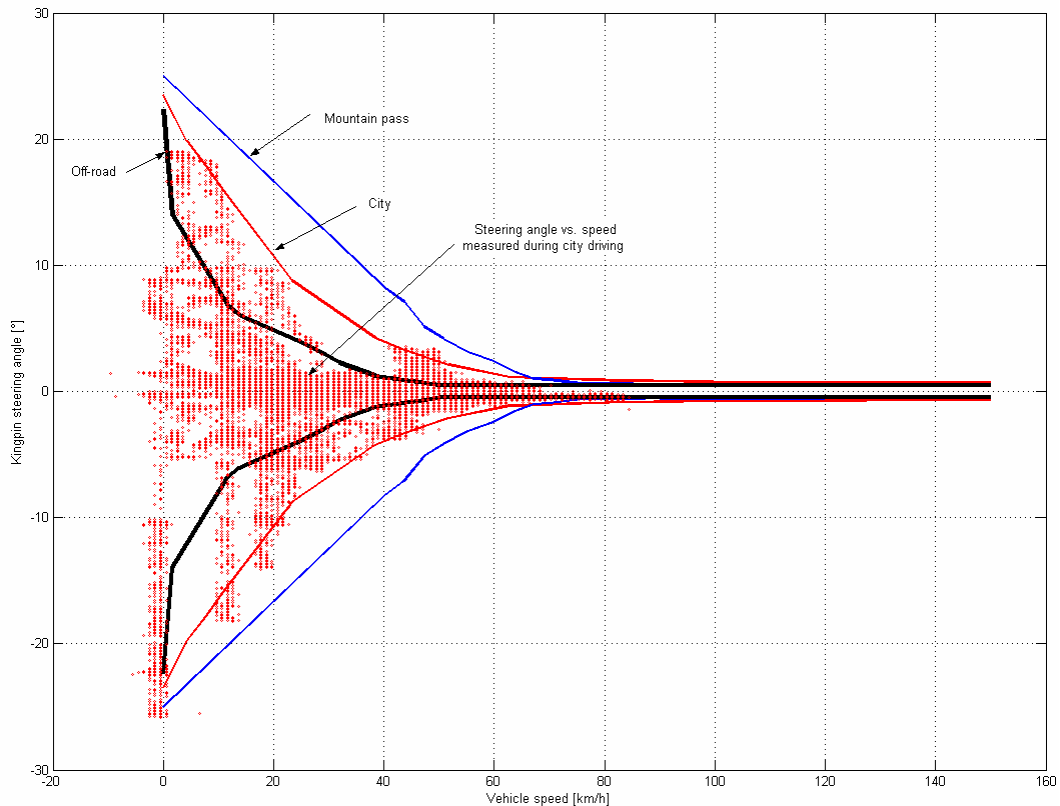


Figure 43: Steering angle vs. speed (Els, 2006a)

The obstacle detection method using laser range sensors have the advantage of detecting the terrain roughness before the vehicle travels over it. The downside of this method is that these sensors are usually expensive and sensitive to lighting and surface colour conditions.

The acceleration histogram method is a simple solution that uses only a small bi-axial accelerometer. Unfortunately the results are not discriminative enough. The different terrains do have similarities and this is the reason for the large areas of overlap.

Fuzzy logic is an algorithm that is easy to set up and can just as easily be changed, but this manual adjustment is cumbersome due to the many variables that need to be considered. This method can probably be improved if a lot of time is spent on a formal optimization analysis of the parameters of the fuzzy inference system. The parameters currently used do not give satisfactory results.

The Self-Organising Map neural network is a multi-dimensional histogram that tries to discriminate all the observations by sorting the data into bins. After the SOM is trained the classification happens

quickly with very little effort. This algorithm has a disadvantage because it is not always able to classify new data. Therefore the training data has to represent each terrain very accurately. The method did on average quite well. The best results (RIDE_HAND_2, 84% correctly classified) were obtained by using the following parameters: relative roughness indicator (RRI), RRMS of the lateral acceleration, vehicle speed and steer angle.

The best results were obtained from the analysis method suggested by the Department of Statistics at the University of Pretoria. A Quadratic discriminant function together with eleven measured parameters was used to classify the five terrain types. This method was able to correctly identify all the terrains for 89.5% of the time. The maximum of a moving histogram was used to improve the classification to 96.2%. This result is good considering that the Double lane change and the city traffic tests can be very similar at some stages. The same can be said for the Belgian paving and the Off-road track. In cases where doubt exists (e.g. the terrain cannot be classified) the control system should switch the suspension system to the handling mode to ensure safe operation of the vehicle.

In view of the potential and remaining ambiguity to discern different terrains, the question arises when is it essential to switch the $4S_4$ system from the ride comfort to the handling mode.

4 Ride comfort vs. Handling switching strategies

Results from the previous chapter showed that the terrain cannot be identified unambiguously by means of Fuzzy logic, SOM, Histograms, etc. without further refinement of the algorithms. These methods appear to be successful when identifying pure uneven terrain (Belgian paving and Off-road track), but discrimination of terrains where handling manoeuvres (Double lane change and Ride and handling track) were performed is less successful. Even if the terrain could be identified without uncertainty, the suspension must still be switched between the ride comfort and handling mode if and when it is needed. The main aim of the investigation in this chapter is to find a method that will make a ride comfort or handling decision based on measurements taken from the vehicle. Therefore switching signals based on logic was investigated and compared to a benchmark signal that is an ideal strategy based on expert knowledge.

4.1 Benchmark switch

Dr. **Els (2006b)** from the University of Pretoria, who developed the $4S_4$ semi-active suspension system, created the switch signal seen in the bottom graph of Figure 44, based on the steer angle, speed, vertical acceleration and lateral acceleration of the vehicle (top four graphs in Figure 44). This signal was created from intuition using the experience gained during fifteen years of vehicle dynamic research and testing. It should also be noted that the complete time history was available and this signal thus includes some form of “preview”, i.e. switching happens earlier than would be detectable using any sensors on the vehicle.

All the proposed ride comfort vs. handling switching strategies were subsequently compared to and evaluated with this signal.

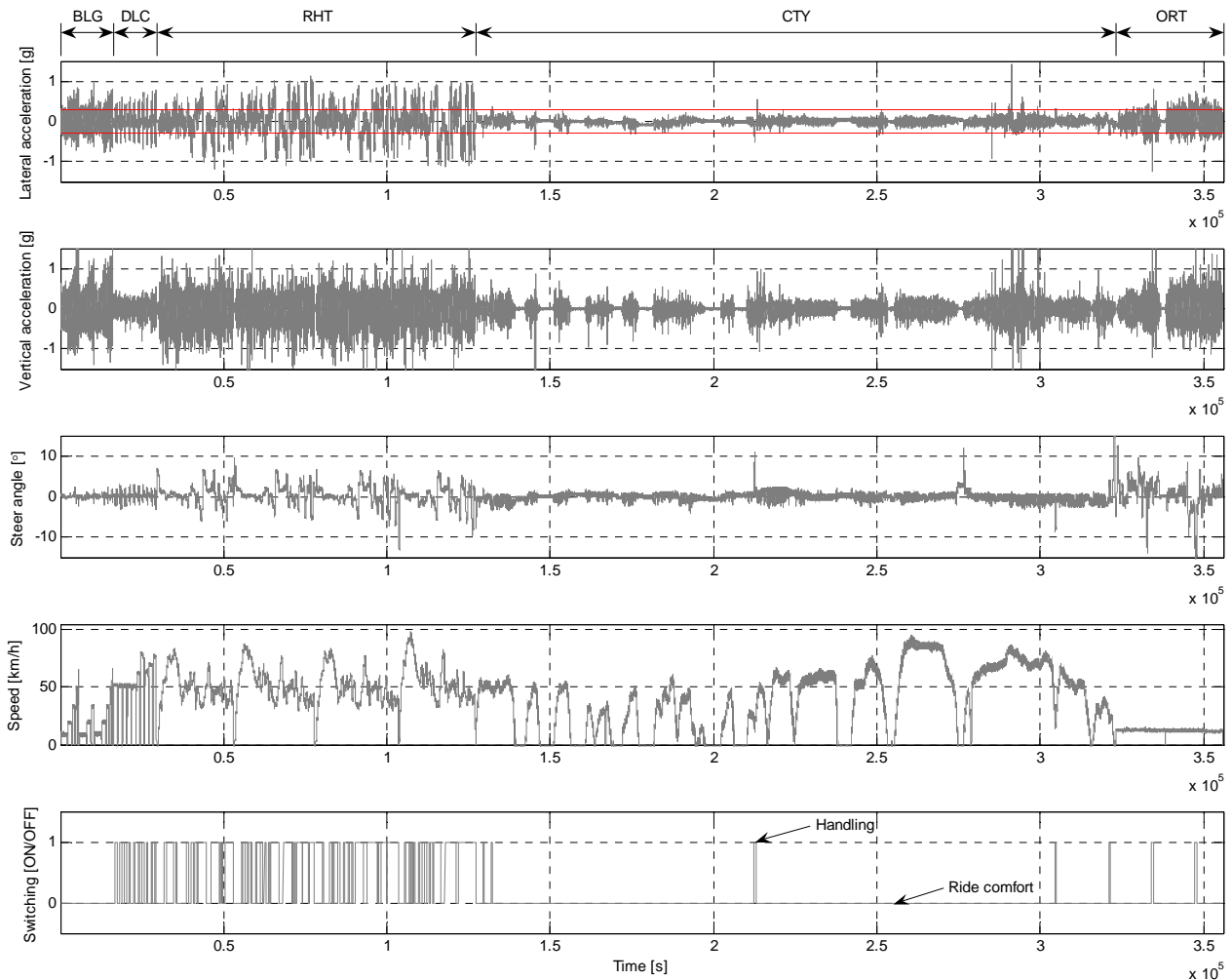
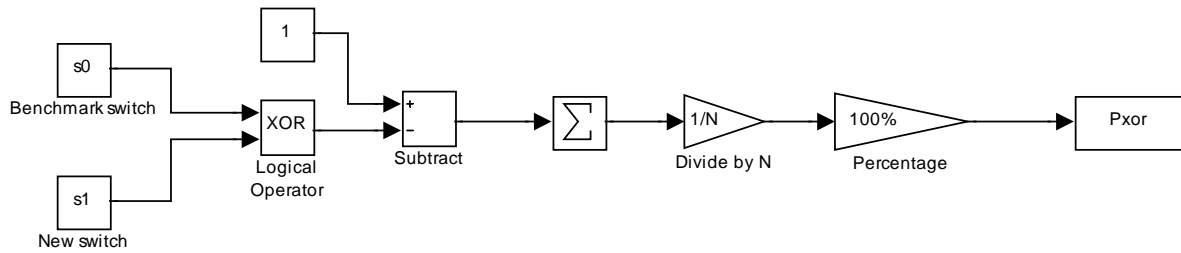


Figure 44: Data used (top four graphs) to generate the Benchmark switch (bottom graph) Els (2006b)

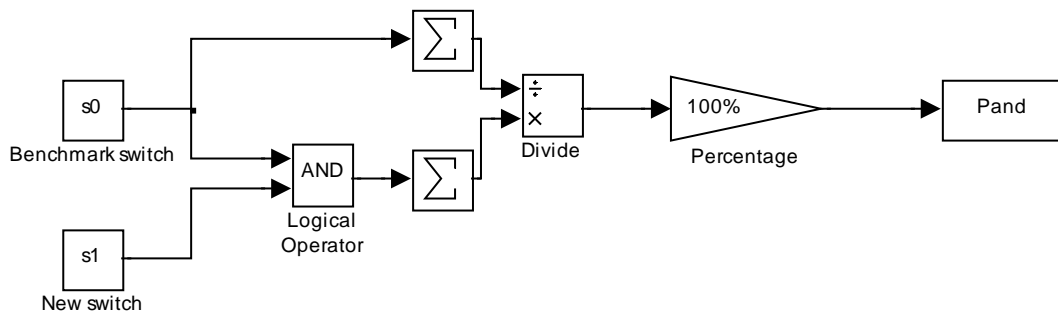
4.2 Comparison metrics

Three main characteristics of each switching signal were used to evaluate any proposed switching strategy when compared to the benchmark. The first characteristic is the number of times that the strategy switches between hard and soft (P_{nsw}). A signal that switches too much causes the valves to chatter. Because it is dangerous if the strategy switches to the soft suspension setting during a handling manoeuvre, the second parameter is an indication of the time that the algorithm and the benchmark are both in handling mode at the same time (P_{and}). Finally, the similarity between both the on and off state of the suspension was compared at a specific point in time (P_{xor}). The mathematical descriptions of these three comparison metrics are given in MATLAB code (www.mathworks.com) in Eq. 10 to Eq. 12 and also graphically in the form of flow diagrams shown in Figure 45 to Figure 47.


Figure 45: P_{xor} flow diagram

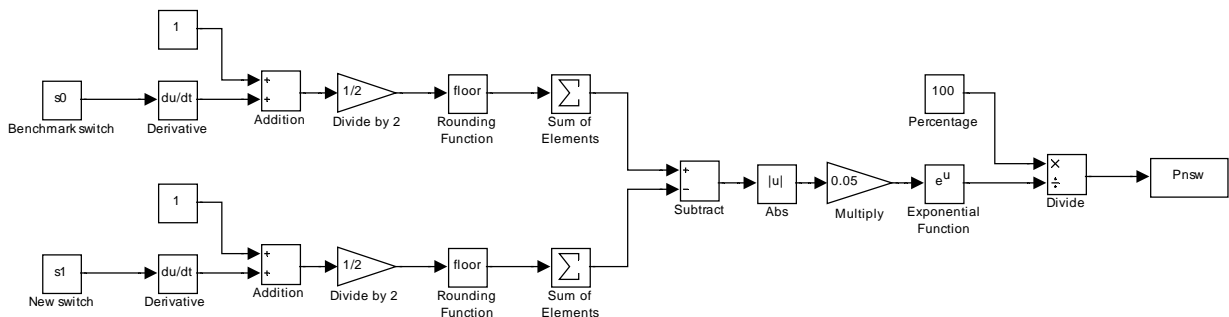
$$P_{xor} = 100 * \text{sum}(1 - \text{xor}(s_0, s_1)) / (\text{length}(s_0))$$

[MATLAB code] Eq. 10


Figure 46: P_{and} flow diagram

$$P_{and} = 100 * \text{sum}(\text{and}(s_0, s_1)) / (\text{sum}(s_0))$$

[MATLAB code] Eq. 11


Figure 47: P_{nsw} flow diagram

$$P_{nsw} = 100 / \exp(0.05 * \text{abs}(\text{sum}(\text{floor}((\text{diff}(s_0) + 1) / 2)) - \text{sum}(\text{floor}((\text{diff}(s_1) + 1) / 2))))$$

[MATLAB code] Eq. 12

Where

s_0 is the benchmark switching signal

s_1 is the proposed switching signal

N or $\text{length}(s_0)$ is the length of the benchmark signal.

The characteristics were weighted differently in order to quantify whether the algorithm performed well. The amount of switching was less important, because it could have exactly the same amount

as the benchmark but could be completely wrong for the other two parameters. On the other hand if P_{nsW} was left out, the strategy could rank high with the on/off characteristic but the switching would happen spuriously and could be dangerous. To prevent the suspension being in soft mode when handling is required, due to spurious switching, the following two solutions were considered namely:

- Delaying the switch to ride comfort mode from the handling mode.
- To have different threshold values (hysteresis) for switching to handling or ride comfort mode.

4.3 Single switch with delay vs. Hysteresis switch

The Single switch strategy is based on an if-statement. If the measured or calculated parameter is above or below a single threshold value, the switch changes its state to OFF or ON depending on what is required. To prevent the switch from chattering around the threshold value, a delay can be added. The delay causes the switch to turn off only after a certain period of time and then only if the algorithm has not switched it back on again. The Hysteresis switching strategy works in a similar way but does not have a delay. The ON threshold value is higher than the OFF threshold value. This inherently causes a delay if the frequency of the measured signal is low enough. If the signal contains a lot of high frequency noise, chattering may occur again. Figure 48 illustrates the difference between these concepts.

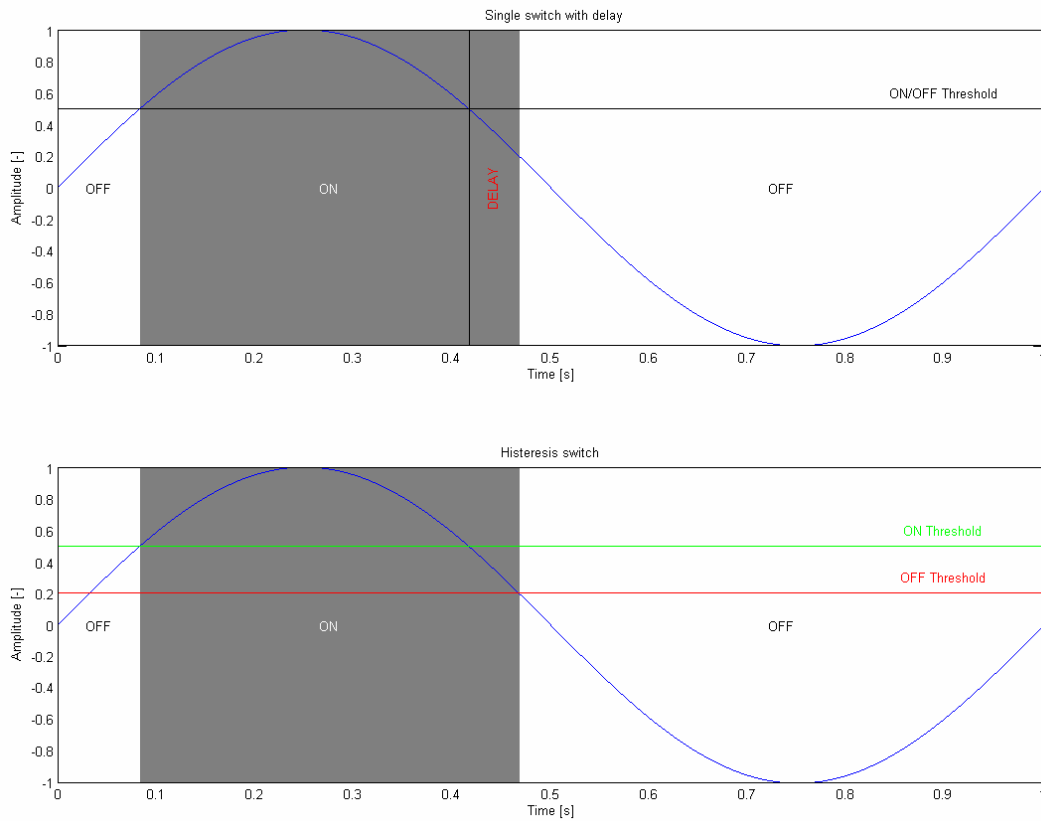


Figure 48: Single switch with delay vs. Hysteresis switch

The disadvantage of the single switch is that the delay can cause the suspension to be stuck in the handling mode while ride comfort is actually required. The disadvantage of the Hysteresis switch is that if the zero value shifts, it can also cause the suspension to be in handling mode for too long, as will be seen in Chapter 5.

The first proposed switching strategy is based on the low frequency content at which most handling manoeuvres take place and will be discussed in the following paragraph.

4.4 Fast Fourier Transform analysis

Fourier analysis is extremely useful when working with periodic signals. The concept is based on the fact that any signal can be represented as the sum of an infinite number of sine waves with different frequencies, amplitudes and phase shifts.

When the vehicle is experiencing a handling manoeuvre, the measurements (e.g. lateral acceleration, yaw velocity, suspension displacements, etc.) from most of the onboard sensors, have very distinct low frequency content. The idea is to use the lateral acceleration as a measure of handling. The lower frequencies are very important but the DC or constant offset and drift should

be zero and can become a problem when calculating the FFT. Therefore the frequency band from 0.4 to 3.5 Hz is used. The Fast Fourier Transform or FFT algorithm in MATLAB (www.mathworks.com) is used to transform the measured data to the frequency domain. At each time step the last 256 data points are used to compute the FFT of the vehicle's lateral acceleration. The discrete Fourier transform can be calculated faster with the FFT algorithm if the number of points is a multiple of 2 ($2^8 = 256$). The average amplitude over a 0.4 - 3.5 Hz frequency band is calculated and is used in the two switching strategies (Single switch and Hysteresis switch). Figure 49 shows one frame from an animation that displays the time domain input, the FFT and averaged FFT. The last graph is a bar plot that compares the proposed strategy with the Benchmark.

The Single switch strategy had an ON/OFF threshold value of 0.04 and no delay. The Hysteresis switch had an ON threshold value of 0.04 and an OFF threshold value of 0.01. Figure 50 compares the Single switch and the Hysteresis switch to the benchmark for all the tests. Appendix A.2 gives a more detailed view of each test (Figure 74 to Figure 78). Table 10 and Table 11 reveal the actual performance of each strategy compared to the benchmark.

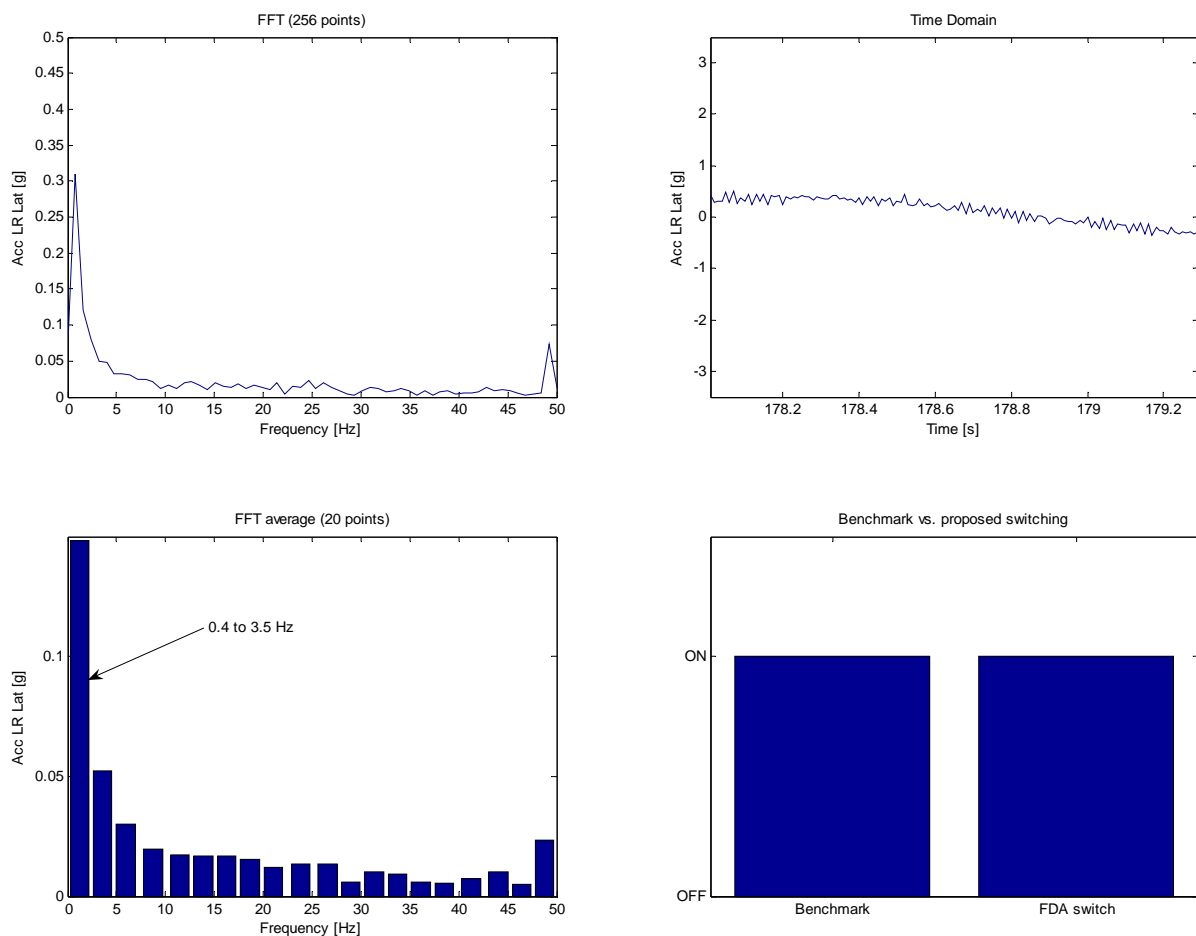


Figure 49: The FFT plots, Lateral acceleration and Benchmark comparison

The comparison metrics are used to evaluate their performance. The “nsw” is the number of switches that took place for the proposed strategy and in brackets is the benchmark’s number of switches for that specific test.

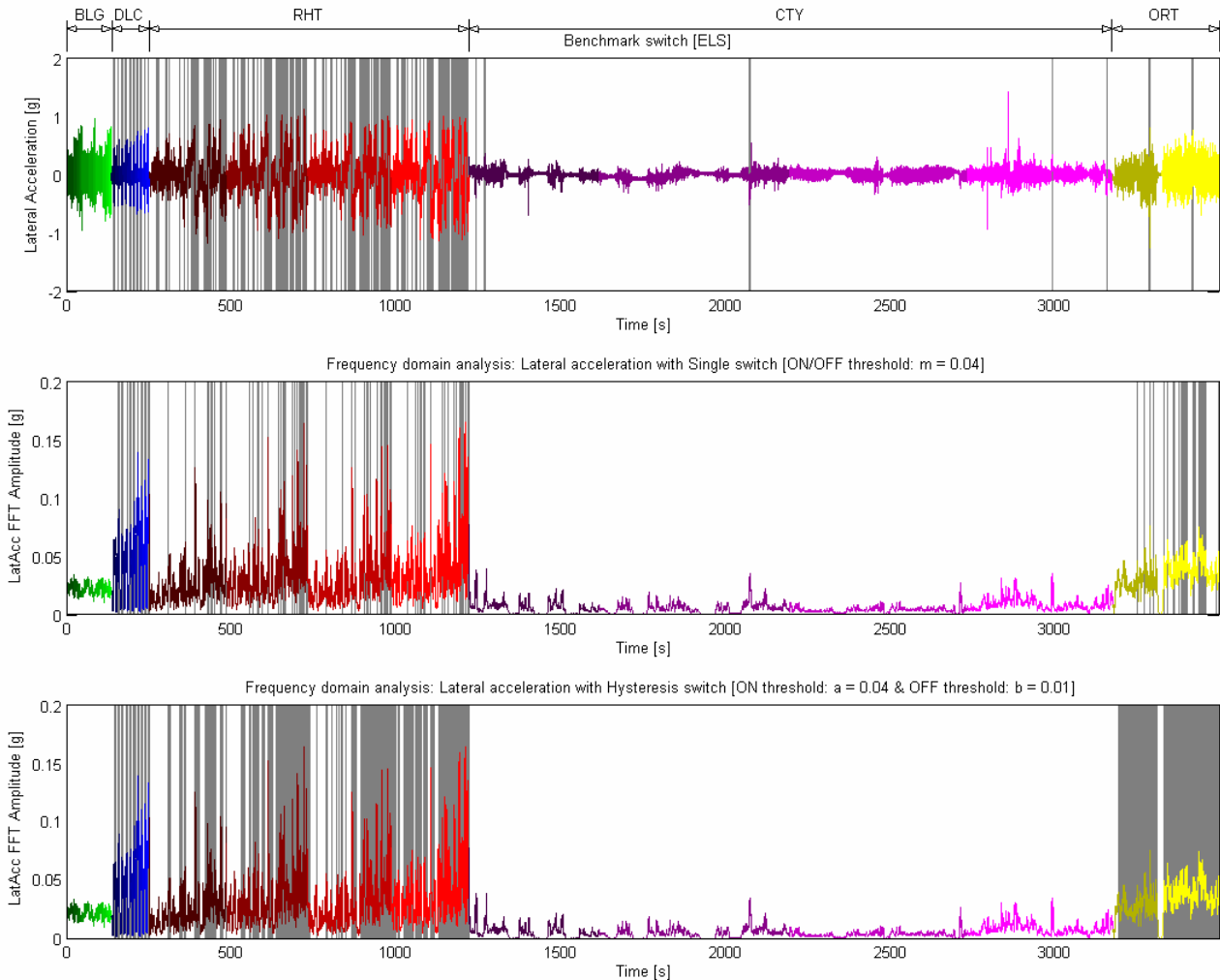


Figure 50: Comparing the Benchmark switch with the Single switch and the Hysteresis switch

Parameter	BLG	DLC	RHT	CTY	ORT	ALL
P_{xor} [%]	100.0	73.8	70.9	98.8	14.6	82.2
P_{and} [%]	100.0	90.4	79.5	0.0	100.0	78.0
P_{nsw} [%]	100.0	100.0	47.2	77.9	100.0	36.8
nsw	0 (0)	10 (10)	34 (49)	0 (5)	2 (2)	46 (66)

Table 10: Performance of the lateral acceleration frequency domain analysis using the Hysteresis switch strategy

Parameter	BLG	DLC	RHT	CTY	ORT	ALL
P_{xor} [%]	100.0	74.4	56.6	98.8	70.3	83.6
P_{and} [%]	100.0	79.5	35.8	0.0	27.7	38.0
P_{nsw} [%]	100.0	57.7	0.1	77.9	0.6	0.0
nsw	0 (0)	21 (10)	187 (49)	0 (5)	106 (2)	314 (66)

Table 11: Performance of the lateral acceleration frequency domain analysis using the Single switch strategy

The colour code for the tables is black: 90 to 100 %, dark grey: 80 to 90 %, light grey: 70 to 80 % and white: below 70 %). This will be used with all the performance tables that follow. The Hysteresis switch works better than the Single switch in general. Both methods did very well with the Belgian paving (no switching). There is however, still a problem with the switching over the Ride and handling track and the Off-road track.

The same strategy was repeated using yaw velocity instead of lateral acceleration. For this instance it was found that the Hysteresis switch again produced better results than the Single switch, specifically with the Double lane change and Ride and handling track tests.

The ON threshold value, $a = 0.8$, and the OFF threshold value, $b = 0.3$, were determined by optimizing the following objective function:

$$P_{comb} = 100(0.6P_{xor} + 0.3P_{and} + 0.1P_{nsw}) \quad \text{Eq. 13}$$

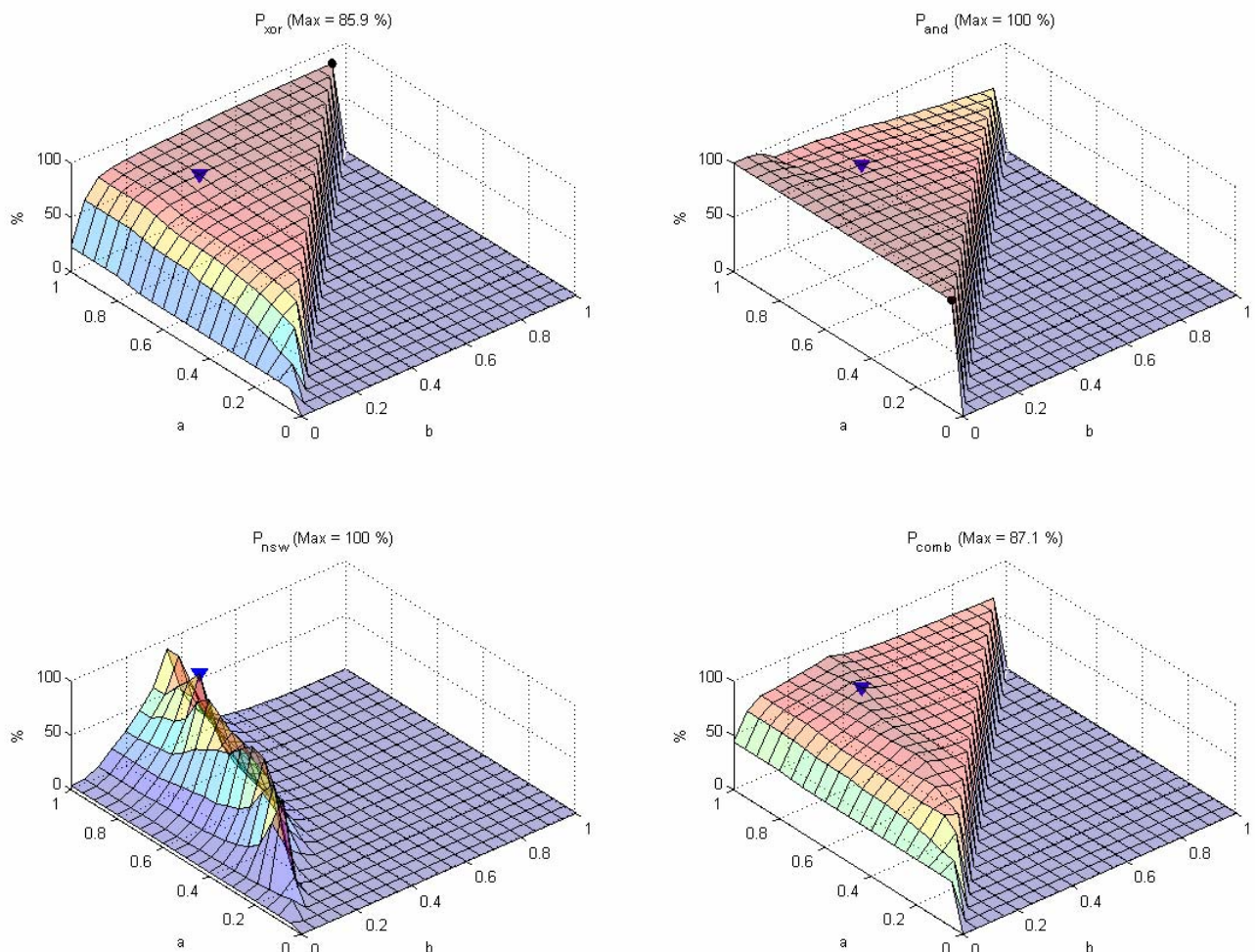


Figure 51: Optimization of ON and OFF threshold values for the Hysteresis switch (based on yaw velocity)

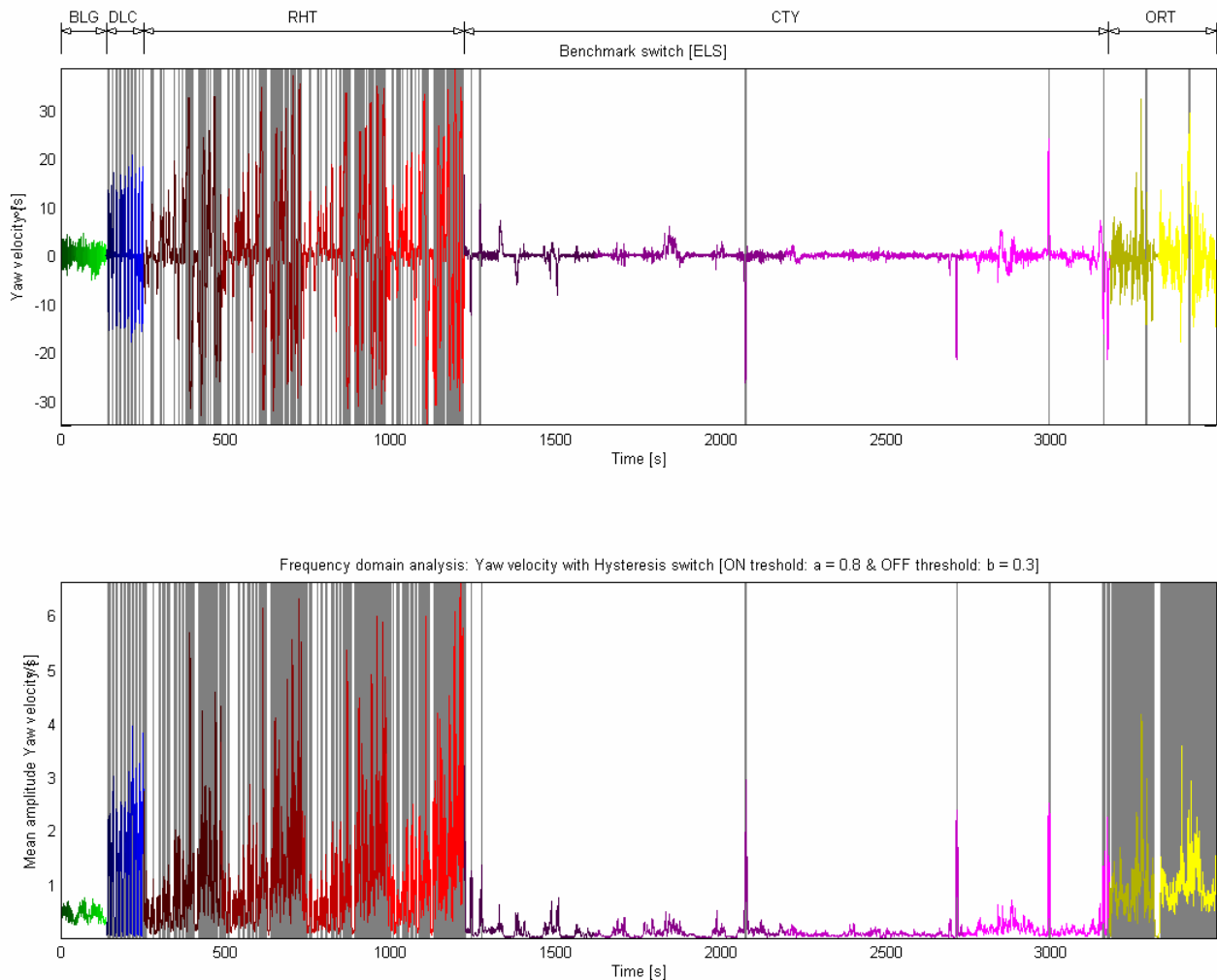


Figure 52: A comparison between the Benchmark switch and the Hysteresis switch (Yaw velocity frequency domain analysis)

Parameter	BLG	DLC	RHT	CTY	ORT	ALL
P_{xor} [%]	100.0	77.0	74.1	98.0	10.1	82.6
P_{and} [%]	100.0	95.0	91.8	78.4	100.0	91.8
P_{nsw} [%]	100.0	100.0	90.5	90.5	100.0	100.0
nsw	0 (0)	10 (10)	47 (49)	7 (5)	2 (2)	66 (66)

Table 12: Performance of the yaw velocity frequency domain analysis using the Hysteresis switch strategy

Figure 51 shows the objective function and each term separately. The domain where $a \geq b$ is used because the time to compute the rest of the domain increased dramatically. This however is the only logical combination of these two parameters. The black dot shows the maximum for that specific term and the blue triangle represents the position of the optimum point for the whole objective function. Figure 52 and Table 12 display the results for this strategy. More detail is shown in Appendix A.3 (see Figure 79 to Figure 83). This method performed well with the exception of the Off-road track section. The low frequency yaw velocity content when moving over rocky terrain is relatively high compared to the Belgian paving.

Another frequency domain method is discussed in the next section and uses the correlation between two signal's phase information, also called coherence.

4.5 Coherence

Coherence can be explained by considering waves in a body of water. When two waves are coherent they will superimpose on top of each other and become a larger wave. If the same two waves are out of phase or are not coherent they will cancel each other out. Coherence is also a frequency based analysis and is a function of the power spectra and the cross spectrum of two separate signals (MATLAB, www.mathworks.com). In other words it compares the phase angles of two signals. Signals with exactly the same phase information will have a coherence of one. On the other hand if the two signals are completely out of phase the coherence will be zero. Thus the degree of correlation between the two signal's phases can be computed with coherence.

$$C_{xy} = \frac{|P_{xy}|^2}{P_{xx}P_{yy}} \tag{Eq. 14}$$

Where C_{xy} is the coherence of the two signals

P_{xy} is the cross power spectral density function between the signals

P_{xx} and P_{yy} are the power spectral density functions of signal x and y

(MATLAB, www.mathworks.com)

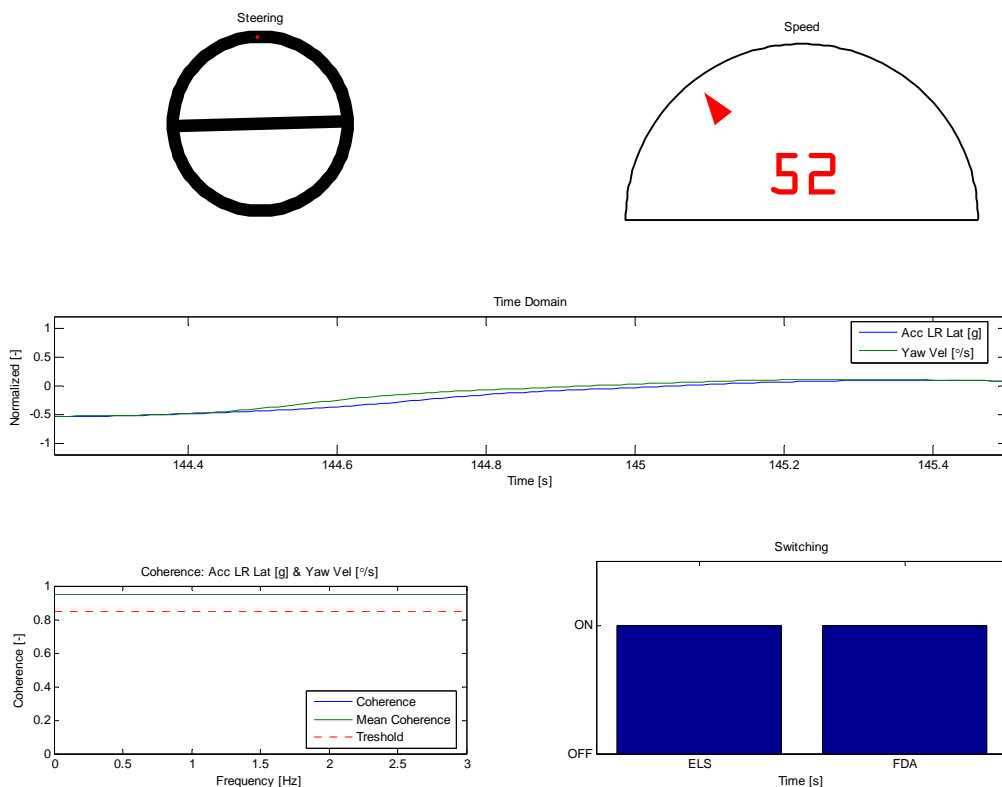


Figure 53: Normalised steering angle and speed (maximum = 1, minimum = -1), Coherence and the comparison of the strategy with the Benchmark

As mentioned in the previous section, some measurements contain similar low frequency characteristics. This is also true for low frequency phase angles of these signals. Good coherence is achieved when two signals are in phase. Figure 53 indicates one frame of an animation that shows the steering input, the speed, two normalised signals, the computed coherence and it's mean. A bar plot shows the proposed switching strategy compared to the benchmark switch signal for the specific time step. A coherence value of 0.85 was used as the ON/OFF threshold.

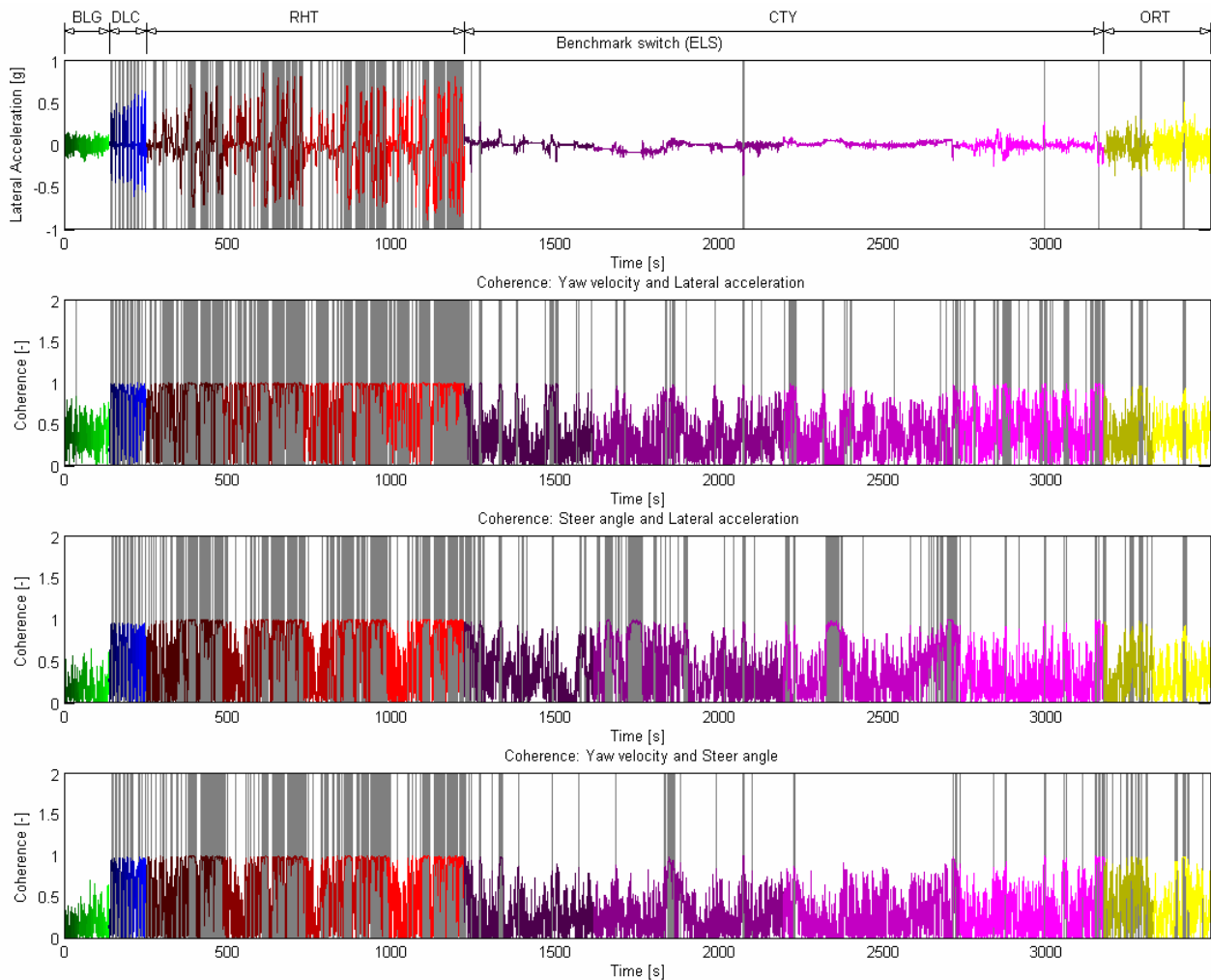


Figure 54: A comparison between the Benchmark switch and the three possible coherence strategies

The performance of the coherence strategies is shown in Figure 54. Each type of test is displayed in more detail in Appendix A.4 (see Figure 84 to Figure 88). The three possibilities are the coherence of all the combinations from two of the following parameters: yaw velocity, steer angle and lateral acceleration. Table 13 to Table 15 give a summary of the performance of each strategy in each test. It is clear that the coherence of the yaw velocity and the lateral acceleration produced the best overall results although it switched twice on the Belgian paving. An excessive amount of switching did however occur in most of the tests.

Parameter	BLG	DLC	RHT	CTY	ORT	ALL
P_{xor} [%]	98.3	80.5	75.6	81.5	92.0	81.4
P_{and} [%]	0.0	96.7	96.2	93.5	100.0	96.2
P_{nsw} [%]	90.5	77.9	36.8	1.5	70.5	0.3
nsw	2 (0)	15 (10)	69 (49)	89 (5)	9 (2)	183 (66)

Table 13: Performance of Hysteresis switch [Coherence between: yaw velocity and lateral acceleration]

Parameter	BLG	DLC	RHT	CTY	ORT	ALL
P_{xor} [%]	100.0	75.1	73.3	79.6	90.1	79.5
P_{and} [%]	100.0	70.0	81.1	85.8	95.2	80.6
P_{nsw} [%]	100.0	60.7	18.3	1.7	67.0	0.1
nsw	0 (0)	20 (10)	83 (49)	87 (5)	10 (2)	200 (66)

Table 14: Performance of Hysteresis switch [Coherence between: steer angle and lateral acceleration]

Parameter	BLG	DLC	RHT	CTY	ORT	ALL
P_{xor} [%]	100.0	77.4	74.7	90.8	76.7	84.9
P_{and} [%]	100.0	83.0	81.8	83.5	94.2	82.2
P_{nsw} [%]	100.0	70.5	24.7	6.1	42.7	0.5
nsw	0 (0)	17 (10)	77 (49)	61 (5)	19 (2)	174 (66)

Table 15: Performance of Hysteresis switch [Coherence between: yaw velocity and steer angle]

Coherence did not produce acceptable results. Fuzzy logic was already used as a terrain classification method and will now be investigated further as a switching strategy.

4.6 Fuzzy logic switching strategy

Using Fuzzy logic to get a switching signal can be very complicated because of the immense number of parameters that can be set by the user. To really use the full potential of this method it is advised that a formal optimization analysis of these parameters be done. It is however possible to obtain a relatively good answer with little effort based on the user's knowledge about the system as shown in the next few figures. Figure 55 shows the Graphic User Interface (GUI) in which the Fuzzy Inference System (FIS) was created. The left window displays the input membership functions and the right the output membership functions.

Two simple rules were used to govern this switch namely:

- If the Lateral acceleration is equal to Ride comfort then the suspension should be Soft
- If the Lateral acceleration is equal to Handling then the suspension should be Hard

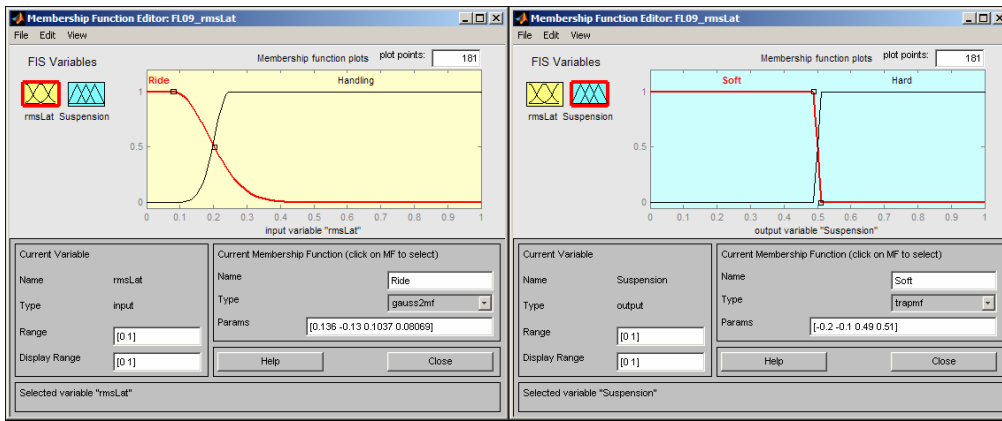


Figure 55: Fuzzy logic input and output membership functions

Figure 56 and Table 16 compares the Fuzzy logic output to the benchmark switch. The results are shown in more detail in Appendix A.5 (see Figure 89 to Figure 93).

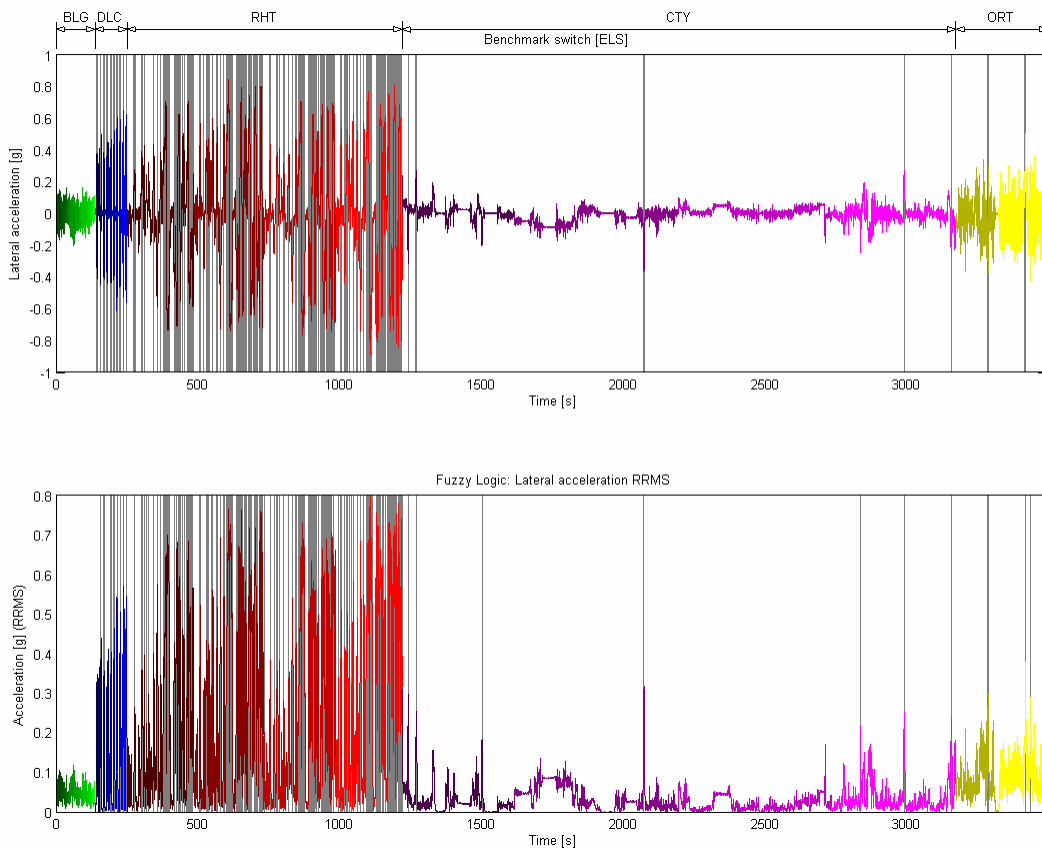


Figure 56: Comparison between the Benchmark switch and the Fuzzy logic switch

Parameter	BLG	DLC	RHT	CTY	ORT	ALL
P_{xor} [%]	100.0	88.1	89.1	99.4	95.6	95.8
P_{and} [%]	100.0	80.2	87.8	65.6	60.8	85.8
P_{nsw} [%]	100.0	63.8	4.7	70.5	27.3	0.6
nsw	0 (0)	19 (10)	110 (49)	12 (5)	28 (2)	169 (66)

Table 16: Performance of Fuzzy logic switch

The Fuzzy logic did not do particularly well in any of the tests. There is however a lot of possible combinations of different parameters that might improve this method.

Many of the methods discussed switch too late to the handling mode. In an attempt to have a faster switch response, polynomial fits are used to predict the future based on a short history of the data.

4.7 Polynomial prediction

This method is used to predict what a signal will do a few time steps in the future. This is done by fitting polynomial functions of a specific order to the data and extrapolating to a point in the future. The functions are fitted using the least-squares approximation.

The first to fourth order polynomial functions were fitted to a running window of lateral acceleration. This is an attempt to produce an early warning for the suspension control system. The lateral acceleration was filtered with a 3 Hz ideal low pass filter to obtain a smoother signal for better polynomial fits. The window is 2 seconds (200 points) long and a further 200 milliseconds (20 points) are extrapolated into the future. These functions are averaged to get a combined function that closely approximates the signal. Two averaging methods were used. Every function approximates the signal to a certain degree. The Least error mean method weighted each polynomial function inversely proportionate to the least mean square error. A large weight is multiplied with the function that has the smallest least mean square error and *vice versa*. The second method, Equal weight mean, applied an equal weight to all the functions. This furthest extrapolated point is then used in the switching strategy. Unfortunately the polynomial fits are very laborious and take a long time to compute therefore the calculations are done every 0.5 s. Figure 57 shows the four polynomial functions in the first graph, the two averaging methods in the second graph and the result of the two methods in the bottom graph.

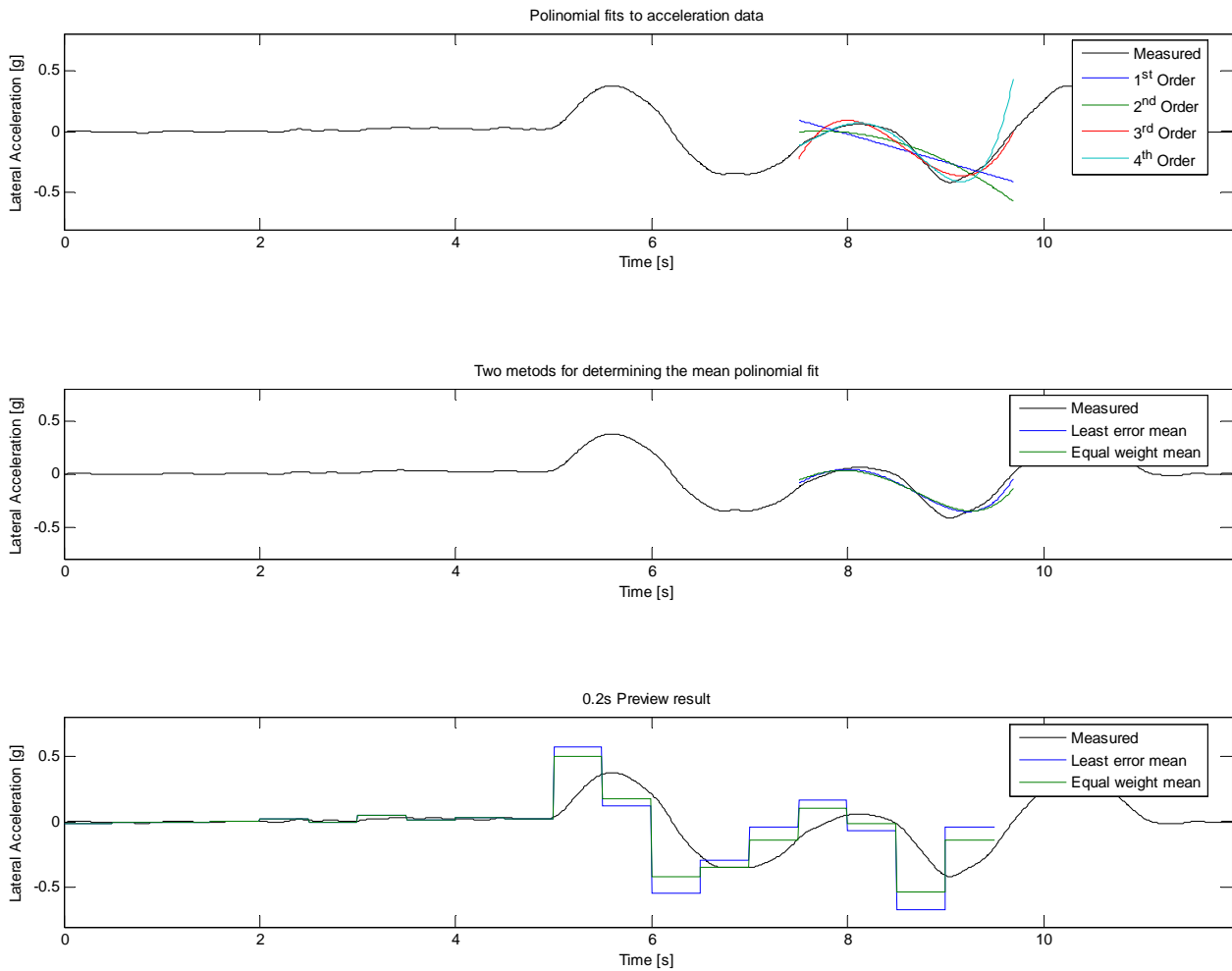


Figure 57: The process of determining the Polynomial prediction

The performance of these two strategies is shown in Figure 58. A figure of each test type is shown in Figure 94 to Figure 98 (Appendix A.6). Table 17 and Table 18 confirm that the strategies fail on the Off-road track once again. A Single switch was used with a threshold value of 0.2 g and no delay. The terrain classification methods of chapter 3 could be implemented to adjust the switching thresholds for example over rough terrain in order to get better results.

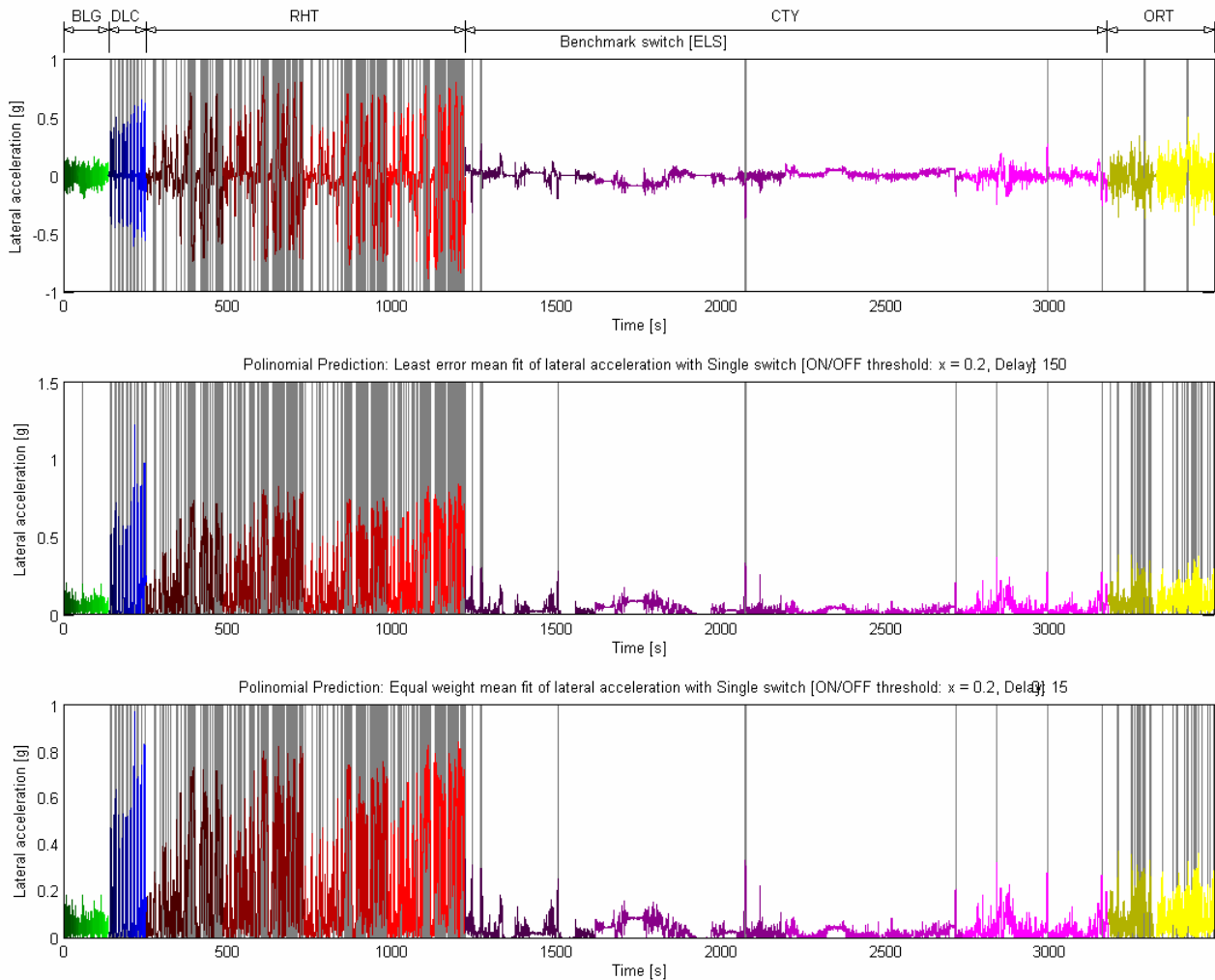


Figure 58: Comparing the Least error mean and the Equal weight mean strategies to the Benchmark

Parameter	BLG	DLC	RHT	CTY	ORT	ALL
P_{xor} [%]	97.1	86.4	86.7	99.0	72.5	92.5
P_{and} [%]	0.0	99.6	97.4	89.9	80.6	97.4
P_{nsw} [%]	90.5	100.0	36.8	77.9	25.9	5.2
nsw	2 (0)	10 (10)	69 (49)	10 (5)	29 (2)	125 (66)

Table 17: Performance of Polynomial prediction with Least error weighted mean method

Parameter	BLG	DLC	RHT	CTY	ORT	ALL
P_{xor} [%]	100.0	89.5	87.2	99.1	74.3	93.2
P_{and} [%]	100.0	99.6	97.3	84.6	88.3	97.3
P_{nsw} [%]	100.0	100.0	35.0	81.9	27.3	6.4
nsw	0 (0)	10 (10)	70 (49)	9 (5)	28 (2)	121 (66)

Table 18: Performance of Polynomial prediction with Equal weighted mean method

Figure 59 shows the difference in reaction time for the absolute of the lateral acceleration and its polynomial prediction during the Double lane change. The top graph shows the reaction time of the absolute lateral acceleration compared to the benchmark switch. The dashed lines are the proposed

ON switch and the solid lines show the Benchmark's ON switch signal. Similarly the second graph shows the Polynomial prediction strategy's reaction time relative to the Benchmark. The third graph on this figure shows a stem plot depicting the difference. A positive value indicates that the switch was activated before the benchmark switch signal. Negative values represent a late switch compared to the benchmark. From these results it can be concluded that the polynomial prediction can improve the reaction time of the control system. Unfortunately it switches too many times when compared to the other strategies.

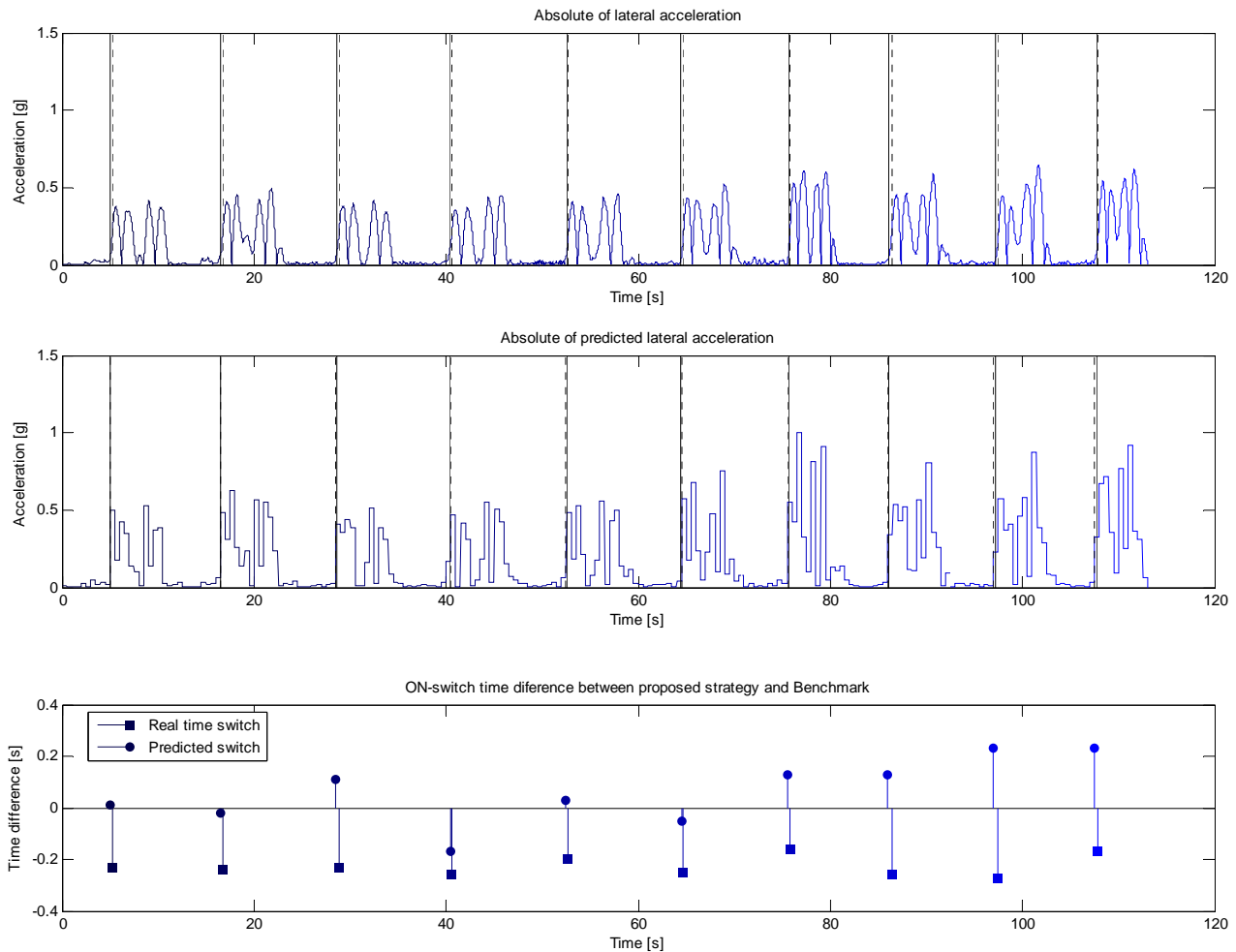


Figure 59: Comparing the ON-switch delay, using polynomial prediction, with the Benchmark

4.8 Running Root Mean Square (RRMS) of the lateral acceleration

Statistics is a powerful way of describing large datasets. Most statistical functions (e.g. mean, standard deviation, etc.) give a single value output of an input vector. In order to make an informed decision the most recent values of a signal is used to calculate some statistical property. This window moves over the signal obtaining a new point and discarding the oldest value at each time step. The term running window is used for this reason. The number of points in the window is of

great importance because it acts like a low-pass filter, cutting off higher frequency content. Large windows have lower cut-off frequencies. If the window is too short statistical content may be lost.

To obtain an indication of the average amplitude of the signal the Root Mean Square (RMS) is used. The RMS of the signal x , y_{rms} , can be calculated as follows.

$$y_{rms} = \sqrt{\frac{\sum_{i=1}^N x_i^2}{N}} \quad \text{Eq. 15}$$

Where x is the signal and N is the number of data points in x .

The Running Root Mean Square (RRMS) method was the first strategy implemented by **Els (2006a)**. A running RMS or RRMS means that the RMS is calculated from the last N points of the signal. The new RRMS signal represents the change in amplitude of the original signal. A window of 100 data points ($N = 100$ or 1 second of data at 100 Hz sampling frequency) was used in the following analysis. The size of this window is the same as was used by **Els (2006a)**. This parameter was not optimized but in a study of eight different values it produced both the least amount of chattering and had the quickest response time. The strategy used running RMS lateral acceleration compared to the running RMS of the vertical acceleration. Ride comfort mode is selected if the RRMS lateral acceleration is less than 0.05 g. The Handling mode is selected if the RRMS lateral acceleration is larger than the RRMS vertical acceleration and greater than 0.05 g or if the RRMS lateral acceleration exceeds 0.3 g. The strategy worked well except for the Double lane change test where the ride comfort mode was selected halfway through the test. The challenge was to see if it could be improved upon. Changing parameters always produced a trade-off between response time and the frequency of switching.

The two switching strategies: Single switch with delay and Hysteresis switch, were again considered. The vehicle will be in ride comfort mode most of the time and will only switch to handling mode when it is needed. For this reason only the lateral acceleration was considered as the input to these switching strategies. A crude optimization method was used to determine the best parameters for each method. The two parameters for the single switch strategy were the ON/OFF threshold (m) and the number of data points (N) to delay the OFF switch. The ON (a) and OFF (b) threshold values were optimized for the Hysteresis switch.

The same objective function was used as before (see Eq. 13), where 0% is poor and 100% is a perfect performance. The three terms are weighted according to their importance. Figure 60 and Figure 61 show the optimization of each term (P_{xor} , P_{and} , and P_{nsw}) in the objective function and the combination of these terms (P_{comb}). The black dots represent the optimum for each term, while the blue triangle represents the combined optimum.

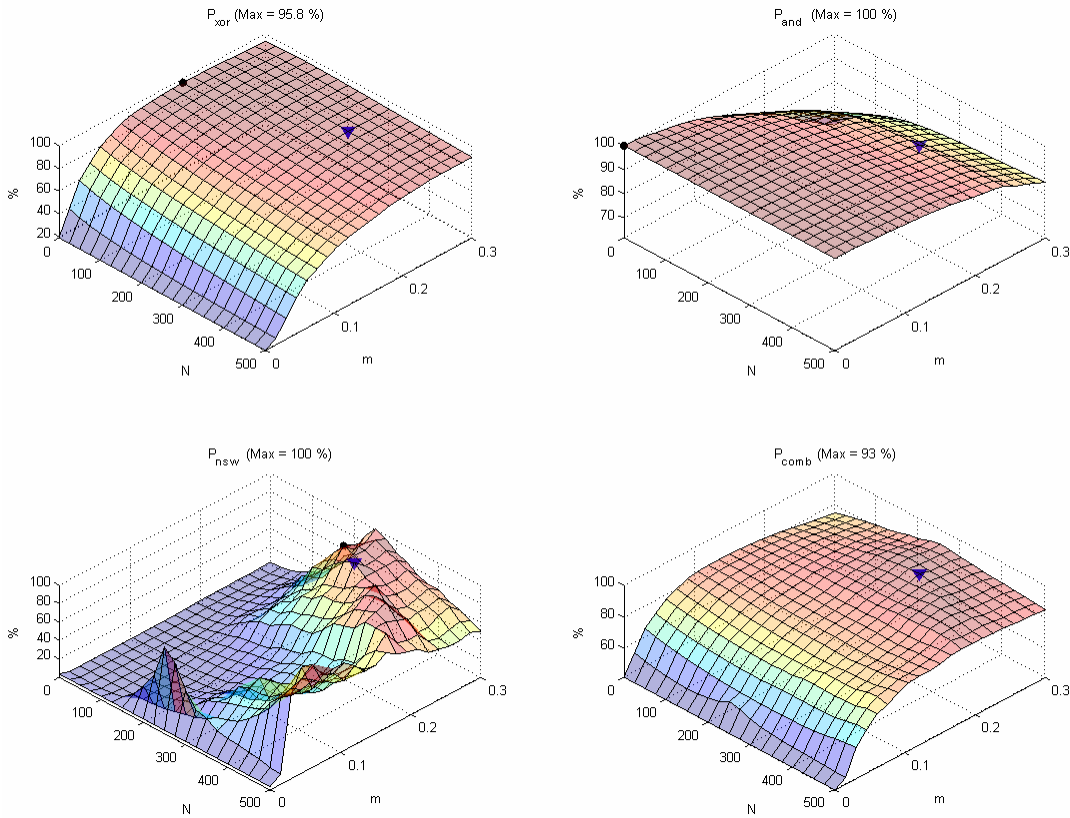


Figure 60: Single switch optimization surfaces

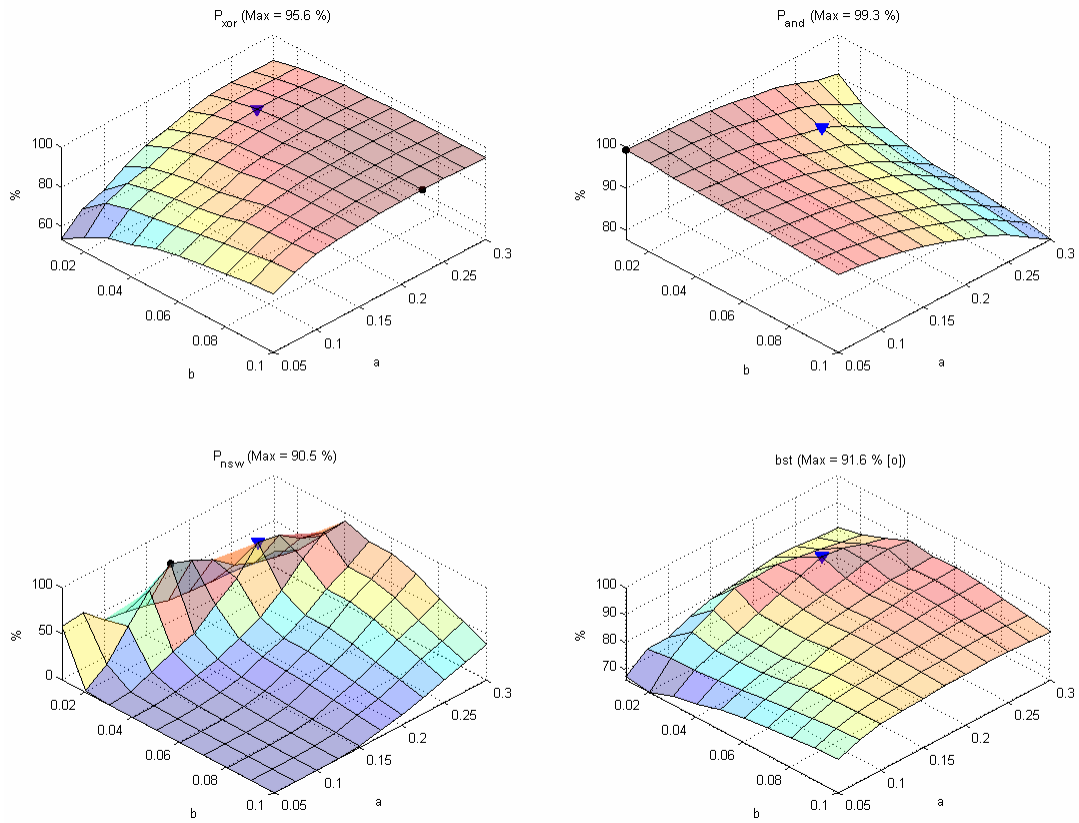
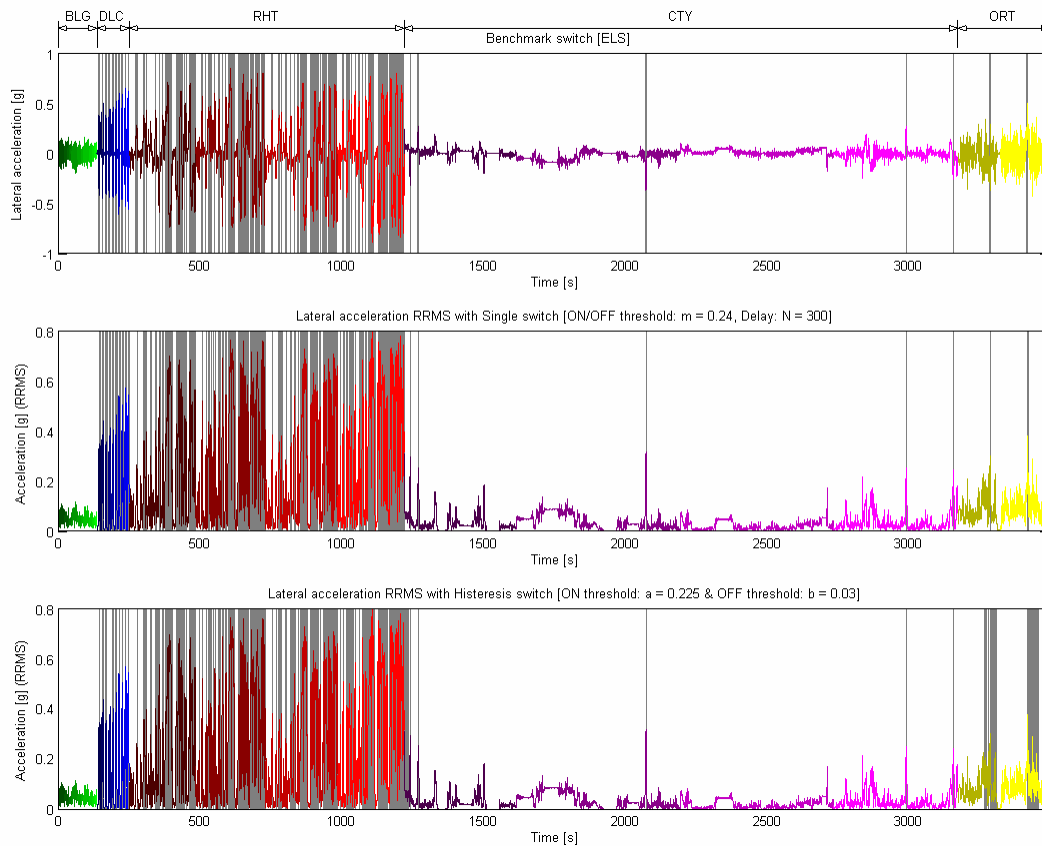


Figure 61: Hysteresis switch optimization surfaces

Figure 62 displays the benchmark comparison with the Hysteresis switch and the Single switch. Each test is shown separately in Appendix A.7 (see Figure 99 to Figure 103). Table 19 and Table 20 give the performance of each strategy on each test.


Figure 62: Comparison of the Benchmark switch, Single switch and Hysteresis switch strategies

Parameter	BLG	DLC	RHT	CTY	ORT	ALL
P_{xor} [%]	100.0	70.8	81.2	99.0	96.2	92.9
P_{and} [%]	100.0	91.0	92.9	62.7	56.5	90.9
P_{nsw} [%]	100.0	100.0	95.1	100.0	95.1	100.0
nsw	0 (0)	10 (10)	48 (49)	5 (5)	3 (2)	66 (66)

Table 19: Performance of RRMS Lateral acceleration Single switch, [ON/OFF threshold: $m = 0.24$ & Delay: $N = 300$]

Parameter	BLG	DLC	RHT	CTY	ORT	ALL
P_{xor} [%]	100.0	87.0	83.8	99.2	75.6	91.9
P_{and} [%]	100.0	89.1	93.5	67.2	64.1	91.6
P_{nsw} [%]	100.0	90.5	90.5	100.0	90.5	90.5
nsw	0 (0)	12 (10)	47 (49)	5 (5)	4 (2)	68 (66)

Table 20: Performance of RRMS Lateral acceleration Hysteresis switch, [ON threshold: $a = 0.225$ & OFF threshold: $b = 0.03$]

The RRMS methods gave the best results thus far. The only serious problem is noticed with the P_{and} parameter on the Off-road track and the city traffic tests, but the P_{nsw} is quite accurate. This means that the handling mode for these tests did not coincide with the benchmark's handling sections. From these results it appears that the Single switch with delay produces the best overall switching signal.

4.9 Conclusion of the Ride comfort vs. Handling switching strategies

The Ride comfort vs. handling decision is crucial to the success of the $4S_4$ system. Table 21 to Table 23 presents the comparisons of each strategy's performance.

Terrain		P_{xor} [%]										
		Strategy										
		Frequency domain			Coherence			Fuzzy Logic	Polynomial prediction		RRMS	
	Single switch, Lateral acceleration	Hysteresis switch, Lateral Acceleration	Hysteresis switch, Yaw velocity	Hysteresis switch, Yaw velocity and Lateral acceleration	Hysteresis switch, Steer angle and Lateral acceleration	Hysteresis switch, Yaw velocity and Steer angle	FIS switch, Lateral acceleration	Least error mean method, Lateral acceleration	Equal weight mean method, Lateral acceleration	Hysteresis switch, Lateral acceleration	Single switch, Lateral acceleration	
BLG	100.0	100.0	100.0	98.3	100.0	100.0	100.0	97.1	100.0	100.0	100.0	
DLC	74.4	73.8	77.0	80.5	75.1	77.4	88.1	86.4	89.5	87.0	70.8	
RHT	56.6	70.9	74.1	75.6	73.3	74.7	89.1	86.7	87.2	83.8	81.2	
CTY	98.8	98.8	98.0	81.5	79.6	90.8	99.4	99.0	99.1	99.2	99.0	
ORT	70.3	14.6	10.1	92.0	90.1	76.7	95.6	72.5	74.3	75.6	96.2	
ALL	83.6	82.2	82.6	81.4	79.5	84.9	95.8	92.5	93.2	91.9	92.9	

Table 21: Performance of switching strategies (P_{xor})

Table 21 shows the percentage of the similarity of the strategy compared to the Benchmark signal. All the strategies performed quite well with the Belgian paving and city traffic for this objective parameter (P_{xor}). The best overall performers were: Fuzzy logic (FIS switch), Polynomial prediction (Equal weight mean method) and both RRMS strategies.

P_{and} [%]

Terrain	Strategy										
	Frequency domain			Coherence			Fuzzy Logic	Polynomial prediction		RRMS	
	Single switch, Lateral acceleration	Hysteresis switch, Lateral Acceleration	Hysteresis switch, Yaw velocity	Hysteresis switch, Yaw velocity and Lateral acceleration	Hysteresis switch, Steer angle and Lateral acceleration	Hysteresis switch, Yaw velocity and Steer angle	FIS switch, Lateral acceleration	Least error mean method, Lateral acceleration	Equal weight mean method, Lateral acceleration	Hysteresis switch, Lateral acceleration	Single switch, Lateral acceleration
BLG	100.0	100.0	100.0	0.0	100.0	100.0	100.0	0.0	100.0	100.0	100.0
DLC	79.5	90.4	95.0	96.7	70.0	83.0	80.2	99.6	99.6	89.1	91.0
RHT	35.8	79.5	91.8	96.2	81.1	81.8	87.8	97.4	97.3	93.5	92.9
CTY	0.0	0.0	78.4	93.5	85.8	83.5	65.6	89.9	84.6	67.2	62.7
ORT	27.7	100.0	100.0	100.0	95.2	94.2	60.8	80.6	88.3	64.1	56.5
ALL	38.0	78.0	91.8	96.2	80.6	82.2	85.8	97.4	97.3	91.6	90.9

Table 22: Performance of switching strategies (P_{and})

The P_{and} parameter was established as the measure of simultaneous time spent in the handling mode of the proposed strategy and the Benchmark. On average all the strategies performed well on the Double lane change and the Ride and handling track as seen in Table 22. The frequency domain Hysteresis switch (yaw velocity), the coherence Hysteresis switch (yaw velocity and steer angle) and the Polynomial prediction with equal weight mean (lateral acceleration) showed the most potential in this category. The coherence Hysteresis switch (yaw velocity and lateral acceleration)

and the Polynomial prediction with least error mean (lateral acceleration) also did well but both of them switched twice over the Belgian paving which none of the other strategies did.

Terrain		$P_{nsw} [\%]$										
		Strategy										
		Frequency domain			Coherence			Fuzzy Logic	Polynomial prediction		RRMS	
Single switch, Lateral acceleration	Hysteresis switch, Lateral Acceleration	Hysteresis switch, Yaw velocity	Hysteresis switch, Yaw velocity and Lateral acceleration	Hysteresis switch, Steer angle and Lateral acceleration	Hysteresis switch, Yaw velocity and Steer angle	FIS switch, Lateral acceleration	Least error mean method, Lateral acceleration	Equal weight mean method, Lateral acceleration	Hysteresis switch, Lateral acceleration	Single switch, Lateral acceleration		
BLG	100.0	100.0	100.0	90.5	100.0	100.0	100.0	90.5	100.0	100.0	100.0	100.0
DLC	57.7	100.0	100.0	77.9	60.7	70.5	63.8	100.0	100.0	90.5	100.0	100.0
RHT	0.1	47.2	90.5	36.8	18.3	24.7	4.7	36.8	35.0	90.5	95.1	95.1
CTY	77.9	77.9	90.5	1.5	1.7	6.1	70.5	77.9	81.9	100.0	100.0	100.0
ORT	0.6	100.0	100.0	70.5	67.0	42.7	27.3	25.9	27.3	90.5	95.1	95.1
ALL	0.0	36.8	100.0	0.3	0.1	0.5	0.6	5.2	6.4	90.5	100.0	100.0

Table 23: Performance of switching strategies (P_{nsw})

The number of switches that a strategy produces is compared to the Benchmark signal and with an exponential function is translated into a performance percentage (P_{nsw}). A low percentage means that the number of switches was either too high or too low compared to the benchmark signal. All the strategies performed well on the Belgian paving because no switching was ever required over

this terrain. The frequency domain Hysteresis switch (yaw velocity) and the two RRMS (lateral acceleration) strategies performed extremely well compared to the others.

The overall best performing strategies were determined using the objective function that was used to optimize some of the methods (see Eq. 13). The bottom three strategies, shown in Table 24, produced the best results overall.

Methodology	Strategy	Performance (%)
Frequency domain	Single switch, Lateral acceleration	71.6
	Hysteresis switch, Lateral acceleration	68.8
	Hysteresis switch, Yaw velocity	81.7
Coherence	Hysteresis switch, Yaw velocity and Lateral acceleration	79.7
	Hysteresis switch, Steer angle and Lateral acceleration	79.5
	Hysteresis switch, Yaw velocity and Steer angle	80.8
Fuzzy Logic	FIS switch, Lateral acceleration	85.3
Polynomial prediction	Least error mean method, Lateral acceleration	82.3
	Equal weight mean method, Lateral acceleration	88.5
RRMS	Hysteresis switch, Lateral acceleration	88.4
	Single switch, Lateral acceleration	88.5

Table 24: Overall results for all the strategies

These results are theoretical and needed to be verified with real vehicle tests. The polynomial prediction method requires a lot of processing power and could not be implemented in the current system. The next chapter shows the results of the two RRMS strategies.

5 Experimental results

A set of tests were performed to verify some of the proposed strategies. In this case the passengers' reaction was used as the benchmark switching signal.

5.1 *Passenger response*

Four digital input channels were used for measuring the reaction of the passengers to the movement of the vehicle. Spring loaded pushbuttons were connected to the recording computer. (See Figure 63) The buttons were pushed in if the passenger felt that a handling manoeuvre was being performed. The benchmark signal was defined as ON (handling), if two or more buttons were being pushed at the same time. This benchmark signal is not based on expert knowledge but rather human reaction from the forces that act on a person's body when severe handling manoeuvres are experienced.



Figure 63: Passenger response button

5.2 *Measurements*

The following list of measurements were recorded for this set of tests

- Left front suspension displacement [*mm*]
- Right front suspension displacement [*mm*]
- Left rear suspension displacement [*mm*]
- Right rear suspension displacement [*mm*]
- Left rear lateral acceleration [*g*]
- Left rear vertical acceleration [*g*]
- Right rear lateral acceleration [*g*]

- Right rear vertical acceleration [g]
- Right rear longitudinal acceleration [g]
- Roll velocity [$^{\circ}/s$]
- Yaw velocity [$^{\circ}/s$]
- Left distance laser sensor (not used for this study) [mm]
- Right distance laser sensor (not used for this study) [mm]
- Kingpin angle [$^{\circ}$]
- Vehicle speed from left rear wheel [km/h]
- Vehicle speed from driveshaft [km/h]
- Digital buttons [OFF (0) / ON (1)] (Passenger response)
- Spring setting [Hard (0) / Soft (1)]
- Damper setting [Hard (0) / Soft (1)]
- Digital Butterworth IIR filtered left rear lateral acceleration [g]
- Real-time computed RRMS of filtered left rear lateral acceleration [g]

The spring and damper settings were recorded in order to know exactly when the suspension switched. An IIR Butterworth 3 Hz low pass filter was applied to the lateral acceleration in order to increase the signal to noise ratio (see Eq. 1). The RRMS of this signal was also logged for later analysis.

5.3 Test results

Figure 64 to Figure 73 show selected tests that were done with two of the proposed strategies. These strategies are the Single switch with RRMS lateral acceleration and Hysteresis switch with RRMS lateral acceleration. Both these strategies use the Running Root Mean Square to calculate the RMS of the lateral acceleration of 1 s of data every 0.01 s. Threshold values are then used to determine when the suspension should be set to ride comfort or handling mode. The passenger response can be seen in the top graph of each figure. The passengers' response is displayed in the background of the graph as shades of grey sections. The darkness of these sections represents the number of buttons that are being pressed at that specific time. At first glance there are some problems that can be seen. First of all the real-time filtered data does not seem to have the correct zero value. The reason for this can be explained as follows: when the control program starts, it first obtains the zero values of all the channels while the vehicle is stationary. If the vehicle is not completely horizontal at this time, the lateral acceleration will read an offset of the true zero value. In post-processing the signal can be shifted up or down to get the correct zero value. In addition to this there is also a problem

with zero value drift when extended tests are performed. This may be the result of temperature fluctuations.

Another problem that is evident when looking at the lateral acceleration from the Double lane change (Figure 65 and Figure 66) is the long delay that is caused by the phase shift of the Butterworth IIR filtering and RRMS calculations. This causes delays in the reaction time of the switching strategies and is a serious safety problem that still needs to be addressed.

The RRMS, Single and Hysteresis switching strategies, were programmed into the control computer of the suspension system. The following threshold values were used in the algorithms. The Single switch had an ON threshold of $m = 0.24 \text{ g}$ but no delay was implemented. The Hysteresis switch had an ON threshold of $a = 0.225 \text{ g}$ and an OFF threshold of $b = 0.04 \text{ g}$. It was soon realised that because of the incorrect zero value, the OFF threshold ($b = 0.04 \text{ g}$) of the Hysteresis switch was too low, forcing the vehicle to stay in the handling mode for longer then necessary. This value was increased ($b = 0.1 \text{ g}$) and better results in some cases were observed.

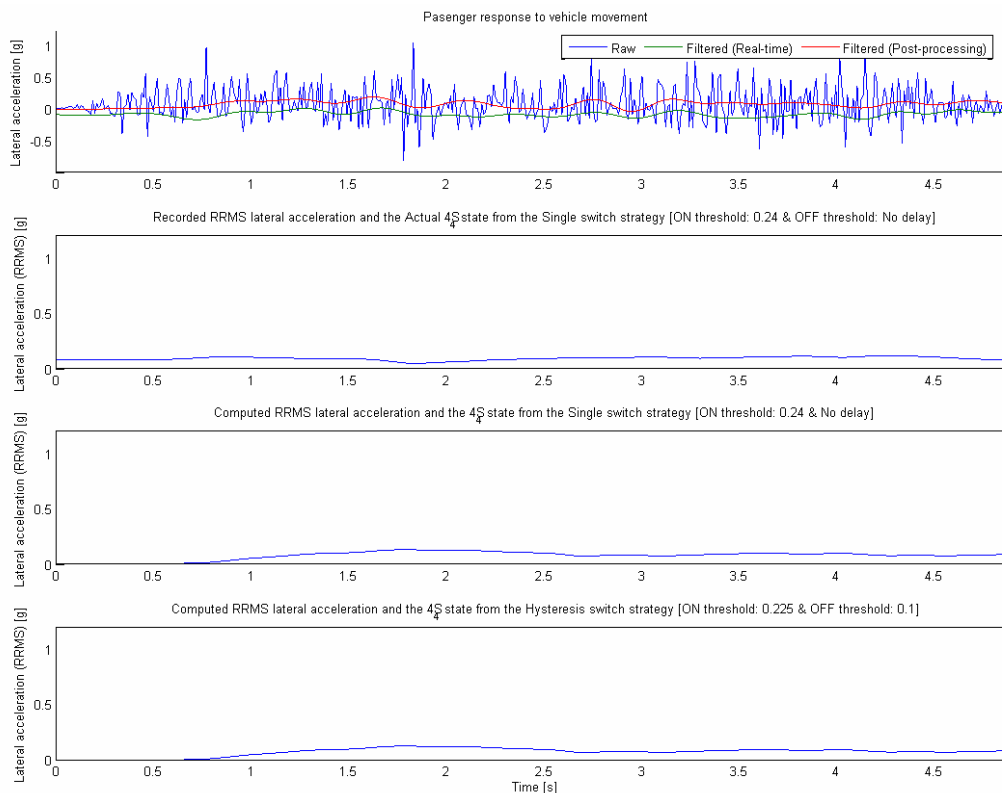


Figure 64: Comparing the actual Single switch [$m = 0.24$, No delay] to the recalculated strategies (BLG)

All the strategies were able to correctly stay in the ride comfort mode when the vehicle travelled over the Belgian paving (see Figure 64).

Figure 65 and Figure 66 shows the results of the Double lane change. The time difference between when the passengers indicated that better handling was needed and the actual switching is more than half a second. At higher speeds this could result in a rollover accident even before the switching will have occurred. It is also clear that better zero values were obtained for the test depicted in Figure 66. The best strategy for the Double lane change appears to be the Hysteresis switch with $a = 0.225$ and $b = 0.04$.

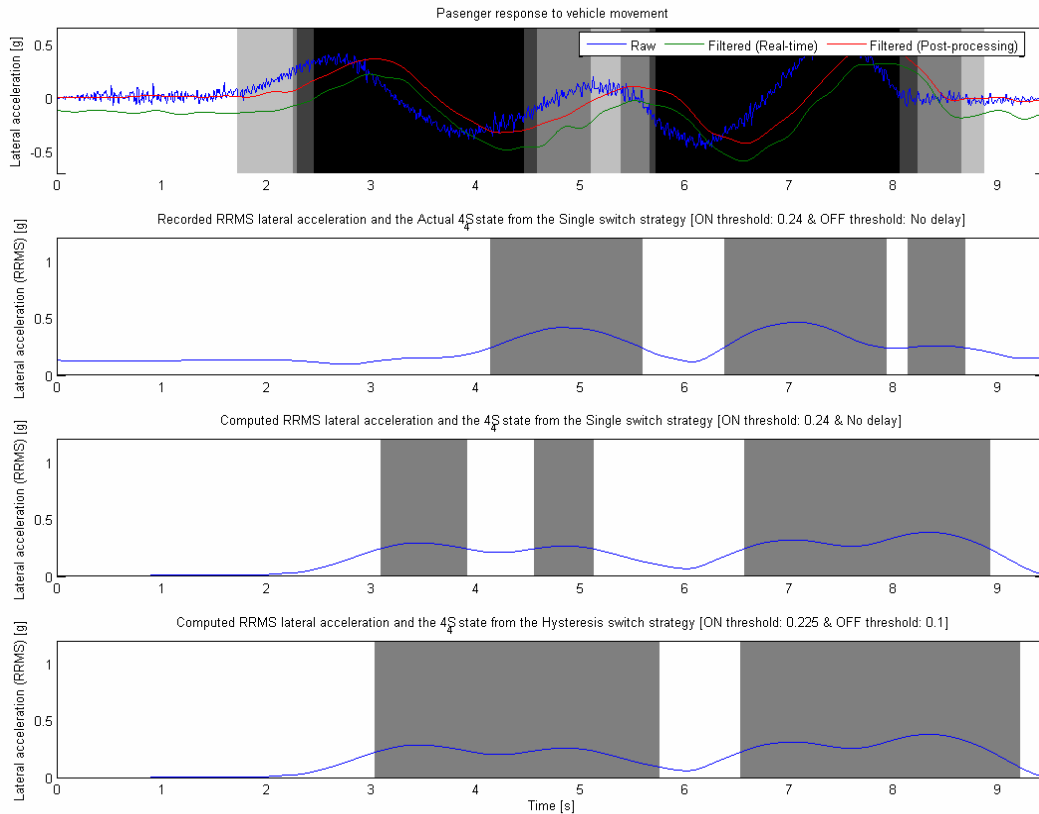


Figure 65: Comparing the actual Single switch [$m = 0.24$, No delay] to the recalculated strategies (DLC)

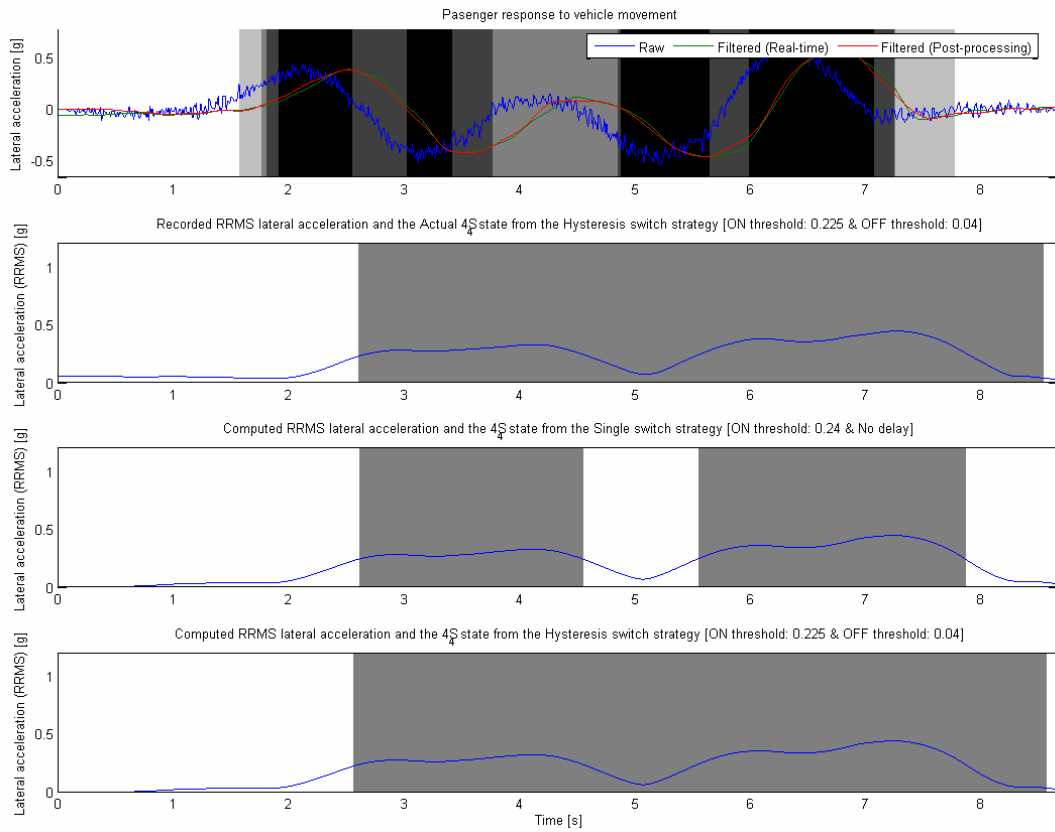


Figure 66: Comparing the actual Hysteresis switch [$a = 0.225$, $b = 0.04$] to the recalculated strategies (DLC)

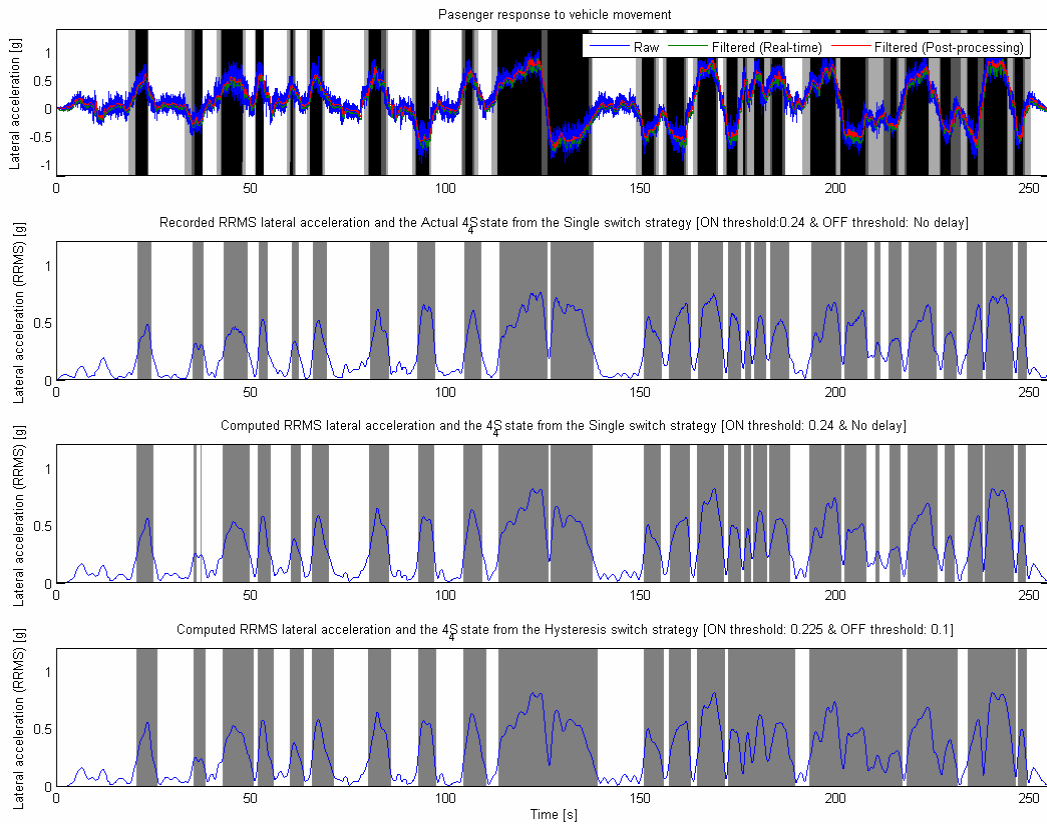


Figure 67: Comparing the actual Single switch [$m = 0.24$, No delay] to the recalculated strategies (RHT)

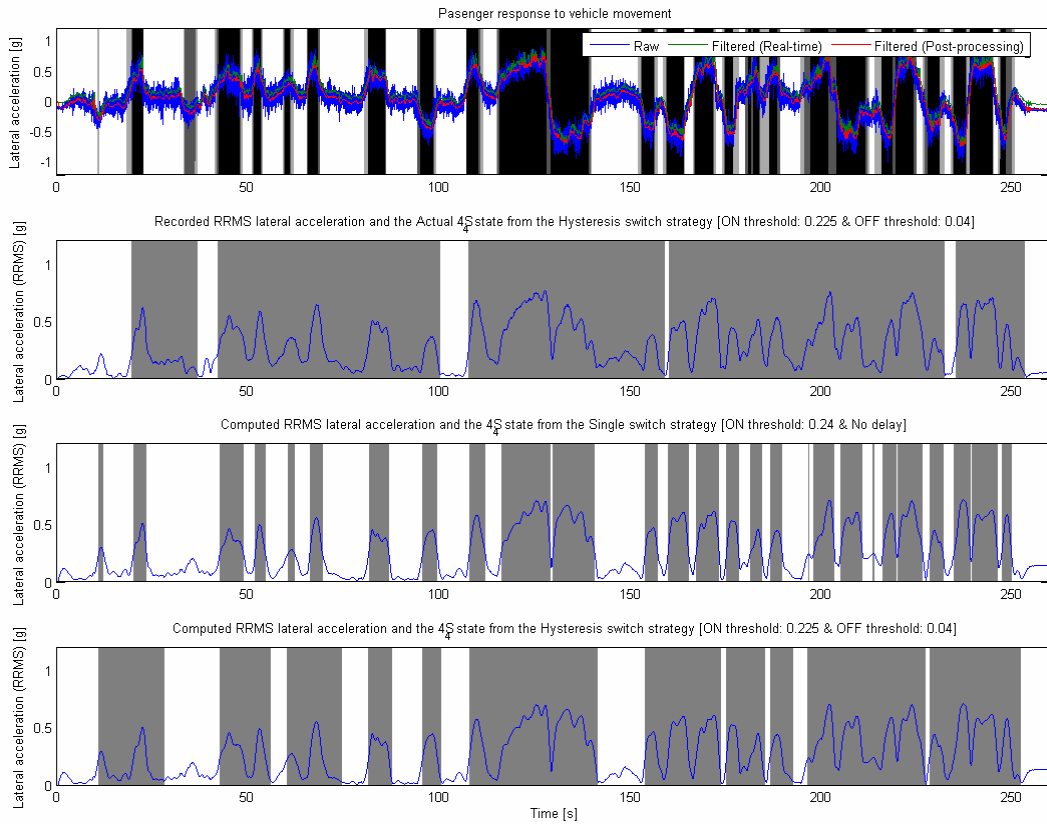


Figure 68: Comparing the actual Hysteresis switch [a = 0.225, b = 0.04] to the recalculated strategies (RHT)

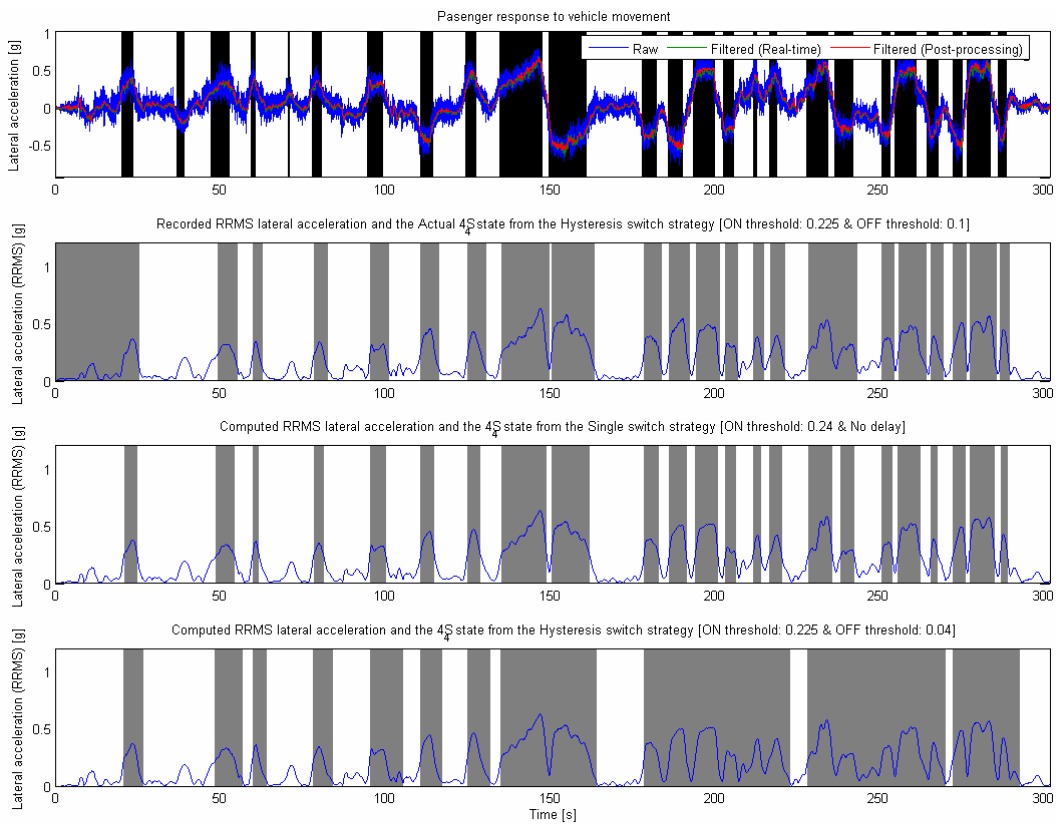


Figure 69: Comparing the actual Hysteresis switch [a = 0.225, b = 0.1] to the recalculated strategies (RHT)

The Ride and handling track tests are shown in Figure 67 to Figure 69. At this point it became clear that the OFF threshold of the Hysteresis switch was not sensitive enough. Figure 68 shows large sections where the suspension stayed in handling mode unnecessarily. The Single switch appeared to be the best strategy for the Ride and handling track.

The City traffic tests are the only tests that are not really repeatable. Traffic is random and the quality of the roads varies. (see Figure 70 and Figure 71) It is therefore more difficult to establish which strategy would work best. This however is where the SUV would spend most of its time. Once again the Single switch strategy performed the best.

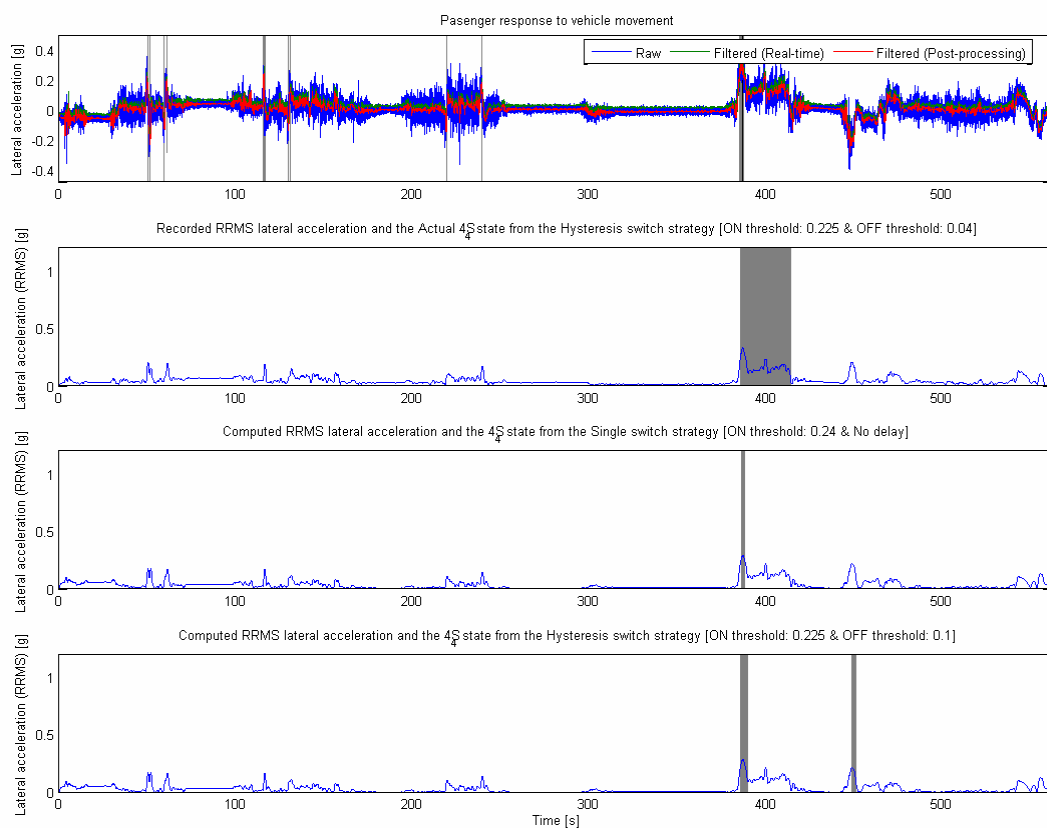


Figure 70: Comparing the actual Hysteresis switch [a = 0.225, b = 0.04] to the recalculated strategies (CTY)

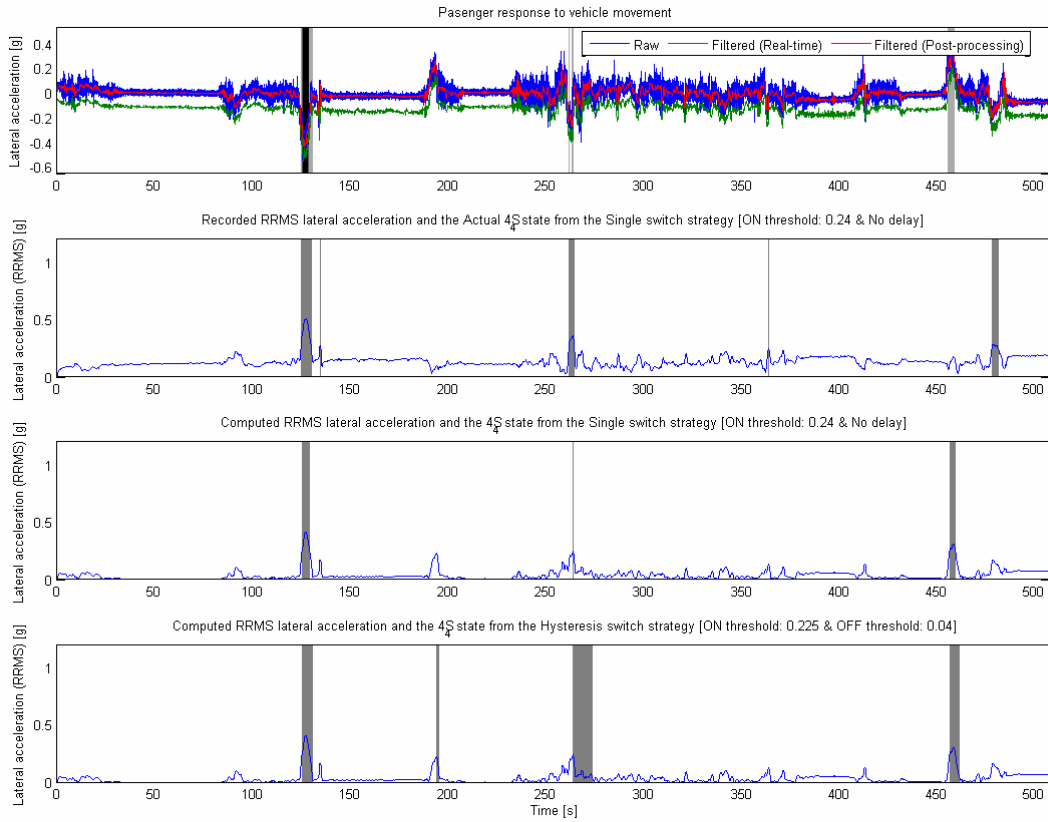


Figure 71: Comparing the actual Single switch [$a = 0.24$, No delay] to the recalculated strategies (CTY)

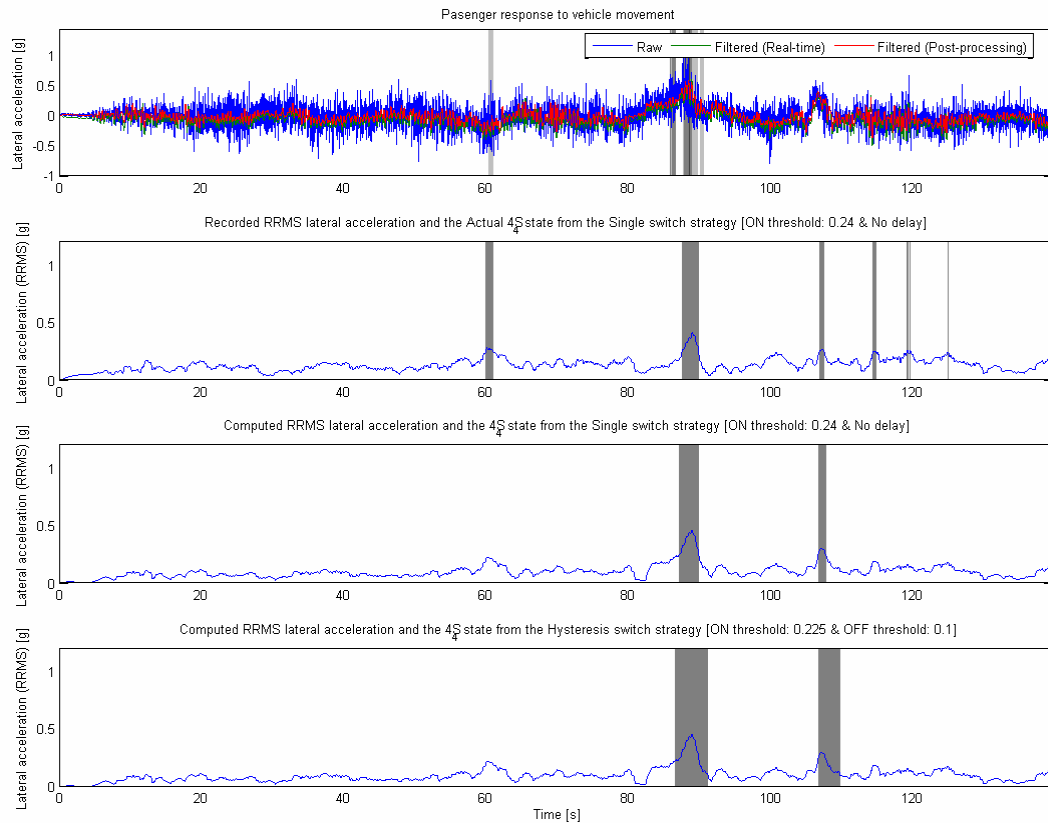


Figure 72: Comparing the actual Single switch [$a = 0.24$, No delay] to the recalculated strategies (ORT)

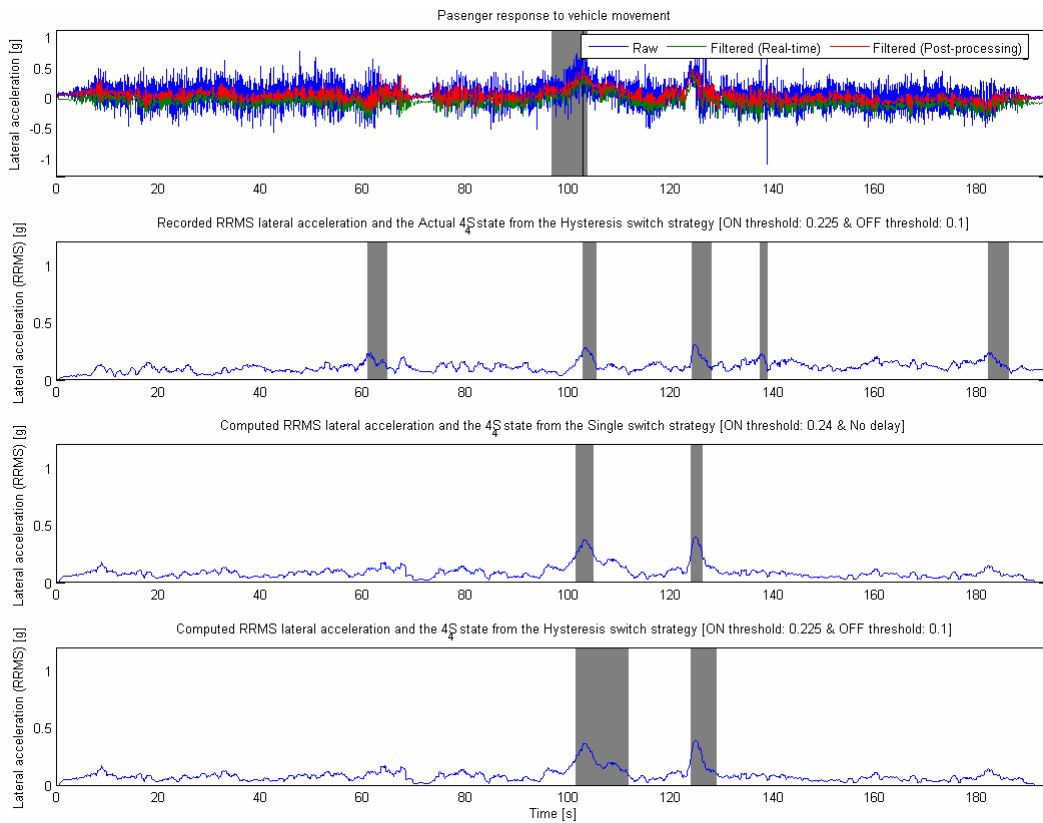


Figure 73: Comparing the actual Hysteresis switch [$a = 0.225$, $b = 0.1$] to the recalculated strategies (ORT)

The Off-road track jerks the vehicle in all directions. This causes the lateral acceleration to be higher than normal even though it is not dangerous from a handling point of view. Both strategies performed poorly on this track, but the Single switch strategy did better than the Hysteresis switch strategy. (see Figure 72 and Figure 73)

5.4 Conclusion of experimental results

The effect of the changing suspension characteristics was not taken into account when the different switching strategies were formulated. This could not be done because the vehicle is a highly non-linear system. It would be close to impossible to know what the effect of changing the suspension characteristics would be on every measurement. There is however a possibility of using a simulation model of the vehicle to investigate this phenomenon, but the computational time it needs to run disqualified this as a viable option at the time.

Parameter	BLG	DLC	RHT	CTY	ORT	ALL
P_{xor} [%]	100.0	75.6	60.2	94.2	-	77.3
P_{and} [%]	100.0	84.7	97.3	27.3	-	62.1
P_{nsw} [%]	100.0	100.0	18.3	63.8	-	11.6
nsw	0 (0)	1 (1)	12 (46)	1 (10)	-	14 (57)

Table 25: Hysteresis switch with lateral acceleration [$a = 0.225$, $b = 0.04$]

Parameter	BLG	DLC	RHT	CTY	ORT	ALL
P_{xor} [%]	-	76.5	73.8	-	89.1	79.7
P_{and} [%]	-	77.7	86.0	-	15.0	58.8
P_{nsw} [%]	-	95.1	81.9	-	81.9	100.0
nsw	-	3 (2)	21 (25)	-	5 (1)	29 (29)

Table 26: Hysteresis switch with lateral acceleration [$a = 0.225$, $b = 0.1$]

Parameter	BLG	DLC	RHT	CTY	ORT	ALL
P_{xor} [%]	100.0	70.7	84.1	98.8	96.7	95.0
P_{and} [%]	100.0	57.7	86.4	100.0	67.6	92.2
P_{nsw} [%]	100.0	90.5	86.1	81.9	77.9	49.7
nsw	0 (0)	5 (3)	27 (24)	5 (1)	8 (3)	45 (31)

Table 27: Single switch with lateral acceleration [$m = 0.24$, No delay]

From Table 25 to Table 27, showing the percentage similarity of the strategies compared to the passenger response, it is clear that the Single switch algorithm performed better than any of the Hysteresis strategies.

6 Conclusions and Recommendations

In this study two main topics were investigated: terrain classification and the ride comfort versus handling switching strategies. The conclusions and recommendations discussed below follow from the results obtained.

6.1 Terrain classification

The main conclusions from the terrain classification analysis are as follows:

- The different terrains and driving styles made it possible to discriminate between the five different test tracks.
- The obstacle detection method utilizes non-contact distance sensors that could be used to detect terrain roughness. Cost and measuring sensitivity are considerations that must be taken into account.
- The acceleration histogram method can be obtained by using a relatively inexpensive accelerometer. This method gives an indication of the ride comfort and handling criteria for each test track.
- A Fuzzy logic algorithm is easy to set up, but the manual adjustment of each parameter is not accurate and can take a long time. A formal optimization analysis of the parameters is needed to fully exploit this method.
- Self-Organising Maps are trained with a set of sample data and is then able to classify the terrain types efficiently. The training data has to represent each terrain very accurately to get good results. A combination of ride comfort and handling parameters resulted in correctly classifying the terrain types for 84% of the time.
- A Quadratic discriminant function together with eleven measured parameters was used and was able to correctly identify all the terrains for 89.5% of the time. The 10.5% of incorrect classification is mainly due to the fact that there are similarities between the terrains. This was further improved to 96.2% of correctly classifying terrain types by using a moving histogram method.

These methods can still be improved by optimizing the parameters of each classifying function. The most promising method would be the statistical quadratic discriminant function, but there are other statistical procedures that might perform better. One such method could be a non-parametric discriminant function. The data was captured at 100 Hz or 100 observations per second. It might not

be necessary to know the terrain type at such a high frequency. Taking an average of the classifications periodically will also produce better results.

6.2 Switching strategies

The safety aspect of the handling mode is the main drive for having a semi-active suspension system. The handling mode is unfortunately very uncomfortable, even in city traffic. This is due to the stiff suspension that is needed to do relatively high speed cornering. A switching strategy is required that will enable the vehicle to drive in ride comfort mode most of the time and only switch to handling mode when needed. Five methodologies and eleven strategies were formulated and investigated in this study. The most reliable parameter that gave a good indication of when handling manoeuvres were performed was the lateral acceleration of the vehicle. The Running Root Mean Square of this measurement was used in the RRMS strategies. When compared to the frequency domain, coherence, Fuzzy logic and polynomial prediction, the RRMS strategies performed the best. Theoretically the RRMS Single switch strategy produced a switching signal that resembled the benchmark signal the closest.

These RRMS algorithms did not perform as well in the experimental tests when compared to the passenger response. They still have great potential to become the standard of measuring handling manoeuvres. The RRMS strategies can be improved if the correct zero values of these measurements could be obtained. It is proposed that the global pitch and roll angle should be used to calculate the x, y and z components of the accelerations relative to the vehicle's local axis system. This will indicate the actual slope of the vehicle's body and can therefore be used to compensate for the global lateral acceleration that is currently measured. By improving filtering techniques, signals with smaller phase shifts can be produced and also a quicker response time for the switching strategies.

Both in terms of terrain classification and switching strategies potential methods have been identified. These methods can be developed further and possibly combined to ensure the safe and comfortable performance of SUV's and other off-road vehicles.

Bibliography and References

AL-Holou, N., Joo, D. S. and Shaout, A., (1995), *The development of Fuzzy logic based controller for semi-active suspension system*, 0-7803-2428-5/95 \$4.00 ©1995 IEEE, pp. 1373-1376.

Braghin, F., Brusarosco, M., Cheli, F., Cigada, A., Manzoni, S. and Mancosu, F., (2005), *Measurement of contact forces and patch features by means of accelerometers fixed inside the tire to improve future car active control*, XIX IAVSD Symp., Politecnico di Milano, Milan, Italy, 29 August – 2 September 2005, Paper #19

Department of transport, (2004), *Republic of South Africa, Road traffic and fatal crash statistics: 1990 – 2003, June 2004*

Donahue, M. D., (1998), *Implementation of an Active Suspension, Preview Controller for Improved Ride Comfort*, Unpublished Master's degree, Department of Mechanical Engineering, University of California at Berkeley

Els, P.S., Uys P.E., Snyman, J.A. and Thoresson, M. (2006), *Gradient-based approximation methods applied to the optimal design of vehicle suspension systems using computational models with severe inherent noise*, Mathematical and Computer Modelling 43 (2006), pp. 787 - 801

Els, P.S., (2006a), *The ride comfort vs. handling compromise for off-road vehicles*, Unpublished Doctoral thesis, Faculty of Engineering, University of Pretoria, South Africa

Els, P.S., (2006b), Personal communications, e-mail (2006/06/19)

Eberle, W.R. and Steele, M.M., 1975, *Investigation of Fluidically Controlled Suspension Systems for Tracked Vehicles – Final Report*, Technical Report No. 12072, TACOM Mobility Systems Laboratory, US Army Tank Automotive Command, Warren, Michigan, September 1975

Foda, S.G., (2001), *Neuro-Fuzzy Control of a Semi-active Car Suspension System*, 0-7803-7080-5/01/\$10.00 ©2001 IEEE, pp. 686 - 689

Fuzzy logic Toolbox, User's guide version 2, The Mathworks, www.mathworks.com, p.1.5-1.10

Bibliography and References

- Grimbeek, R. J., (2006), Personal communications, Department of Statistics, University of Pretoria
- Hashiyama, T., Furuhashi, T. and Uchikawa, Y., (1995), *Design of Fuzzy Controllers for Semi-active Suspension generated through the Genetic Algorithm*, 0-8186-7174-2/95 \$04.00 ©1995 IEEE, pp. 166 - 169
- Iagnemma, K. and Dubowsky, S., (2002), *Terrain estimation for high-speed rough-terrain autonomous vehicle navigation*, Department of Mechanical Engineering, Massachusetts Institute of Technology.
- Iagnemma, K., Brooks, C. and Dubowsky, S., (2004), *Visual, Tactile, and Vibration-Based Terrain Analysis for Planetary Rovers*, pp. 1 - 8
- International Standards Organization, (1999), *International Standard ISO 3888-1: Passenger cars - Test track for a severe lane-change manoeuvre: Part 1: Double lane change*, ISO/TR 3888-1: 1999 (E)
- Kohonen, T., (2001), *Self-Organizing Maps*, Berlin: Springer, pp. 51 – 65, 78, 79
- Kyrtsos, C.T., (1998), *Roll-over detector for vehicles*, United States Patent: 6225894.
- Marzbanrad, J., Ahmadi, G., Zohoor, H. and Hojjat, Y., (2004), *Stochastic optimal preview control of a vehicle suspension*, Journal of Sound and Vibration 275 (2004), pp. 973 - 990
- Nagai M., Moran, A., Tamura, Y., & S. Koizumi, (1997), *Identification and control of nonlinear active pneumatic suspension for railway vehicles using neural networks*, Control Eng. Practice, Vol. 5, No. 8, 1997, pp. 1137 - 1144
- Negnevitsky, M., (2002), *Artificial Intelligence, A Guide to Intelligent Systems*, Harlow, England; New York: Addison-Wesley, pp. 164, 165, 203
- Nicolas, C.F., Landaluze, J., Castrillo, E., Gaston, M. and Reyero, R., 1997, *Application of Fuzzy logic control to the design of Semi-Active Suspension systems*, 0-7803-3796-4/97/\$10.00 ©1997 IEEE, pp. 987-993

Bibliography and References

- Pasquier, M., Quek, C. and Toh, M., (2001), *Fuzzylot: a novel self-organising fuzzy-neural rule-based pilot system for automated vehicles*, Neural Networks 14, pp. 1099 - 1112
- Rao, M.V.C. and Prahlad, V., (1995), *A tuneable fuzzy logic controller for vehicle-active suspension systems*, Fuzzy Sets and Systems 85, pp. 11 - 21
- Sadhukhan, D., Moore, C. and Collins, E., (2004), *Terrain estimation using internal sensors*, Proceedings of the 10th IASTED International Conference, Robotics and applications, August 23-25, 2004, Honolulu, Hawaii, USA, pp. 195 - 199
- Schurter, K.C. and Roschke, P. N., (2000), *Fuzzy modelling of a Magnetorheological damper using ANFIS*, 0-7803-5877-5/00/\$10.00 © 2000 IEEE, pp. 122 - 127
- Snyman, J.A., (2005), *Practical mathematical optimization, An Introduction to Basic Optimization Theory and Classical New Gradient-Based Algorithms*, Springer, Applied Optimization, volume 97, ISBN 0-387-24348-8
- Sun, L., (2003), *Simulation of pavement roughness and IRI based on power spectral density*, Mathematics and computers in simulation 61 (2003), pp. 77 - 88
- Theron, N.J. and Els, P.S., (2005), *Modelling of a Semi-active Hydropneumatic Spring-damper Unit*, Accepted for publication in International Journal of Vehicle Design (IJVD), Inderscience Publishers, 3 March 2005
- Thoreson, M.J., (2003), *Mathematical optimization of the suspension system of an off-road vehicle for ride comfort and handling*, Unpublished Master's degree dissertation, University of Pretoria
- Trent, V. and Greene, M., (2002) *A Genetic Algorithm Predictor for Vehicular Rollover*, 0-7803-7474-6/02/\$17.00 ©2002 IEEE, pp. 1752-1756
- Tsunashima, H., Murakami, M. and Miyata, J., (2005), *Vehicle and Road State Estimation Using Interacting Multiple Model Approach*, XIX IAVSD Symp., Politecnico di Milano, Milan, Italy, 29 August – 2 September 2005, Paper #28

Bibliography and References

Tyan, C., Wang, P. P., Bahler, D. R., (1996), *An application on intelligent control using neural network and fuzzy logic*, Neurocomputing 12 (1996), pp. 345 - 363

Wu, Y. and Xu, B., (1999), *Study on the Damping Fuzzy Control of Semi-Active Suspension*, 0-7803-5296-3/99/\$10.00 ©1999 IEEE, pp. 66 - 69

Yoshimura, T., Nakaminami, K., Kurimoto, M. and Hino, J., (1999), *Active suspension of passenger cars using linear and fuzzy-logic controls*, Control Engineering Practice 7 (1999), pp. 41 - 47

Appendix A

- A.1 Statistical analysis of terrain classification*
- A.2 Frequency Domain analysis (lateral acceleration)*
- A.3 Frequency Domain analysis (yaw velocity)*
- A.4 Coherence*
- A.5 Fuzzy logic*
- A.6 Polynomial prediction*
- A.7 RRMS of the lateral acceleration*

Appendix A

A.1 Statistical analysis of terrain classification

Data=Train, Pool=No, var2-var12, Nr=2
2006

982
17:17 Thursday, November 2,

The DISCRIM Procedure
Classification Summary for Calibration Data: BESTER.TRAIN
Resubstitution Summary using Quadratic Discriminant Function

Generalized Squared Distance Function

$$D_j^2(X) = (X - \bar{X}_j)' \text{COV}_j^{-1} (X - \bar{X}_j) + \ln |\text{COV}_j|$$

Posterior Probability of Membership in Each VAR1

$$\text{Pr}(j|X) = \exp(-.5 D_j^2(X)) / \sum_k \exp(-.5 D_k^2(X))$$

Number of Observations and Percent Classified into VAR1

From VAR1	1	2	3	4	5	Total
1	4903 90.71	51 0.94	9 0.17	198 3.66	244 4.51	5405 100.00
2	46 0.64	5859 81.45	146 2.03	1142 15.88	0 0.00	7193 100.00
3	2785 2.01	3102 2.24	129979 93.84	197 0.14	2447 1.77	138510 100.00
4	2649 1.56	4093 2.41	3379 1.99	155942 92.00	3432 2.02	169495 100.00
5	4379 6.29	8 0.01	553 0.79	2361 3.39	62310 89.51	69611 100.00
Total	14762 3.78	13113 3.36	134066 34.36	159840 40.96	68433 17.54	390214 100.00
Priors	0.2	0.2	0.2	0.2	0.2	

Error Count Estimates for VAR1

	1	2	3	4	5	Total
Rate	0.0929	0.1855	0.0616	0.0800	0.1049	0.1050
Priors	0.2000	0.2000	0.2000	0.2000	0.2000	

Appendix A

Data=Test, Pool=No var2-var12, Nr=2

983

17:17 Thursday, November 2,

2006

The DISCRIM Procedure
Classification Summary for Test Data: BESTER.TEST
Classification Summary using Quadratic Discriminant Function

Generalized Squared Distance Function

$$D_j^2(X) = (X - \bar{X}_j)' \text{COV}_j^{-1} (X - \bar{X}_j) + \ln |\text{COV}_j|$$

Posterior Probability of Membership in Each VAR1

$$\text{Pr}(j|X) = \exp(-.5 D_j^2(X)) / \sum_k \exp(-.5 D_k^2(X))$$

Number of Observations and Percent Classified into VAR1

From VAR1	1	2	3	4	5	Total
1	902 90.20	11 1.10	2 0.20	37 3.70	48 4.80	1000 100.00
2	3 0.30	816 81.60	22 2.20	159 15.90	0 0.00	1000 100.00
3	21 2.10	25 2.50	934 93.40	2 0.20	18 1.80	1000 100.00
4	20 2.00	24 2.40	20 2.00	918 91.80	18 1.80	1000 100.00
5	63 6.30	0 0.00	4 0.40	27 2.70	906 90.60	1000 100.00
Total	1009 20.18	876 17.52	982 19.64	1143 22.86	990 19.80	5000 100.00
Priors	0.2	0.2	0.2	0.2	0.2	

Error Count Estimates for VAR1

	1	2	3	4	5	Total
Rate	0.0980	0.1840	0.0660	0.0820	0.0940	0.1048
Priors	0.2000	0.2000	0.2000	0.2000	0.2000	

Appendix A

A.2 Frequency Domain analysis (lateral acceleration)

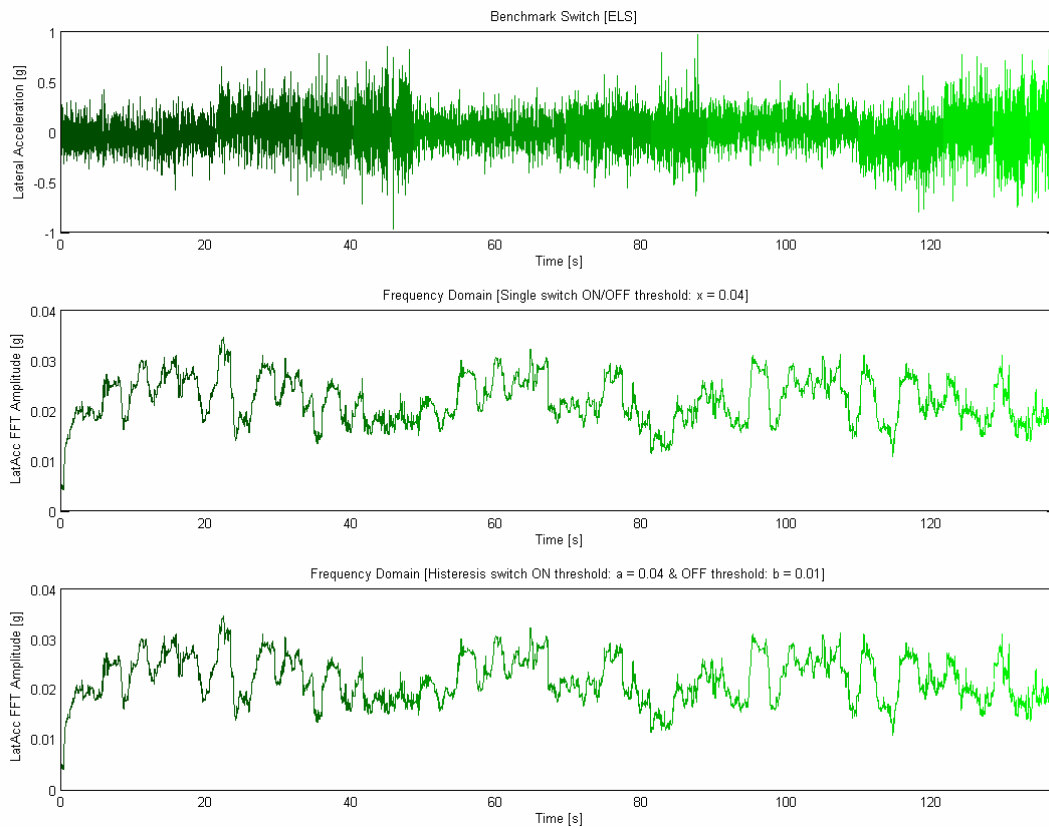


Figure 74: Frequency Domain analysis (lateral acceleration), Belgian paving

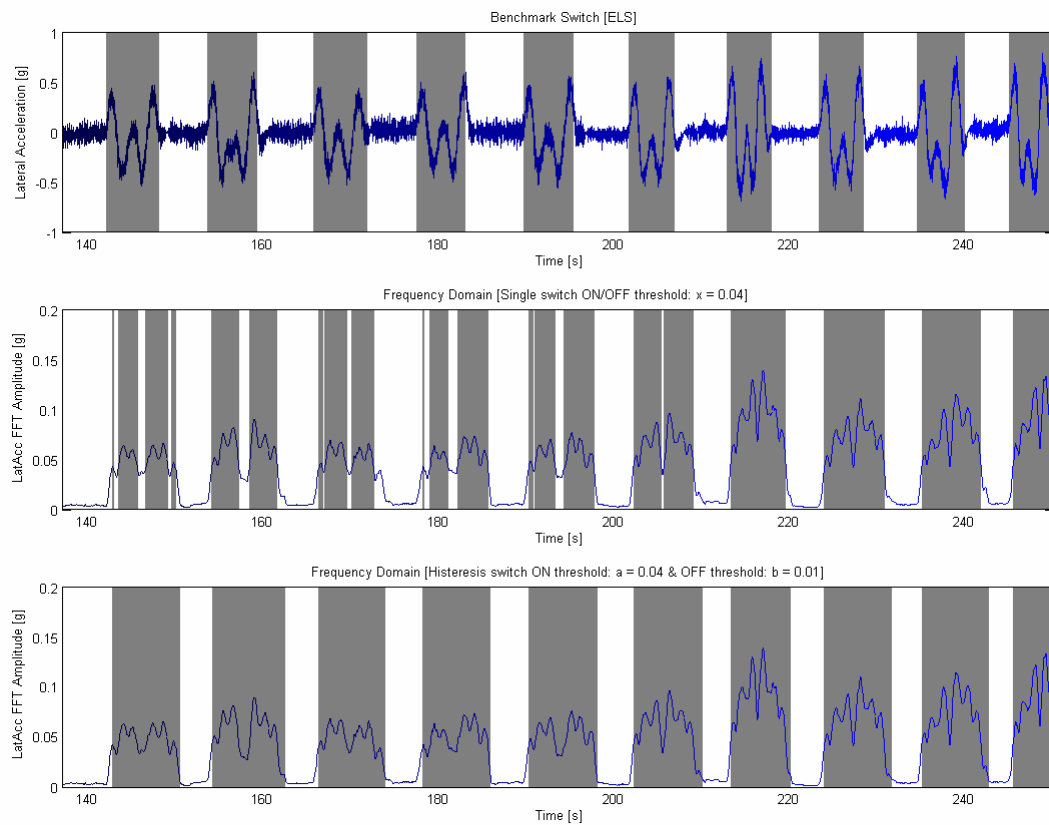


Figure 75: Frequency Domain analysis (lateral acceleration), Double lane change

Appendix A

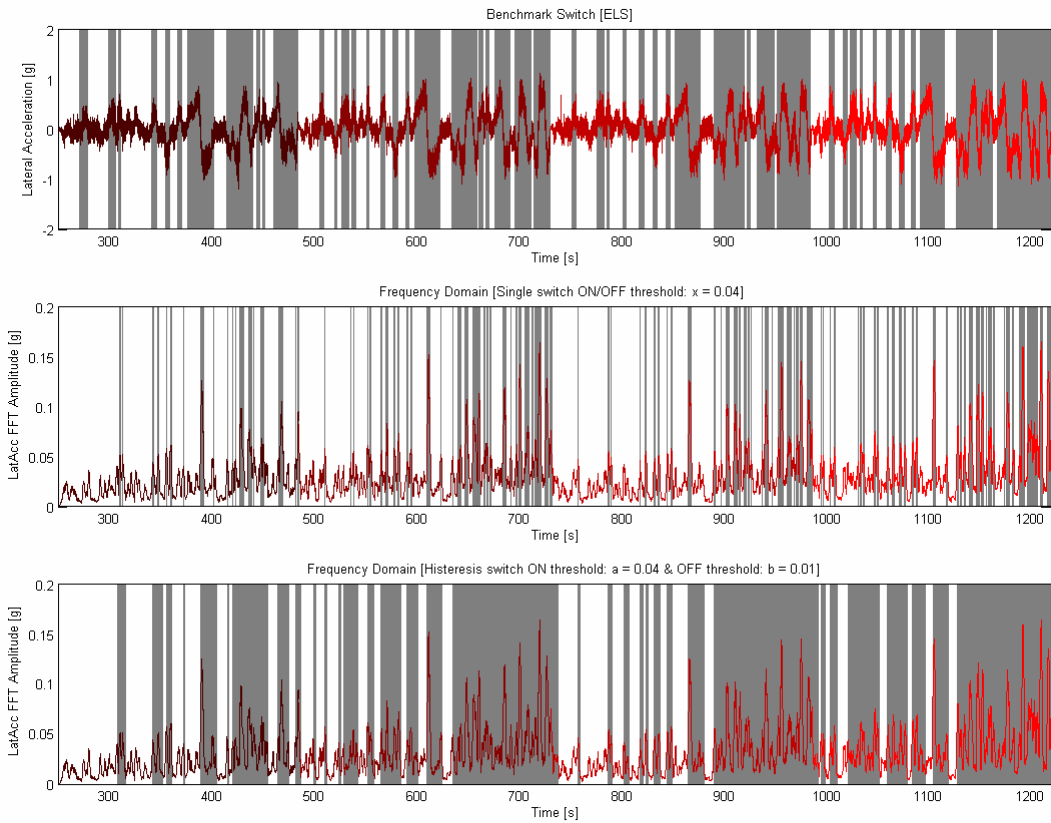


Figure 76: Frequency Domain analysis (lateral acceleration), Ride and handling track

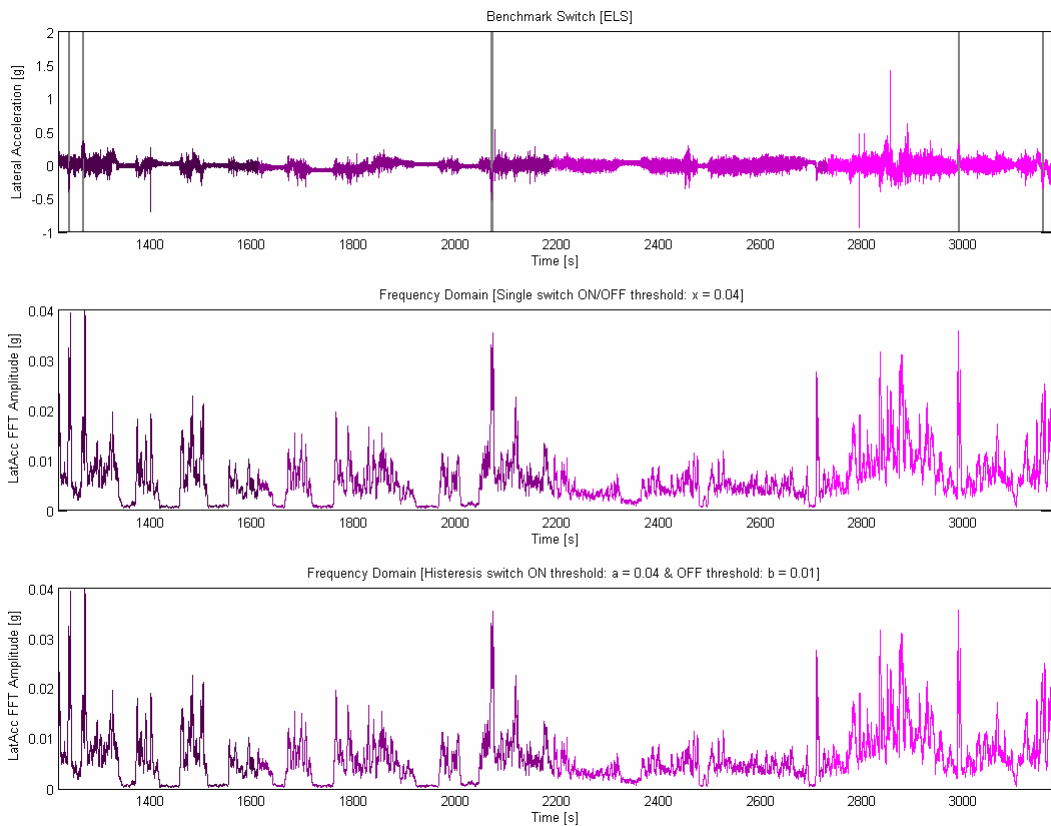


Figure 77: Frequency Domain analysis (lateral acceleration), City traffic

Appendix A

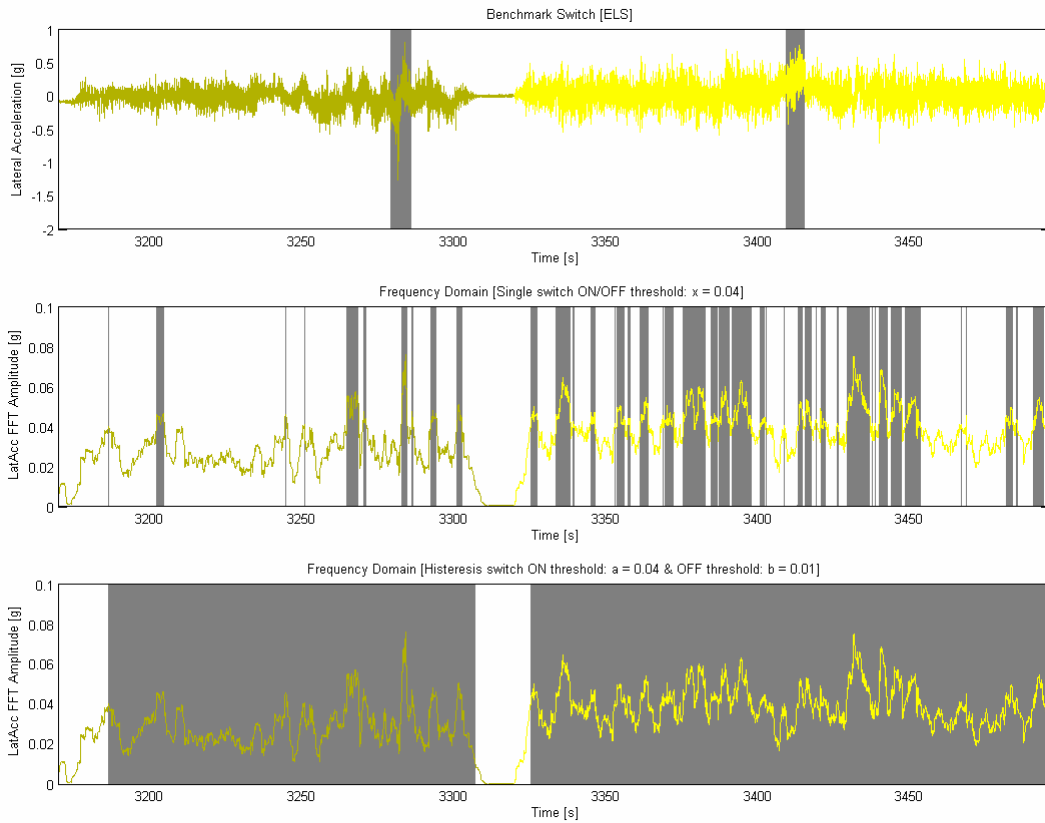


Figure 78: Frequency Domain analysis (lateral acceleration), Off-road track

A.3 Frequency Domain analysis (yaw velocity)

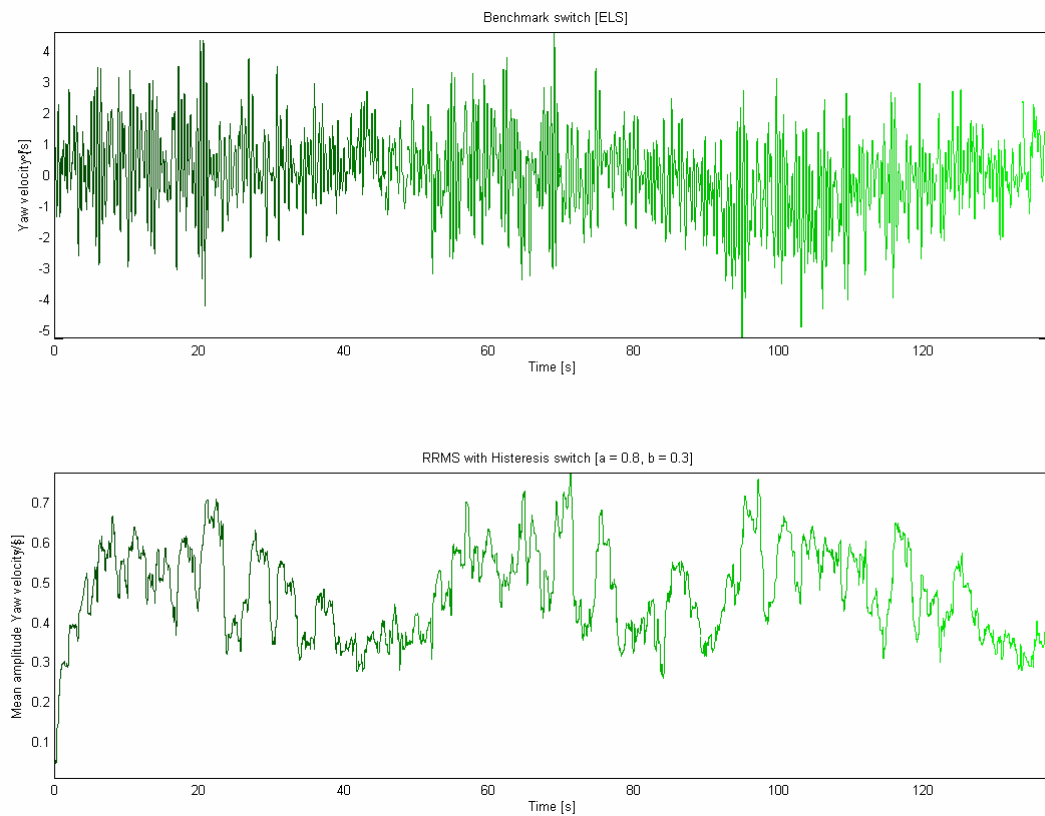


Figure 79: Frequency Domain analysis (yaw velocity), Belgian paving

Appendix A

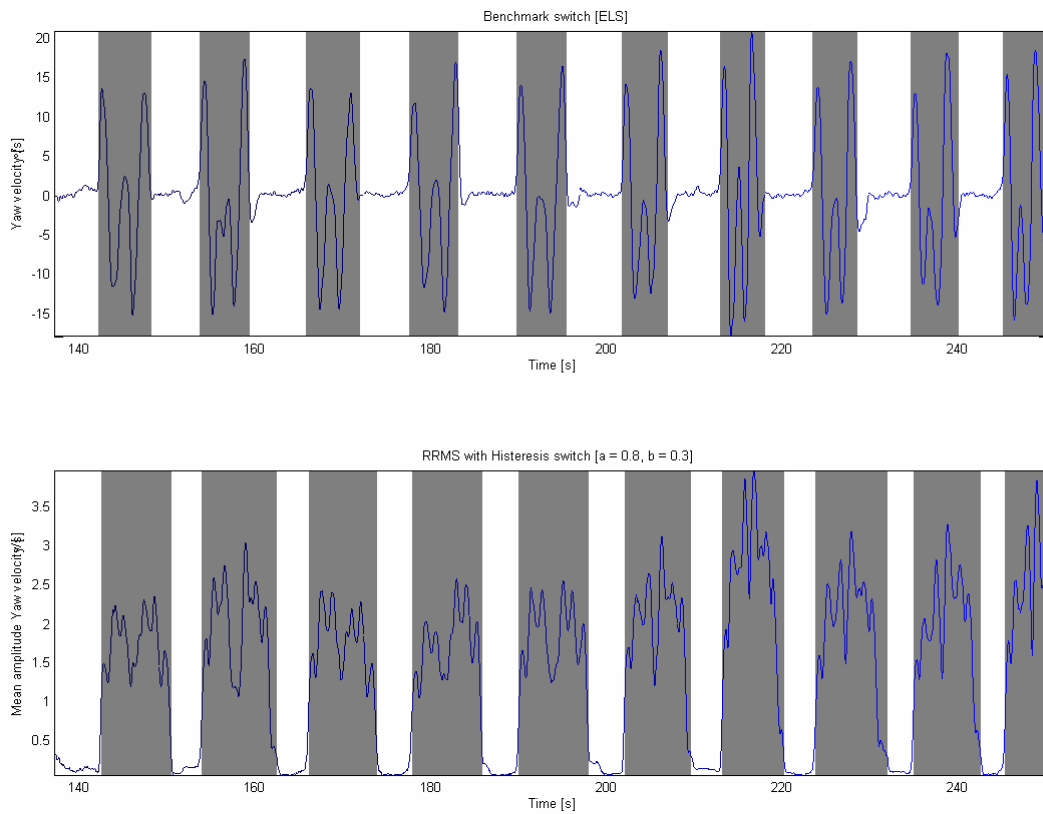


Figure 80: Frequency Domain analysis (yaw velocity), Double lane change

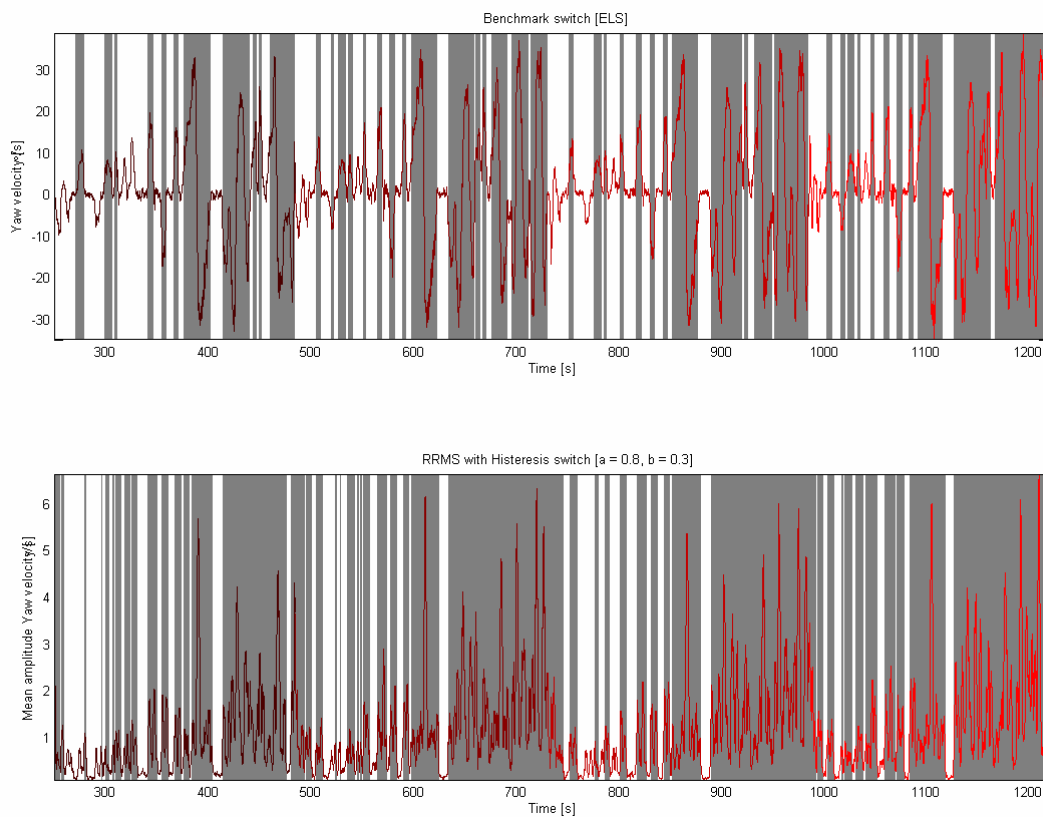


Figure 81: Frequency Domain analysis (yaw velocity), Ride and Handling Track

Appendix A

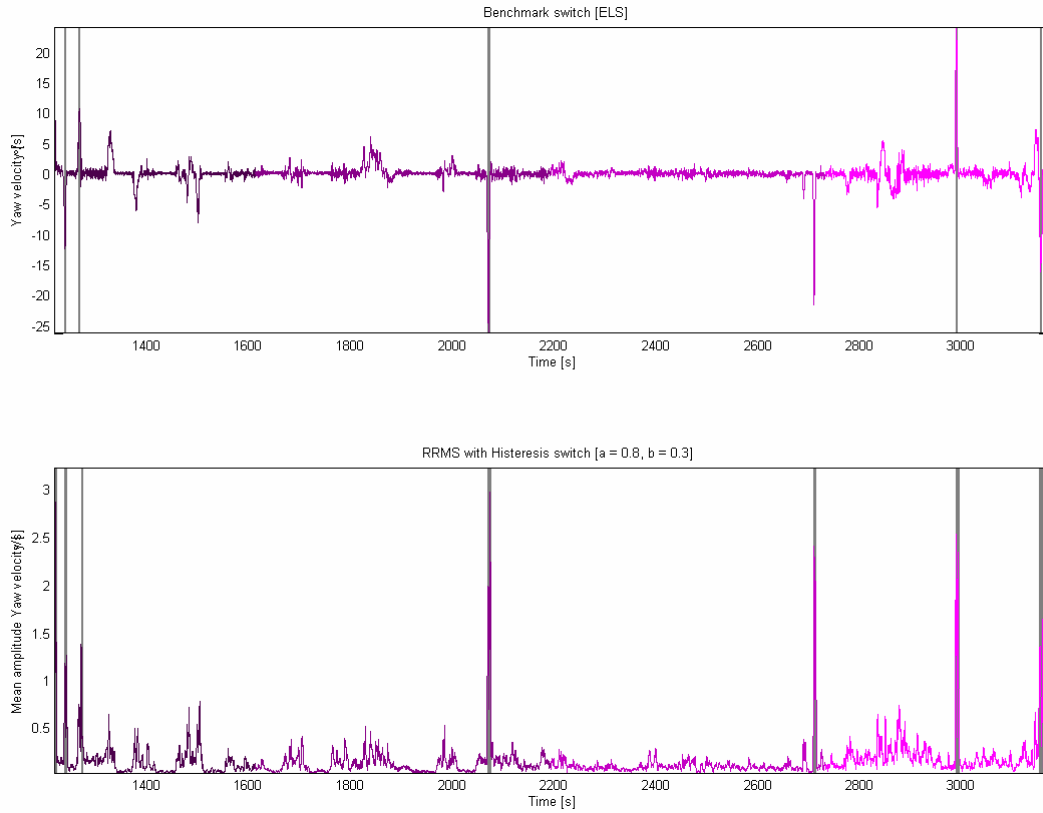


Figure 82: Frequency Domain analysis (yaw velocity), City traffic

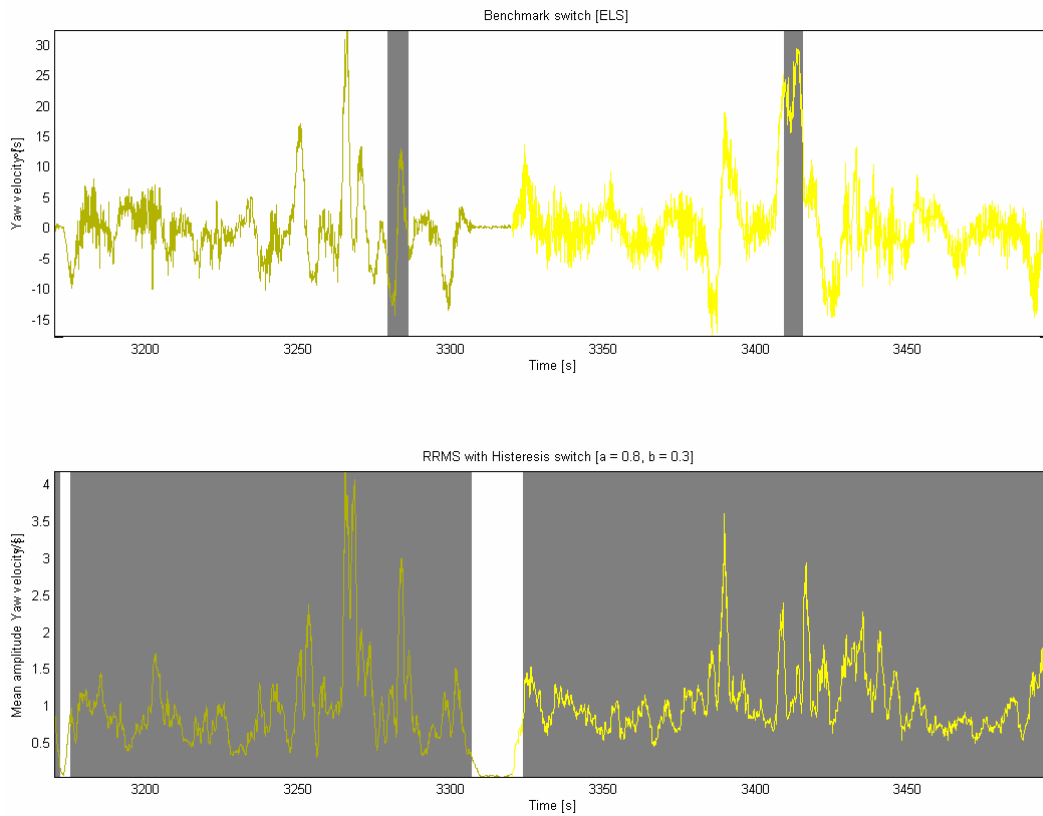


Figure 83: Frequency Domain analysis (yaw velocity), Off-road track

Appendix A

A.4 Coherence

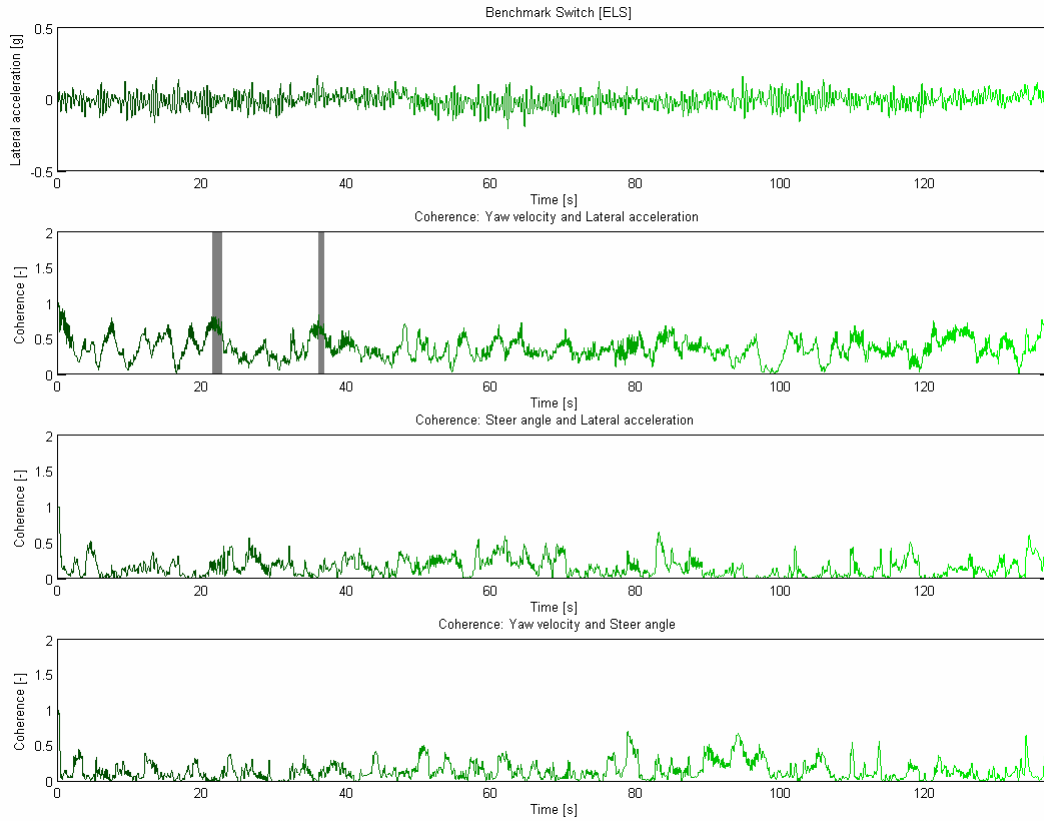


Figure 84: Coherence, Belgian paving

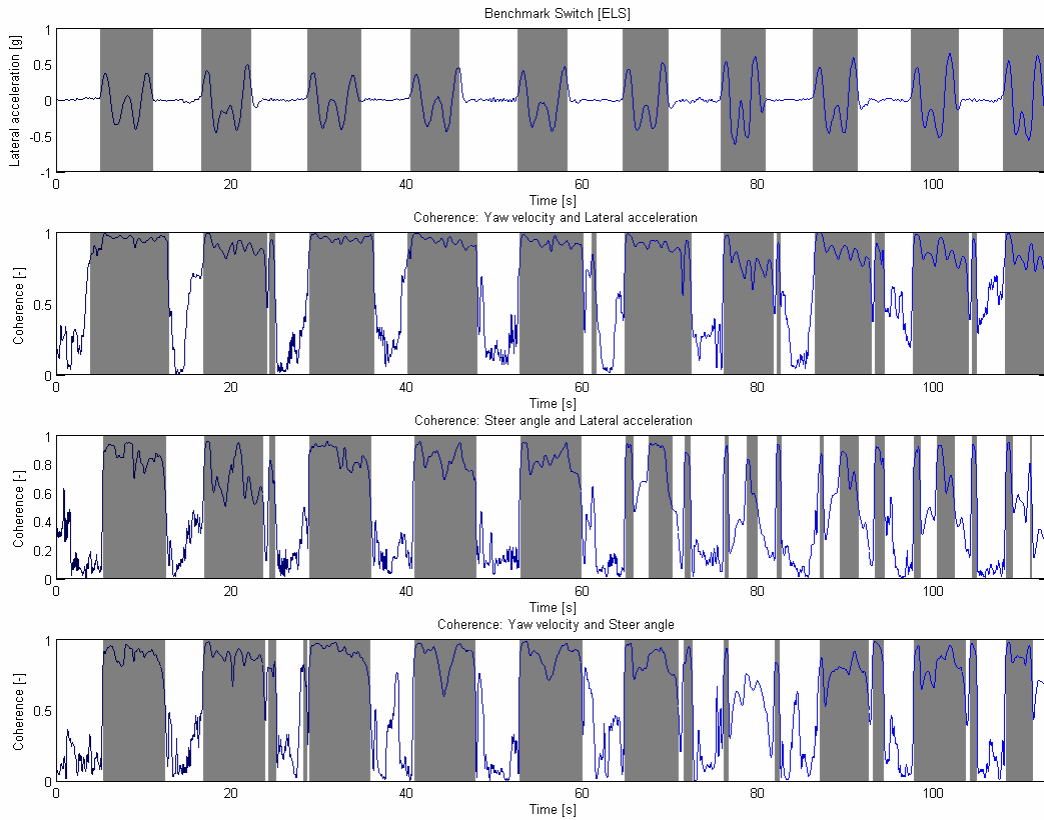


Figure 85: Coherence, Double lane change

Appendix A

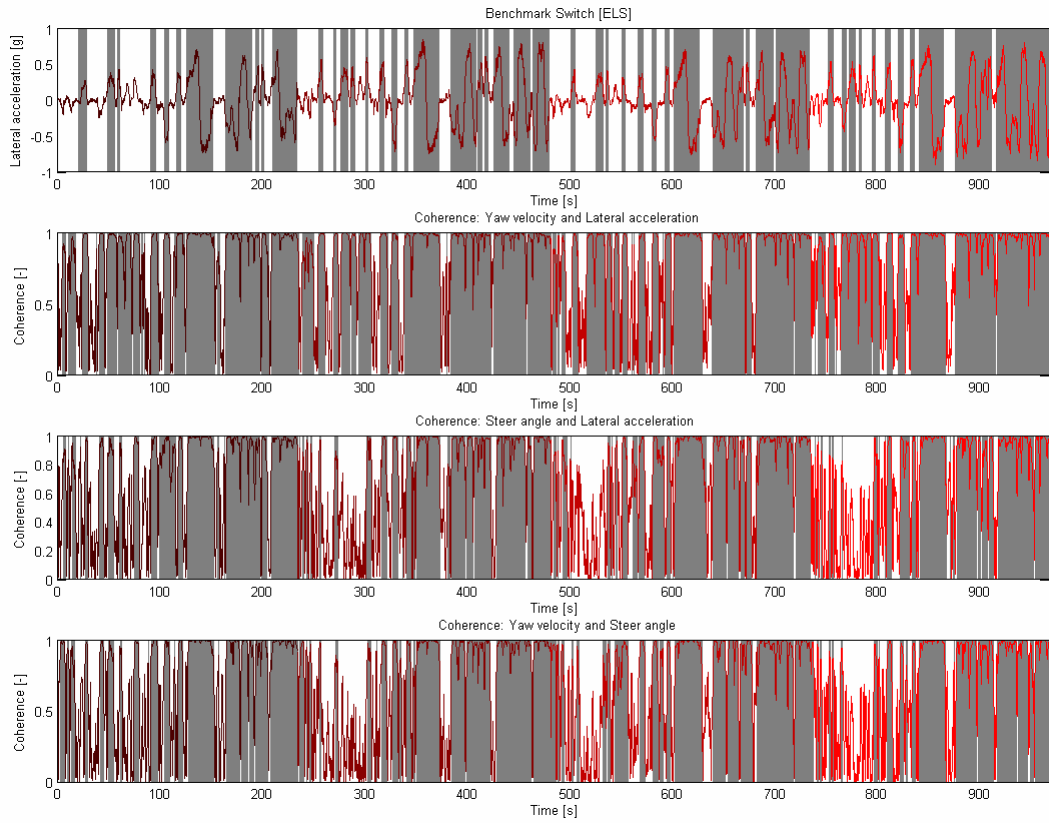


Figure 86: Coherence, Ride and handling track

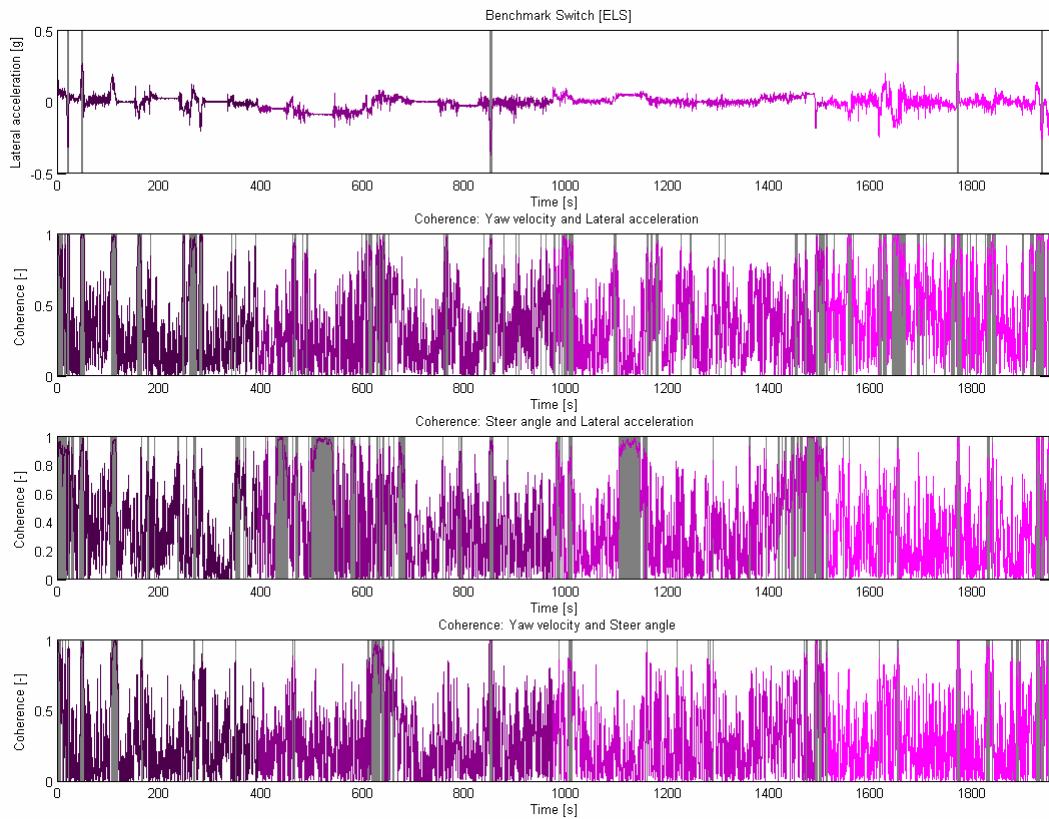


Figure 87: Coherence, city traffic

Appendix A

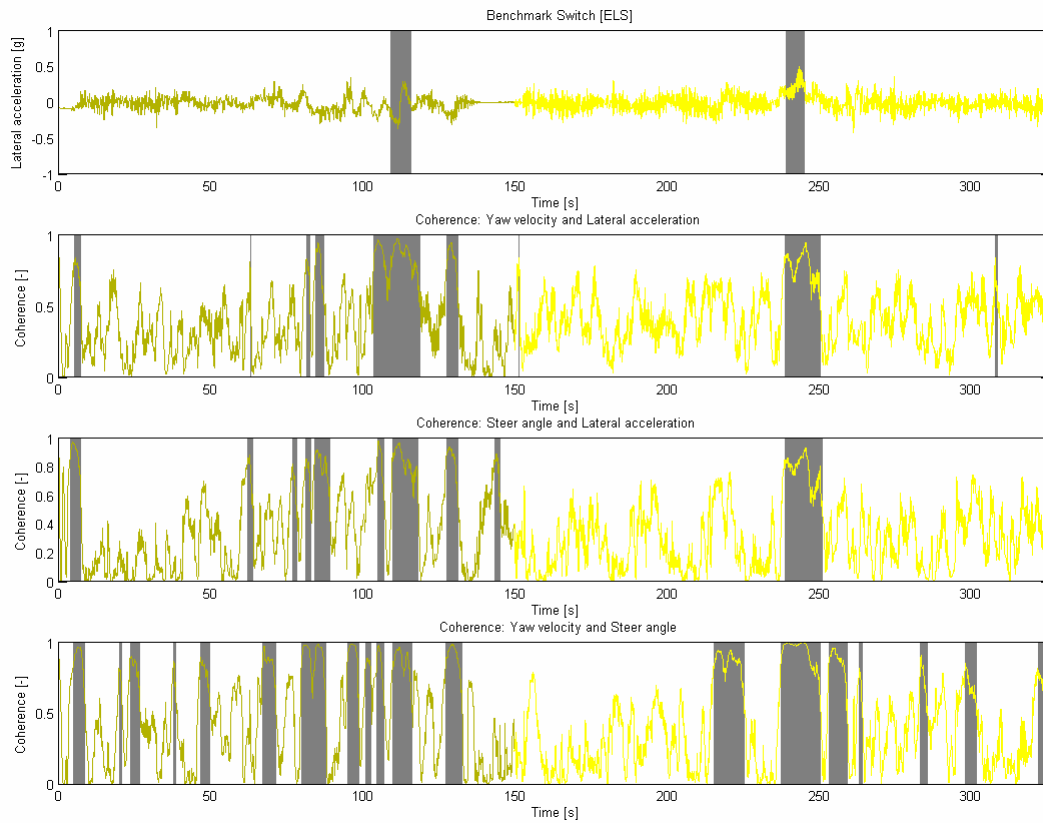


Figure 88: Coherence, Off-road track

A.5 Fuzzy logic

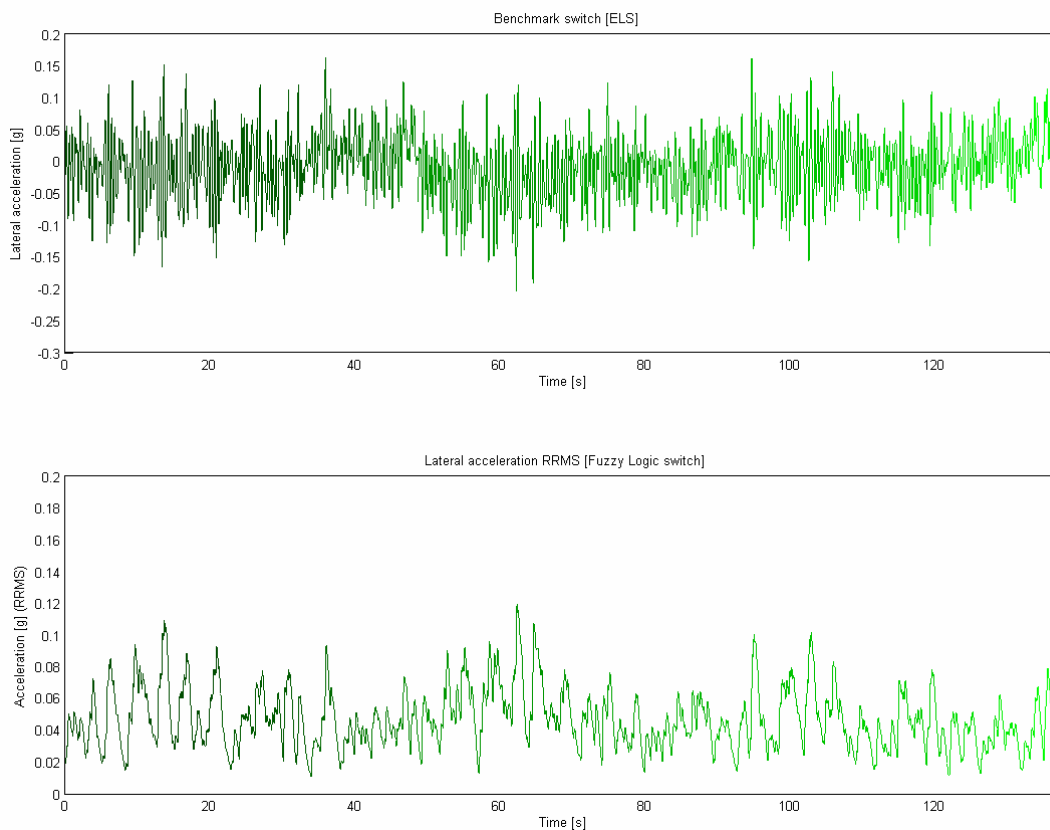


Figure 89: Fuzzy logic, Belgian paving

Appendix A

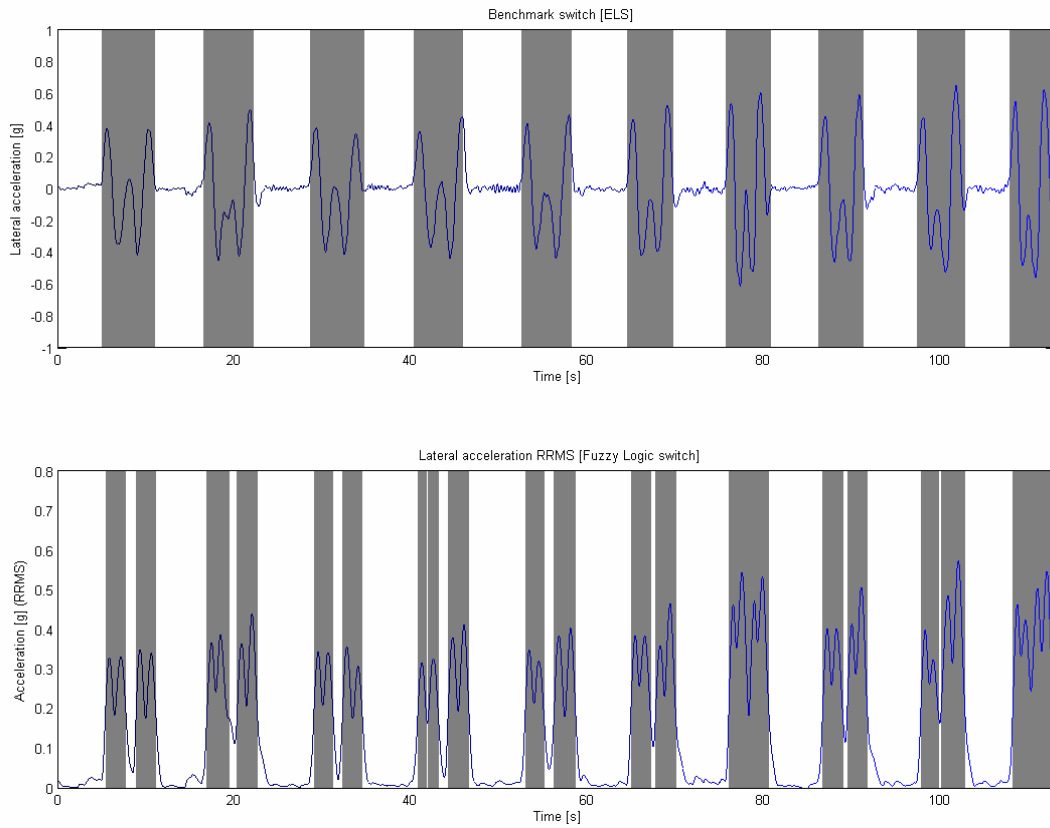


Figure 90: Fuzzy logic, Double lane change

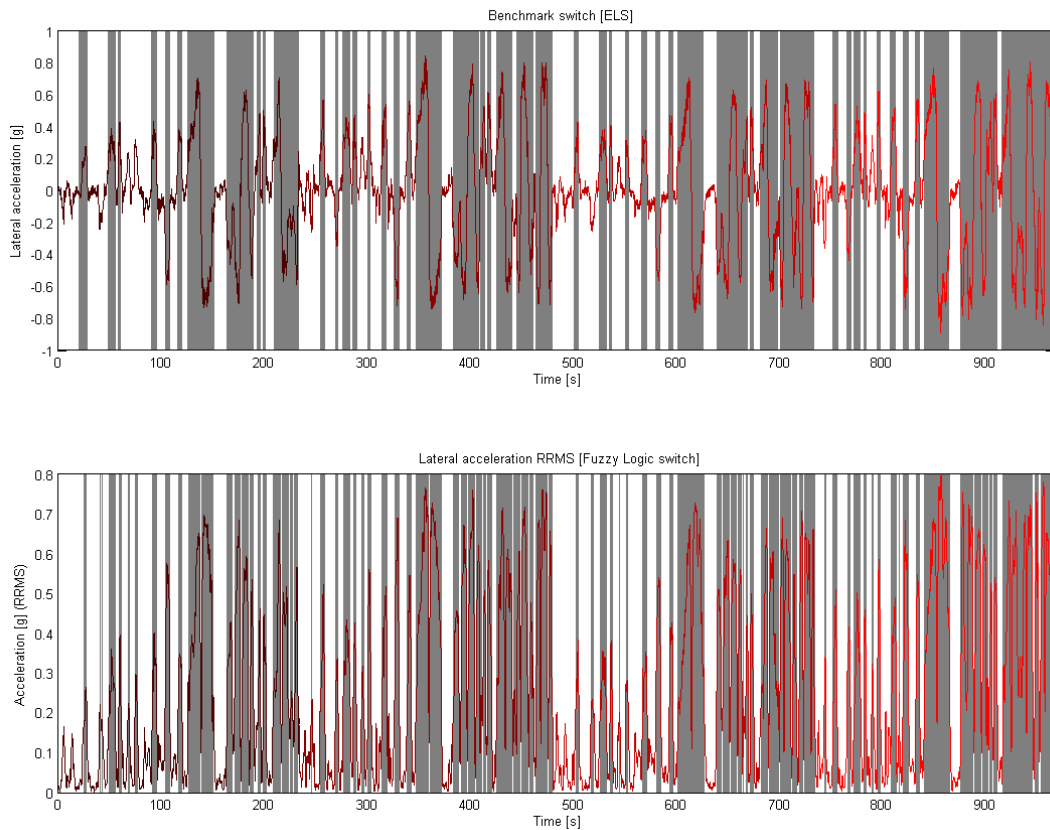


Figure 91: Fuzzy logic, Ride and handling track

Appendix A

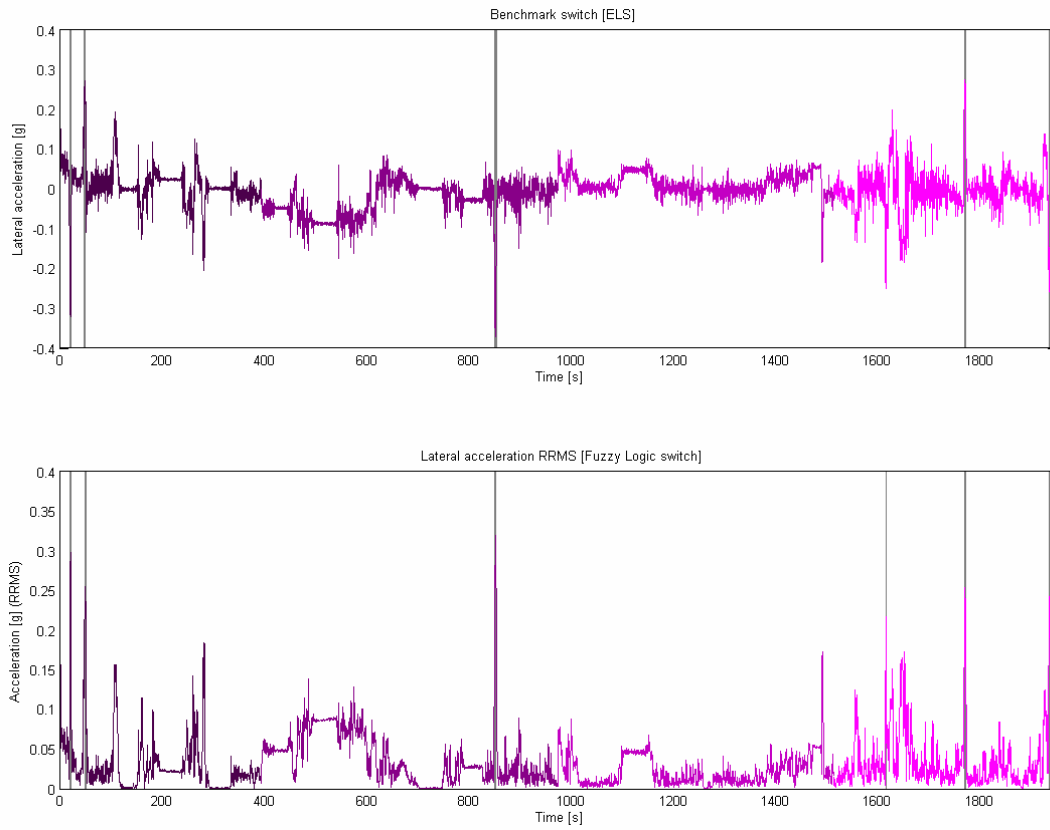


Figure 92: Fuzzy logic, city traffic

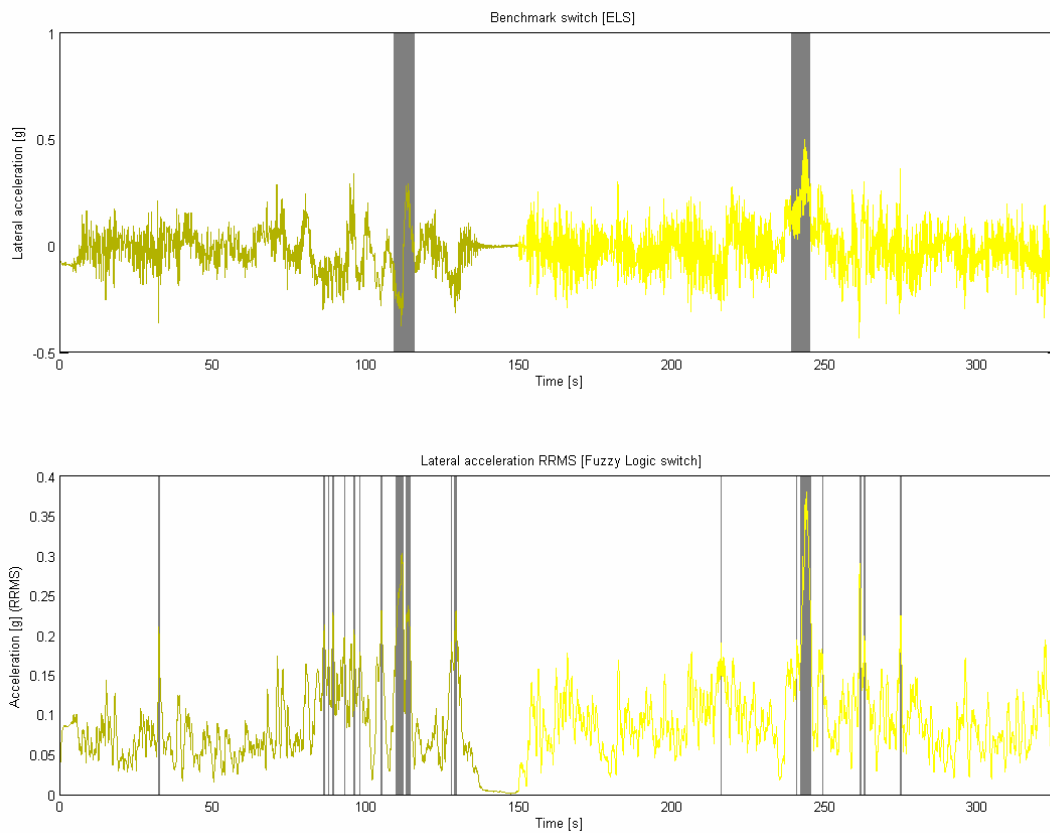


Figure 93: Fuzzy logic, Off-road track

Appendix A

A.6 Polynomial prediction

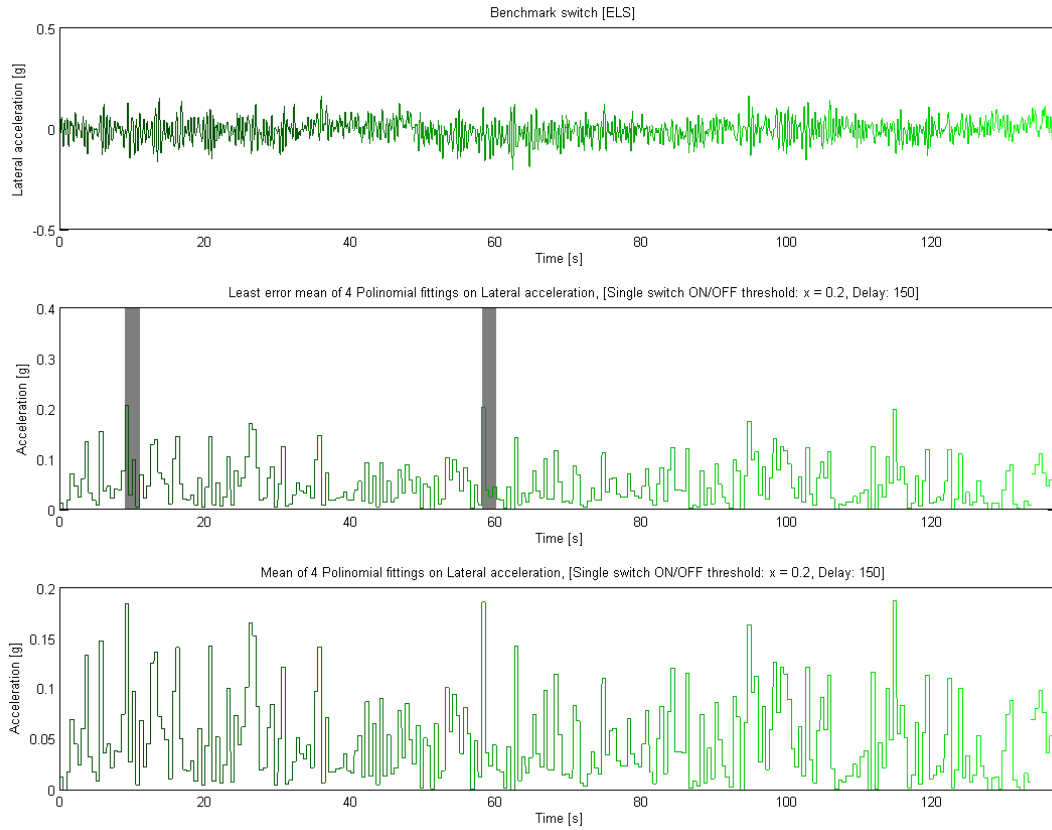


Figure 94: Polynomial prediction, Belgian paving

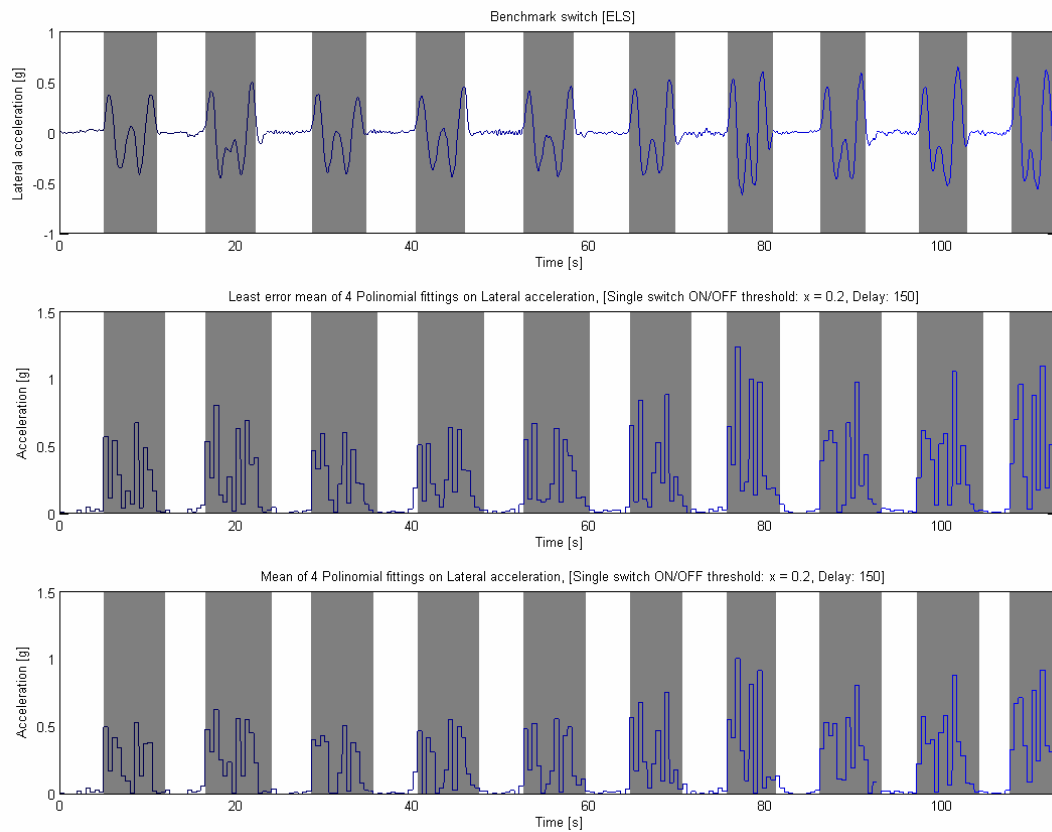


Figure 95: Polynomial prediction, Double lane change

Appendix A

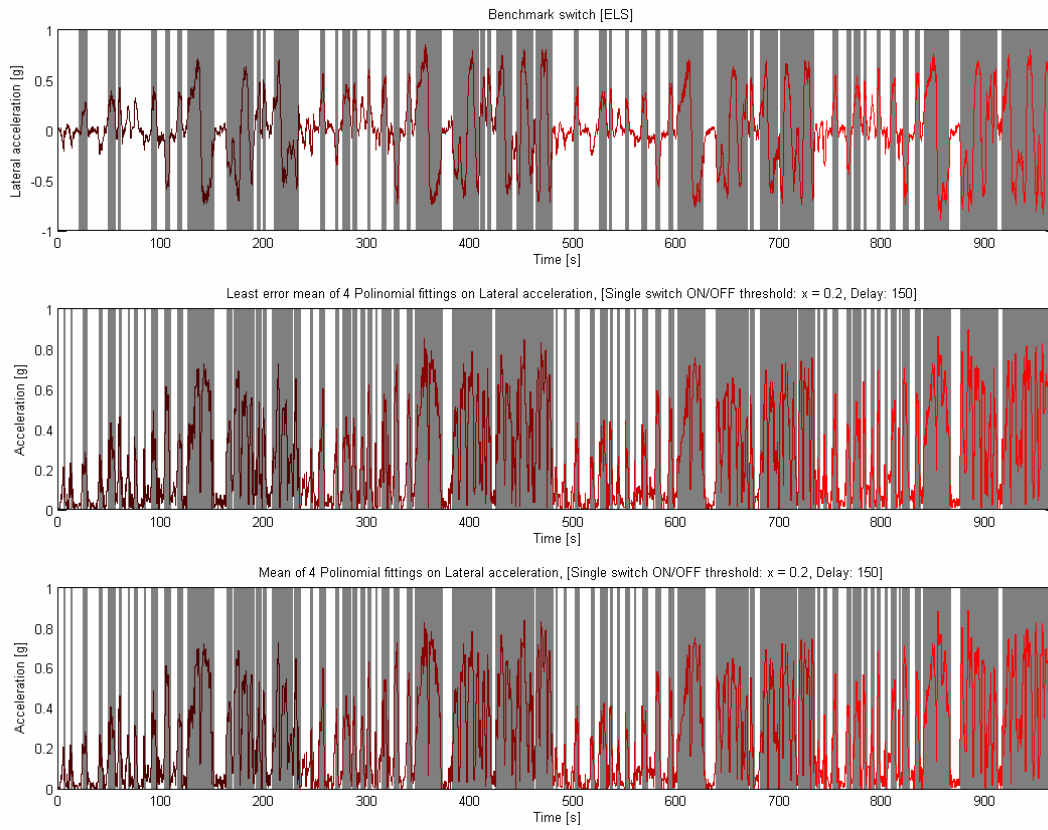


Figure 96: Polynomial prediction, Ride and handling track

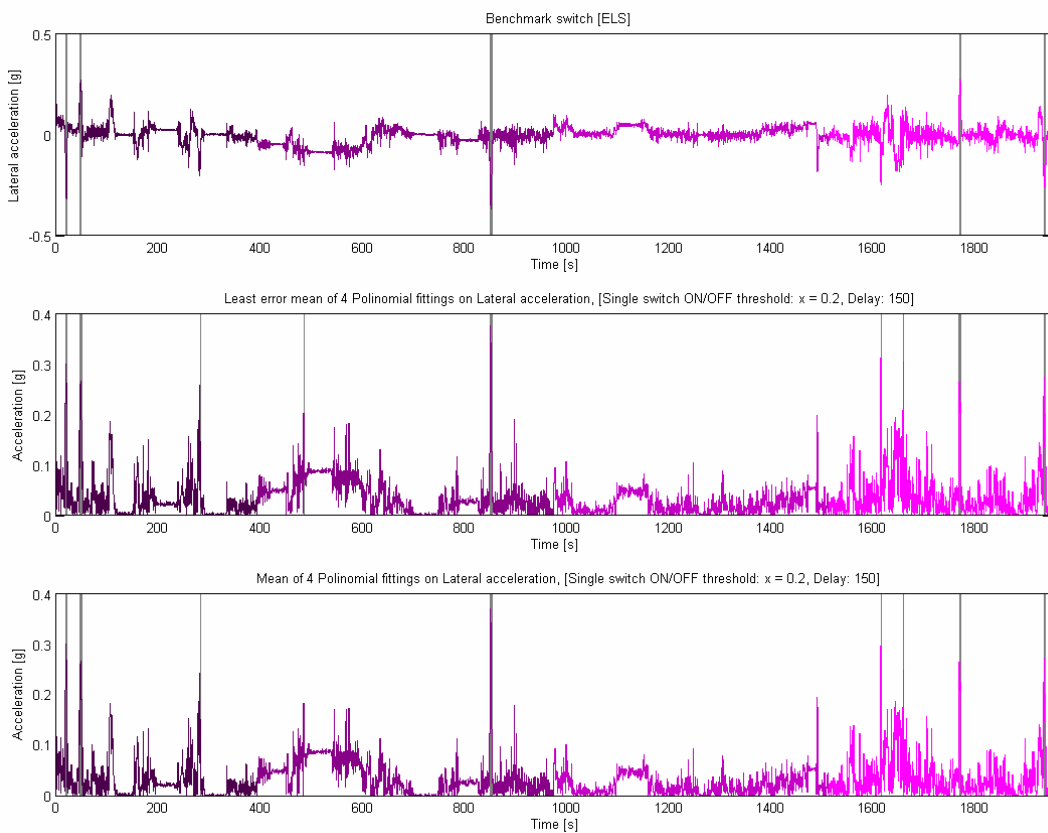


Figure 97: Polynomial prediction, city traffic

Appendix A

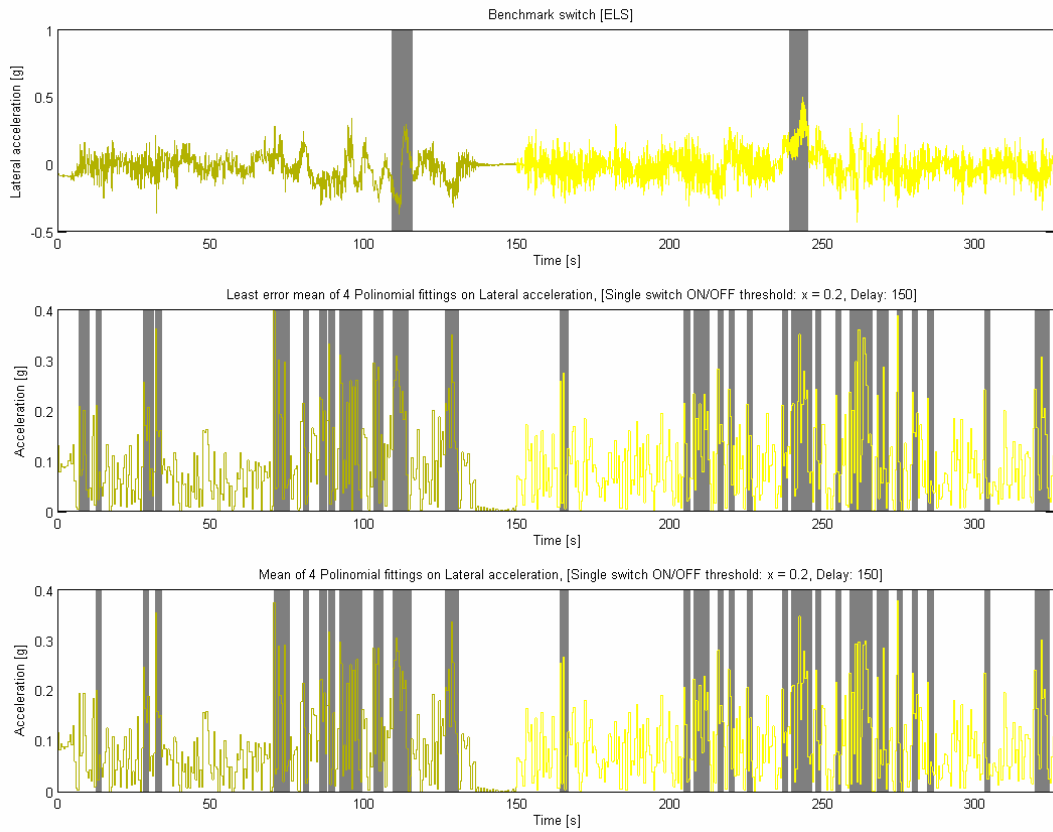


Figure 98: Polynomial prediction, Off-road track

A.7 RRMS of the lateral acceleration

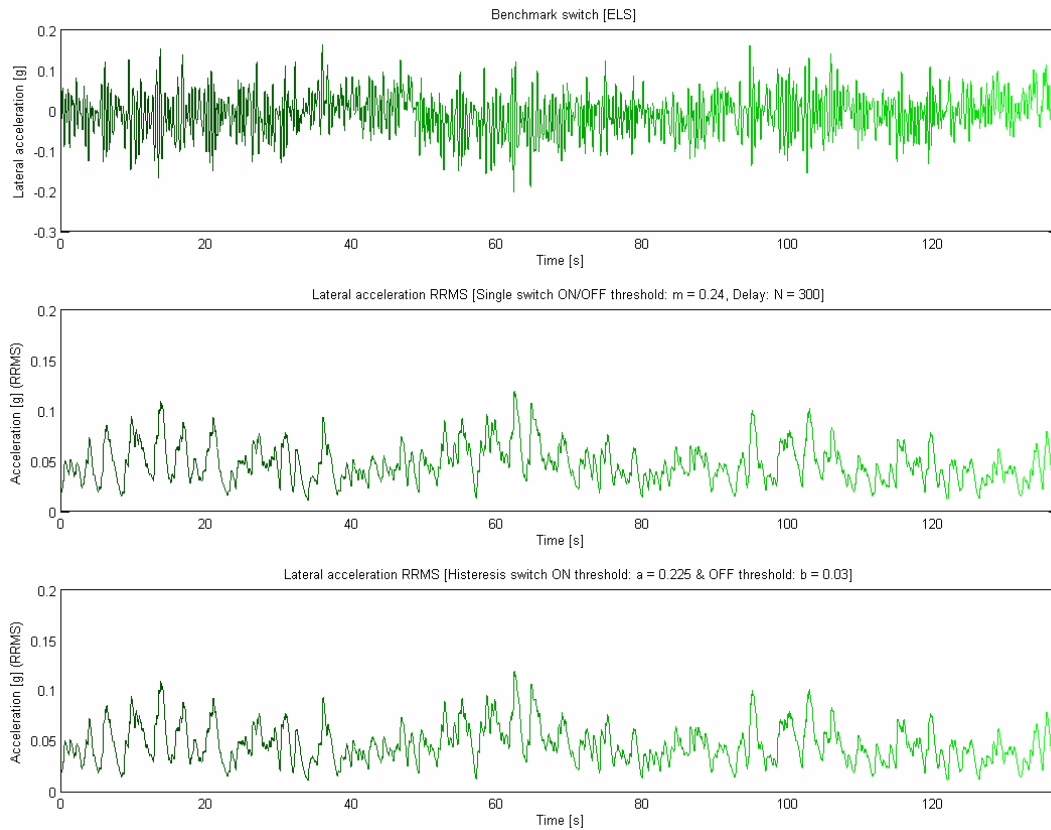


Figure 99: RRMS, Belgian paving

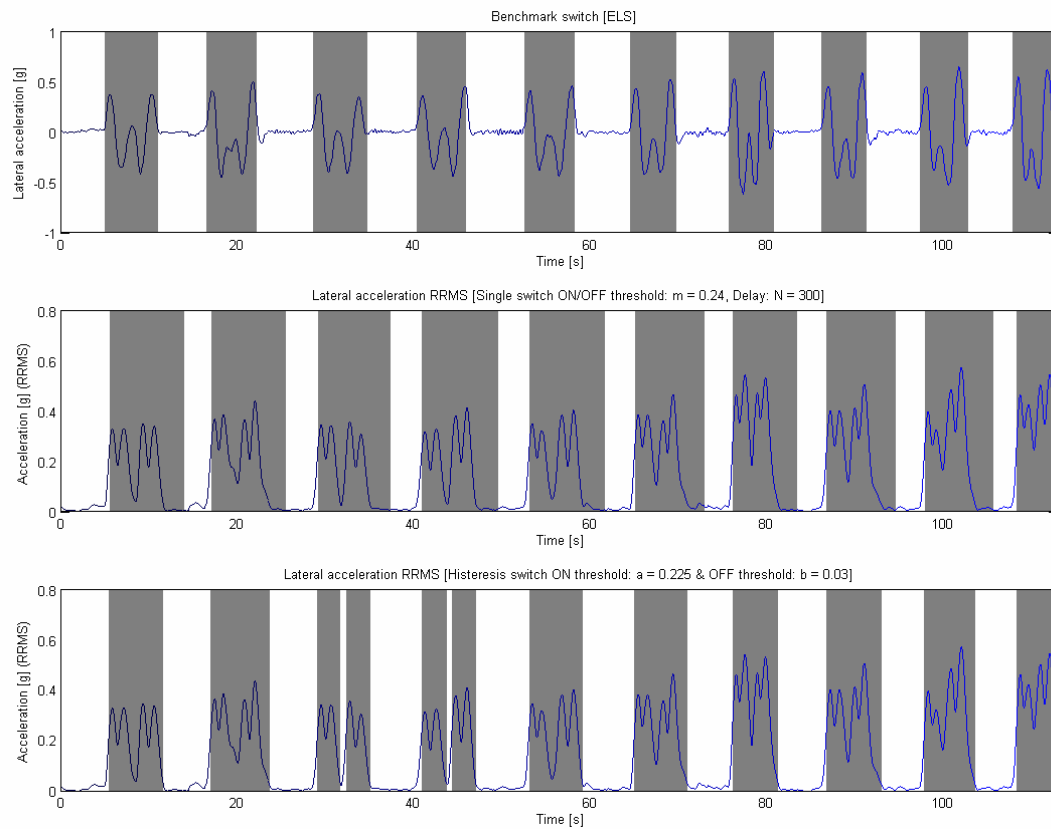


Figure 100: RRMS, Double lane change

Appendix A

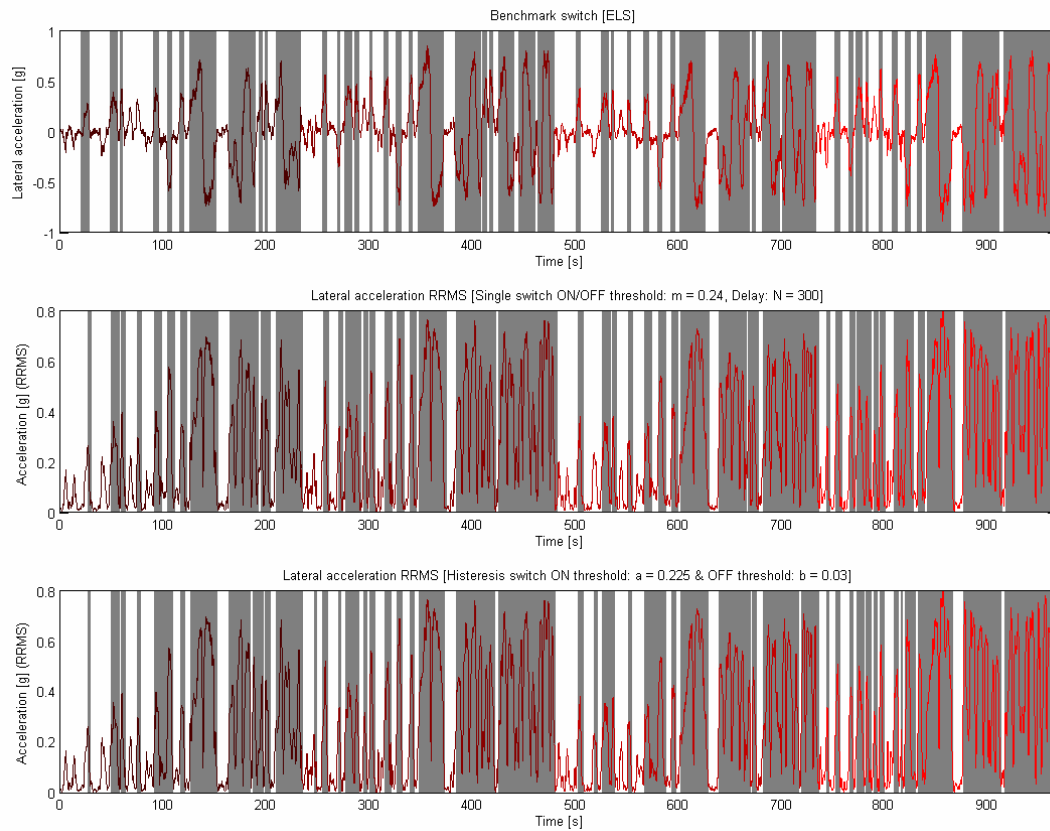


Figure 101: RRMS, Ride and handling track

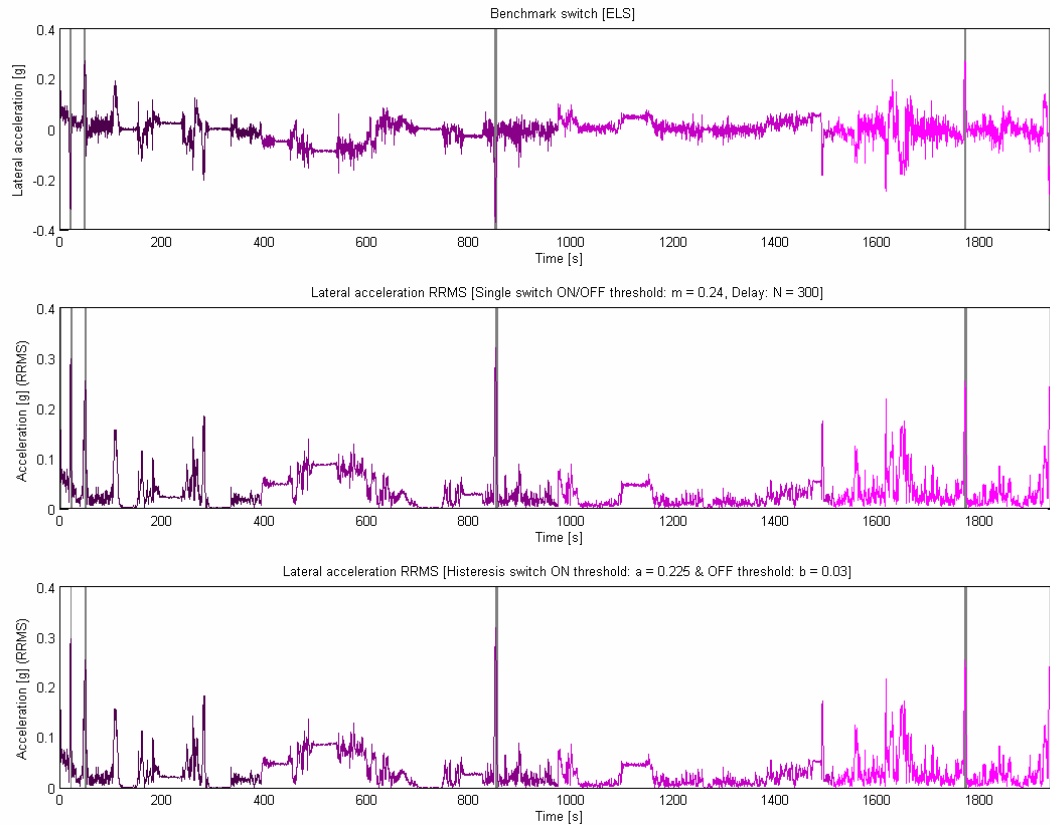


Figure 102: RRMS, city traffic

Appendix A

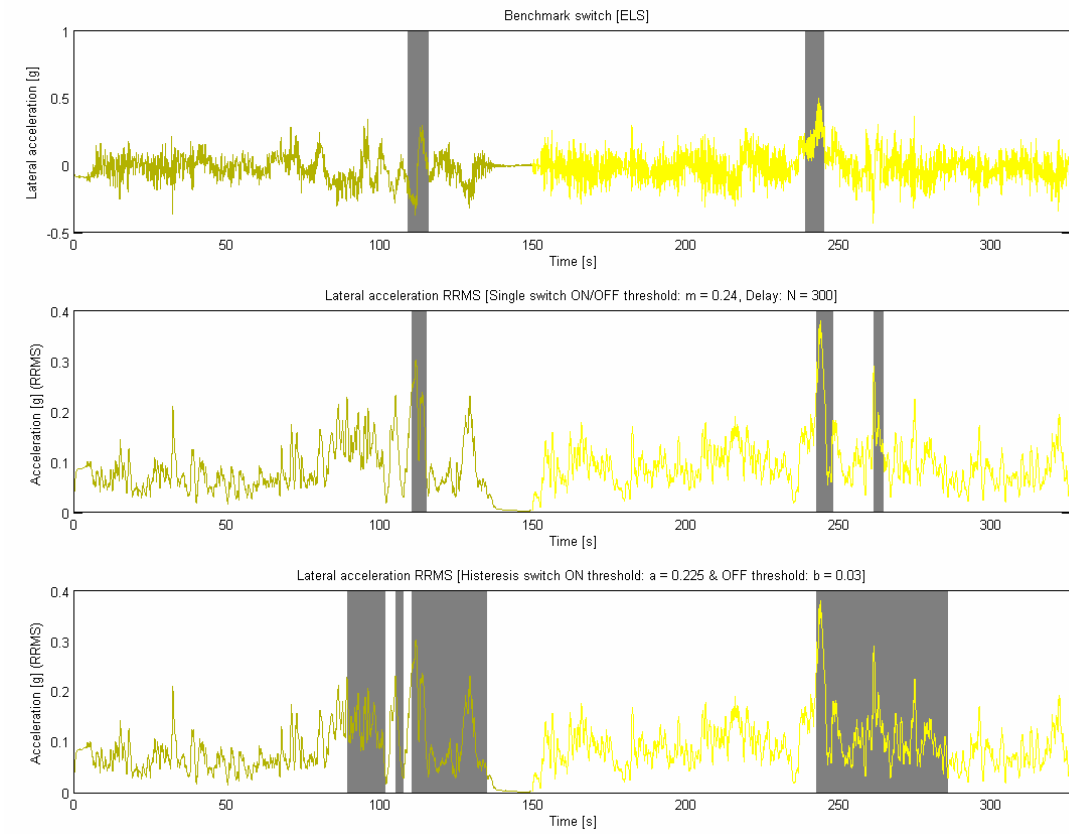


Figure 103: RRMS, Off-road track

